POLYTECHNIQUE MONTRÉAL
affiliée à l'Université de Montréal

Distributed Energy Management in a Network of Prosumers with Thermal Loads Participating in Demand Response Programs

EHSAN REZAEI
Département de mathématiques et de génie industriel

Thèse présentée en vue de l'obtention du diplôme de *Philosophiæ Doctor*
Mathématiques

Décembre 2021

© Ehsan Rezaei, 2021.

POLYTECHNIQUE MONTRÉAL
affiliée à l'Université de Montréal

Cette thèse intitulée :

Distributed Energy Management in a Network of Prosumers with Thermal Loads Participating in Demand Response Programs

présentée par **Ehsan REZAEI**
en vue de l'obtention du diplôme de *Philosophiæ Doctor*
a été dûment acceptée par le jury d'examen constitué de :

Michel GENDREAU, président
Hanane DAGDOUGUI, membre et directrice de recherche
Roland MALHAMÉ, membre
Kodjo AGBOSSOU, membre externe

DEDICATION

To Malihe, my love of life and wonderful wife, who gave me endless support and encouragement in each step of this path ...

ACKNOWLEDGEMENTS

First, I would like to express my appreciation to my research supervisor, Professor Hanane Dagdougui, for all the advice, positive feedback and exciting discussions. I thank her for her support and help, which allowed me to develop my research interests during this Ph.D.

Thanks also to the members of the Department of Mathématiques appliqueés at Polytechnique Montreal for lessons and support. I also would like to thank my friends and colleagues who encouraged and helped me.

Last but not least, I am especially thankful to my parents, Zahra and Javad, for their constant encouragement and my wife, Malihe, who has deeply supported and motivated me throughout this process. Without them, I believe that I couldn't be in this place today.

RÉSUMÉ

Face à la demande croissante d'énergie et aux préoccupations liées au réchauffement climatique, les réseaux électriques, en particulier les réseaux intelligents, s'orientent depuis peu vers l'utilisation de micro-réseaux (MG) intégrant des ressources énergétiques renouvelables (RESs). Le réseau de micro-réseaux (N-MGs) est un concept nouvellement développé qui vise à contribuer au programme de réponse à la demande et à réduire les coûts d'exploitation des MGs tout en répondant à la demande énergétique. La gestion de l'énergie en présence du caractère intermittent des sources d'énergie renouvelable des sources d'énergie renouvelables, la préservation de la confidentialité des MGs données et la fiabilité du réseau sont quelques-uns des défis auxquels les N-MGs sont confrontés.

Compte tenu des défis cités ci-dessus, cette thèse aborde ces aspects dans un contexte hiérarchique et pair-à- pair, tout en l'appliquant à différents secteurs.. En raison de leur économies d'énergies et de leur contribution aux programmes de réponse à la demande, ce travail se concentre principalement sur les réseaux de bâtiment intelligents et des serres agricoles intégrés avec des des microréseaux. Cependant, les méthodes proposées peuvent être généralisées à tous les types des MGs.

Dans la première contribution (Chapitre 4), cette thèse aborde le problème de la gestion de l'énergie dans les bâtiments résidentiels intégrant des ressources énergétiques distribuées et des véhicules électriques. Ce chapitre modélise d'abord un bâtiment résidentiel à logements multiples combinant des panneaux photovoltaïques installés sur le toit et des véhicules électriques. Ensuite, il reformule le problème de gestion de l'énergie en un problème d'optimisation du contrôle prédictif, en tenant compte des contraintes du bâtiment et des véhicules électriques et du confort des occupants.

La seconde contribution (Chapitre 5) aborde le comportement stochastique des sources d'énergie renouvelables dans les réseaux à micro-réseaux selon une architecture pair-en-pair et hiérarchique. Ce chapitre propose d'abord une approche distribuée pour résoudre l'optimisation stochastique avec une distribution connue. Il formule ensuite le problème de gestion de l'énergie du réseau sous la forme d'une optimisation stochastique en deux étapes. Dans la première étape, l'objectif est de trouver les valeurs optimales des températures intérieures. Dans la deuxième étape, le but est de minimiser la puissance achetée sur le réseau principal en présence de comportements stochastiques des ressources énergétiques renouvelables.

La troisième contribution (Chapitre 6), on considère le problème du contrôle énergétique

distribué dans un réseau hiérarchique de serres agricoles. Chaque serre possède plusieurs sous-systèmes qui contrôlent les conditions climatiques intérieures pour la croissance des plantes, ce qui rend le contrôle des serres plus complexe que celui des bâtiments. Pour contribuer aux programmes effacement de la demande, la coordination des serres est essentielle. Ce chapitre présente une méthode distribuée dans laquelle l'agrégateur, entité représentant ce réseau sur le marché, coordonne les serres agricoles et gère des ressources partagées. Dans cette méthode, différentes stratégies d'économie d'énergie linéaires et non linéaires telles que l'écrêtage et le déplacement de la charge sont utilisées pour améliorer les performances du réseau.

Enfin, les simulations réalisées dans chapitres valident, les performances des approches proposées, qui, en raison de leur vitesse de convergence et de leurs réponses rapides, peuvent être utilisées dans des applications pratiques en temps réel.

ABSTRACT

Facing the growing demand for energy and global warming concerns, power system grids, especially smart grids, are recently moving toward using microgrids (MGs) integrated with renewable energy resources (RESs). Network of microgrids (N-MGs) is a newly developed concept that aims to contribute to the demand response program and reduce MGs' operating costs while meeting their loads' needs. Managing energy in the presence of stochastic behaviors of RESs, preserving the privacy of MGs, and having a reliable network are some of the challenges these N-MGs face.

Given the above challenges, this dissertation addresses them in various hierarchical and peer-to-peer network topologies with MGs with different applications. Due to their potential to save energy and contribute to the demand response programs, this work mainly focuses on networks of buildings and greenhouses integrated with RESs. However, the proposed methods and frameworks can be generalized to all types of MGs.

In the first contribution (Chapter 4), this dissertation discusses the energy management problem in residential buildings integrated with RES and electric vehicles (EVs). This chapter first models a multi-unit residential apartment combined with roof-installed photovoltaic panels and EVs. Afterward, it reformulates the building energy management problem to a model predictive control optimization problem, considering the building and electric vehicles constraints and occupants' comforts.

The second contribution (Chapter 5) tackles the RES stochastic behaviors in peer-to-peer and hierarchical network topologies. This chapter first proposes a distributed method for solving two-stage stochastic optimization with known distribution and proves its convergence. It then formulates the network energy management problem as a two-stage stochastic optimization and decomposes it to the level of each MG by using the proposed method. In this framework, there are several coordinators for the coordination of MGs depending on the network topology.

The third contribution (Chapter 6) addresses the distributed energy control in a hierarchical network of greenhouses. Each greenhouse has several subsystems that control the indoor climatic conditions for plant growth, making controlling greenhouses more complex than the buildings. To contribute to the demand response programs, the coordination of greenhouses is essential. This chapter presents a distributed method in which the aggregator, an entity representing this network in the market, coordinates the greenhouses and manages the shared resources. In this method, different linear and nonlinear energy-saving strategies such as load shaving and shifting are used to enhance the network's performance.

Finally, the simulations in each chapter validate, in theory, the performance of proposed approaches, which due to their fast convergence rate and responses, can be used in real-time applications.

TABLE OF CONTENTS

DEDICATION iv

ACKNOWLEDGEMENTS v

RÉSUMÉ vi

ABSTRACT viii

TABLE OF CONTENTS x

LIST OF TABLES xiii

LIST OF FIGURES xiv

LIST OF SYMBOLS AND ACRONYMS xvi

LIST OF APPENDICES xvii

CHAPTER 1 INTRODUCTION 1
- 1.1 Context: Microgrids and Network of Microgrids 1
- 1.2 Challenges of N-MGs 2
- 1.3 Objectives 5
- 1.4 Plan of the dissertation 7

CHAPTER 2 LITERATURE REVIEW 8
- 2.1 Buildings 8
  - 2.1.1 Smart Buildings 8
  - 2.1.2 Integration of Distributed Energy Resources in Buildings 9
  - 2.1.3 Demand Response 11
  - 2.1.4 Building Energy Management Systems 12
- 2.2 Smart Greenhouses 15
- 2.3 Optimization Methods in Networks of Microgrids 16
  - 2.3.1 Centralized 16
  - 2.3.2 Decentralized 17
  - 2.3.3 Distributed 18

CHAPTER 3 SYNTHESIS OF WORK AS A WHOLE 22

CHAPTER 4 ARTICLE 1: OPTIMAL REAL-TIME ENERGY MANAGEMENT IN APARTMENT BUILDING INTEGRATING MICROGRIDS WITH MULTIZONE HVAC CONTROL 24
4.1 Introduction 24
4.2 System Models 27
4.2.1 Energy management structure 27
4.2.2 Model of PV 29
4.2.3 Energy storage system model 29
4.2.4 EVs Model 31
4.2.5 Residential Thermal Model 35
4.2.6 Demand-Supply Balance Constraint 38
4.3 Control Algorithm 39
4.4 Simulations 39
4.5 Conclusion 44

CHAPTER 5 ARTICLE 2: DISTRIBUTED STOCHASTIC MODEL PREDICTIVE CONTROL FOR PEAK LOAD LIMITING IN NETWORKED MICROGRIDS WITH BUILDING THERMAL DYNAMICS 46
5.1 Nomenclature 46
5.2 Introduction 48
5.3 Mathematical Modeling 50
5.3.1 Thermal Dynamic Model of Buildings 51
5.3.2 PV Panels 53
5.3.3 Electrical Storage System 53
5.3.4 Power Balance 54
5.4 Distributed Optimization 55
5.4.1 Single MG Optimization Problem 55
5.4.2 Aggregator Optimization Problem 56
5.4.3 ADMM Introduction 57
5.4.4 ADMM-based Distributed SMPC 58
5.5 Case Study 63
5.6 Conclusion 70
5.7 Appendices 71
5.7.1 Appendix A: Details of Building RC Model 71
5.7.2 Appendix B: Proof of Theorem 1 73

CHAPTER 6 ARTICLE 3: HIERARCHICAL DISTRIBUTED ENERGY MANAGEMENT FRAMEWORK FOR MULTIPLE GREENHOUSE CONSIDERING DEMAND RESPONSE . . . 75
6.1 Introduction . . . 75
6.2 Mathematical Modelling . . . 78
6.2.1 Modelling of Greenhouse Components . . . 78
6.2.2 Modelling of Aggregator Components . . . 85
6.3 Optimisation Problems . . . 87
6.3.1 Greenhouse and Aggregator Optimisation Problems . . . 87
6.3.2 Optimization Problem Decomposition . . . 87
6.4 Case Study . . . 90
6.5 Conclusion . . . 96

CHAPTER 7 GENERAL DISCUSSION . . . 98

CHAPTER 8 CONCLUSION AND RECOMMENDATIONS . . . 100
8.1 Concluding Remarks . . . 100
8.2 Limitations . . . 100
8.3 Future Work . . . 101

REFERENCES . . . 102

APPENDICES . . . 125

LIST OF TABLES

Table 4.1 Standard temperatures to feel comfortable in a room 40
Table 4.2 EVs and Battery Properties 41
Table 4.3 Building Parameters 43
Table 5.1 Wall types and their materials 71
Table 6.1 Control parameters values. 91

LIST OF FIGURES

Figure 1.1	Different control methodologies used in N-MGs.	5
Figure 2.1	Model predictive control (MPC) methodology	13
Figure 2.2	Different optimization methods used in N-MGs	17
Figure 3.1	Synthesis of the Ph.D. project.	22
Figure 4.1	Architecture of a building integrated with microgrid.	28
Figure 4.2	An apartment and its equivalent RC circuit	34
Figure 4.3	Floor map of 8 of studio apartments	37
Figure 4.4	PV Power and Battery SOC.	40
Figure 4.5	Charging and discharging power of ESS	41
Figure 4.6	Zone temperatures	42
Figure 4.7	The total amount of HVAC power consumption	43
Figure 4.8	State of charge of EVs and power generation from PV.	44
Figure 4.9	red The amount of power exchanged with the grid.	45
Figure 5.1	Example of MGs trading energy with the main grid	61
Figure 5.2	Generated PV power of MGs and outside temperature	63
Figure 5.3	Buildings' average temperatures and setpoints	65
Figure 5.4	Buildings' power consumption	66
Figure 5.5	State of charge (SOC) of MGs' batteries	67
Figure 5.6	Charging and discharging status of MGs' batteries	68
Figure 5.8	Total of exchanged power and power exchanged with main grid	68
Figure 5.7	Indoor temperatures of two MGs for each zone.	69
Figure 5.9	Iterations information	70
Figure 5.10	The model of studied triplex home	72
Figure 5.11	An example of thermal network of 3rd floor of mentioned home.	73
Figure 6.1	Conceptual model of the proposed network of greenhouses	79
Figure 6.2	Thermal equivalent circuit of the greenhouse	81
Figure 6.3	PV generated power of each greenhouse and Outside temperature	90
Figure 6.4	Top: Indoor CO_2 level. Bottom: Indoor temperature.	91
Figure 6.5	Greenhouse watering plot	92
Figure 6.6	Greenhouse illumination	93
Figure 6.7	Battery dis/charging power and Battery SOC	94
Figure 6.8	Greenhouse exchanged power, main pump and reservoir info.	95
Figure 6.9	Number of iterations, total time and average time of each step	96

Figure A.1 The network topology 125
Figure A.2 Greenhouse climatic parameters 126
Figure A.3 Greenhouse battery condition 127
Figure A.4 The negotiation process 128
Figure A.5 The power exchanged with the main grid 128
Figure A.6 Total time, average time and total number of iterations 129

LIST OF SYMBOLS AND ACRONYMS

EVs	Electric Vehicles
IoT	Internet of Things
RES	Renewable Energy Resources
PV	Photovoltaic
MG	Microgrids
ESS	Electrical Storage System
N-MGs	Network of Microgrids
MDL	Maximum Demand Load
P2P	Peer-to-Peer
DR	Demand Response
SOP	Stochastic Optimization Problem
ADMM	Alternating Direction Method of Multipliers
EMS	Energy Management System
AI	Artificial Intelligence
DER	Distributed Energy Resources
HVAC	Heating, Ventilation, and Air Conditioning
ZEB	Zero Energy Buildings
BIPV	Building-Integrated Photovoltaics
AHU	Air Handling Unit
BIMG	Building-Integrated Microgrid
BEMS	Building Energy Management System
DSM	Demand Side Management
EE	Energy Efficiency
RO	Robust Optimization
SO	Stochastic Optimization
FAO	The Food and Agriculture Organization
CSA	Climate-Smart Agriculture

LIST OF APPENDICES

Appendix A A P2P Example 125

CHAPTER 1 INTRODUCTION

1.1 Context: Microgrids and Network of Microgrids

During past decades, the demand for electricity has increased significantly to meet the growing usage of electricity in commercial and residential buildings, electric vehicles (EVs), internet of things (IoT). The traditional electrical power plants, mostly fossil or nuclear fuel-powered, are no longer considered a sustainable solution due to their disadvantages, such as CO_2 emissions, air pollution, hazardous waste, and even operational cost. For these reasons, moving towards renewable energy-based resources such as solar and wind plants with lower environmental impacts, cleaner energy, and more economical operating costs is unavoidable [1–3]. In response to these benefits, the number of renewable power plants has considerably increased in the last two decades [4].

According to [5], a microgrid (MG) is a group of sources and loads connected to each other and the main grid. It can operate in grid-connected or island mode. Providing backup for the grid and reducing costs are some advantages of MGs. Due to their clean energy and environmentally friendly aspects, MGs integrated with renewable energy-based distributed resources are of interest. Each renewable-based MG is a set of loads, RESs, and (not necessarily) an electrical storage system (ESS), such as electric batteries [6] or EVs.

Due to the intermittent behaviour of RES, such as insufficient solar radiation for PV power generation, the grid-connected mode is more favourable for MG to maintain the reliability and increase the resilience. At each time step, MG can exchange power with the grid or use its local energy storage system to supply the power to the load.

MG's primary objective is supplying the local loads. However, depending on its application and configuration, MG can support the grid by providing energy and ancillary services, such as frequency and voltage control support, improvement of power quality, and congestion management [7, 8]. Also, MGs can make the markets more competitive by offering energy and power at a reasonable price. On the other hand, MGs can protect their appliances and users by disconnecting from the grid and working in island mode during a power outage in the main grid [9].

Due to the uncertainties and unpredictability of renewable sources, the energy produced at each time step is uncertain and difficult to control. In addition, most renewable-based energy is available only in specific periods. For example, a photovoltaic(PV)-based MG can not generate any power at nighttime. Although using storage systems such as batteries can

help the MG supply the load during energy shortage periods. However, relying only on ESS is not a viable solution due to its high investment costs and physical limitations. A reasonable solution to this problem is a hybrid grid-connected MG with ESS, in which the stochastic behaviours of MG's RES can be handled.

In the Network of Microgrids (N-MGs), microgrids are physically connected following a specific topology and structure. This network can be connected or disconnected from the main grid. In this context, each MG can buy (sell) energy from (to) the main grid or its neighbours, the MGs it is connected to. According to [10], N-MGs are of interest to the main grid due to the robustness improvement they can bring for the main grid. The grid robustness can be mainly damaged by renewable generation uncertainties and loads' stochastic behaviours. To withstand these disturbances and uncertainties, N-MGs can enhance the transient stability performance and enlarge the stability margin by using advanced control and coordination strategies [11–13]. N-MGs can also help to improve grid efficiency in different ways, such as providing distribution system state estimation [14], managing optimal power flow and distributed energy resources (DER) [15–17], and volt and var optimization [18, 19]. Therefore, N-MGs are very serviceable during peak-demand periods in on-peak times, when the demand for electrical energy is higher.

On the other hand, N-MGs can provide a secure, reliable and safe network for MGs they participate in, especially during power outages [11, 17, 20]. Also, a network of MGs provides the most efficient way of DERs utilization, and it can reduce the overall costs of MGs by integrating considerable capacity of DERs power generation [21]. For these reasons, N-MGs are an attractive option for MGs.

1.2 Challenges of N-MGs

Although N-MGs can serve various benefits to both MGs and the main grid, they come with many operational challenges, such as [21, 22]:

1. Individual MGs privacy: three different ownership models are possible for a N-MGs:

   - Utility-owned N-MGs, owned and controlled by a utility company,
   - Privately-owned N-MGs, where different owners control each MG, and
   - Utility–private mixed-owned N-MGs.

   In the private- and mixed-owned N-MGs, maintaining the privacy of MGs is challenging since owners wish to share only the power exchange details.

2. Control and stability issues: high penetration of DERs with intermittent behaviours can result in stability issues for N-MGs. In addition, the management and control of energy exchange in the presence of stochastic behaviours of DERs needs more investigation.

3. Protection coordination: frequent changes of network topology due to different operating modes and optimal flow paths can cause protection coordination problems because fault currents in different topologies are different in size and direction.

4. Efficient communication network: sharing information among MGs and the main grid needs a secure yet fast communication network. Owing to the cyber-attacks, providing a reliable communication network is another challenge in N-MGs.

Three different structures for N-MGs are introduced in the literature to answer these challenges: Centralized, hierarchical, and peer-to-peer (P2P). In the centralized structure, all information of MGs, such as their setpoints, loads and RES generation profiles, should be shared with a central control entity. Then this central controller makes decisions on how energy and power should be distributed in the network [23]. As it sounds, this structure can only work for utility-owned N-MGs or the N-MGs in which MGs' owners are willing to share all of their information. For this reason, hierarchical and P2P have been received attention during the past few years.

Before defining the other two structures, we need to define a new entity known as *aggregator*. In the context of N-MGs, an aggregator can represent a group of MGs which behave as one entity in the market operations [24]. Aggregators are new entities in electric markets, which can improve the flexibility of power systems by moderating their network power consumption and increasing the demand response market players. In this context, the aggregators can participate in energy markets on behalf of MGs and sell their surplus energy to the main grid or other entities. As a result, by providing flexibility to both demand and supply sides, an aggregator helps better integrate its MGs' renewable energy sources.

In a hierarchical structure, all MGs of the network are connected to an N-MGs coordinator (such as an aggregator). This latter plays an interface role with the main grid or distribution network operator. The aggregator's tasks are coordinating the MGs, collecting their power, selling it in the market, and dividing its financial benefits fairly [25, 26]. In addition, in a network with shared resources, it is responsible for how MGs use them. This structure can handle the DERs uncertainties and work in different operation modes of the network. Depending on the optimization method (which we will explain shortly), it also can provide an efficient communication network. For these reasons, this structure is suitable for private- and mixed-owned N-MGs [27, 28].

Though the hierarchical structure can improve the performance of N-MGs in different terms, it suffers from the problem of aggregator failures. In other words, if the aggregator fails due to any reason, such as cyber-attacks, the whole network fails. The P2P structures have been developed to meet this challenge, in which each MG can directly demand its required energy from other resources without the need to share information with any third party [28]. Like hierarchical ones, P2P structures are suitable for both private- and mixed-owned networks and yet do not suffer from aggregator failure problems; however, finding an optimal solution for these structures is more challenging due to their complex structures [28, 29].

As discussed earlier, due to the ownership, sharing information, in either P2P or hierarchical, should not risk the safety of MGs. In other words, to solve the optimization problem of the network, *privacy* of MGs has to be considered. Also, the network should be *reliable*, meaning in the case of single/multiple entity failure, the network should continue to operate. The *computational load* is another important factor in N-MGs concept. Solving a time-consuming optimization problem when the network has to work in a real-time environment is not practical. Privacy, reliability and computational load are the factors that can be used to determine the efficiency of a network [30].

In the literature, the existing approaches to solve the optimization problem of the network are categorized into three main groups: centralized, decentralized and distributed methods. In *centralized* methods, MGs information, including their power consumption, loads models and RES productions, must be shared with a third party, a central controller. The central controller then solves a centralized optimization problem to find the optimal operating point for the whole network and sends back the control signals to MGs [23, 31–33]. On the other hand, *decentralized* methods focus on individual MGs, where each MG solves its optimization problem without sharing information with other MGs or any third party such as aggregator [34–37].

Distributed approaches are a trade-off between centralized and decentralized approaches. In these methods, MGs share a limited version of their information and, in exchange, a global optimal solution and stability of the network can be guaranteed [38–48]. Compared to the centralized methods, distributed ones offer more reliability, better privacy and less computational load. On the other hand, the main grid does not desire selfish behaviours and coordinations similar to decentralized approaches. Therefore, distributed methods are more attractive to the main grid. Despite that, finding the optimal solution in both decentralized and distributed approaches, especially with RES uncertainties, is the main challenge these methods face.

Fig. 1.1 presents a graphical comparison between different optimization approaches from the

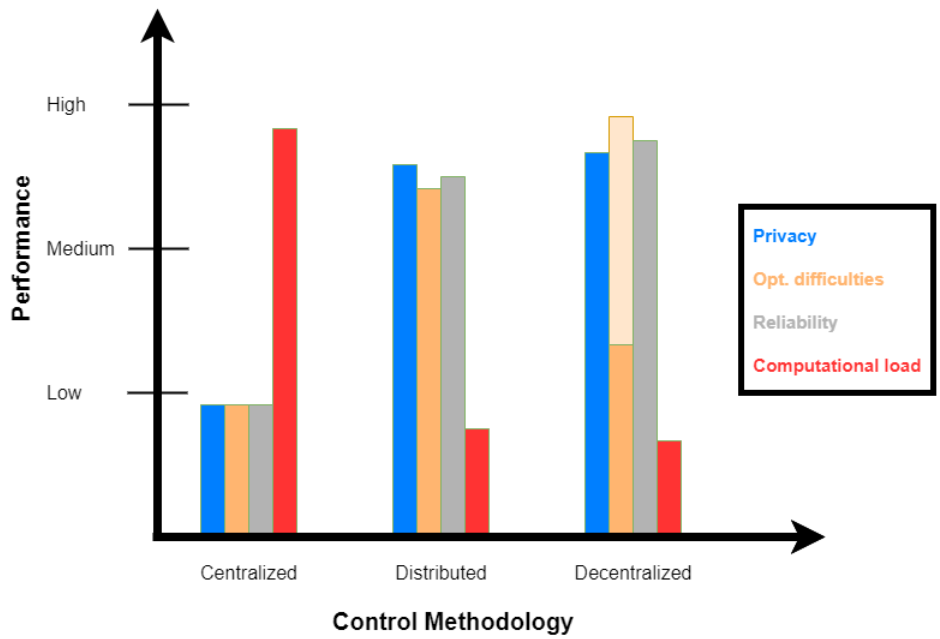

Figure 1.1 Different control methodologies used in N-MGs.

perspective of privacy, reliability and computational load. As seen in this figure, distributed techniques have an acceptable level of reliability and privacy, and since the optimization problem can be solved in parallel at the level of MGs, their computational power is reasonably low. However, these methods are mathematically expensive and complex.

We should mention that, unlike the centralized and decentralized approaches, the distributed methods have the flexibility to work, manage and control power and energy in both structures. For their advantages, these approaches are the main focus of this work.

1.3 Objectives

Buildings integrated RES (especially with roof-installed PV panels) are a new type of MGs developed recently. The building-integrated microgrid (BIMG) refers to a building that uses micro-sources, namely, ESS and RES such as PV panels and batteries, to supply the energy it needs for its load [49]. Due to their potential in influencing the electrical network, these buildings, along with EVs, are good candidates for demand response (DR) programs. Modelling the building's loads, occupants' stochastic behaviours, intermittent behaviours of RES, and managing resources to maximize the building's benefits are some of the challenges that need to be addressed adequately.

In a building, subsystems responsible for comfort parameters consume most of the building's

energy consumption. In residential buildings, a significant part of this energy goes toward controlling occupants' thermal comfort. Hence, from the BIMG perspective, finding an efficient way to model the thermal dynamics of the building is the first challenge.. For instance, considering the occupants' comforts, the nonlinear thermal cross-effects of building's zones, the limitations of heating, ventilation, and air conditioning (HVAC) systems, the integration of local batteries and electric vehicles into the energy management system are challenging tasks that should be adequately addressed.

On the other hand, the second problem is the efficient coordination of MGs hierarchically distributed while limiting total power consumption for the DR program. The control of various and heterogeneous demand response actions while considering occupants' comforts is challenging. Moreover, the control of the shared resources, such as shared batteries in a network of residential buildings or water reservoirs in a network of greenhouses, should be appropriately addressed.

In all structures, the RES stochastic behaviour is another obstacle in finding the optimal solution for the N-MGs. This stochastic behaviour makes it difficult to find the optimal solution, affecting the network's performance. Handling these uncertainties in the distributed and decentralized methods is more complicated than the centralized ones, and thus they need to be studied more.

Given the above problems, the main goal of this dissertation is to solve the problem of energy control and management in a network of buildings integrated with DERs, considering the dynamics of buildings' subsystems and stochastic behaviours of RES for the DR program. To reach this goal, we divide the problem into three specific objectives corresponding to three main contributions:

1. Propose an energy management system for a residential BIMG, where the building participates in the DR program by controlling its thermal dynamic, battery and EVs without violating the occupants' comfort.

2. Construct a stochastic distributed framework to limit peak loads on N-MGs by considering intermittent RES behaviour, in which buildings participate in the DR program using their thermal dynamic and battery.

3. Develop a hierarchical distributed control method for the network of greenhouses with various subsystems for participating in the DR program with different linear and nonlinear strategies such as load shaving and load shifting.

1.4 Plan of the dissertation

This thesis is organized in the following order. Chapter 2 presents the main definitions and related literature. Chapter 3 presents the synthesis of this work as a whole. In Chapter 4, residential buildings integrated with RES and EVs are modelled, their constraints and objective are discussed, and a model predictive control (MPC) approach for controlling the thermal dynamics of the building is proposed. Through simulation, it is shown that the proposed method can reduce the power consumption of buildings without violating the comforts and related technical constraints. In Chapter 5, a stochastic distributed MPC-based framework is presented for both hierarchical and P2P structures, while it considers stochastic behaviours of RES. In this framework, the optimization problem of the network is formulated as a two-stage stochastic optimization problem (SOP), where energies exchanged are second-stage variables. An ADMM-based stochastic decomposition method is then introduced, which can break down the general two-stage SOP to sub-SOPs at the level of each MG. The convergence of the proposed method is proved, and through the simulation, its fast convergence rate is shown. In Chapter 6, a distributed MPC-based control approach is presented for a hierarchical network of greenhouses integrated with PV panels. In this approach, the aggregator is responsible for peak limiting and controlling the shared resources (water reservoir). Therefore, MGs negotiate with the aggregator for the energy exchanged with the main grid and the use of shared resources (water). The proposed approach considers different energy management strategies such as load shaving and shifting, resulting in a nonlinear objective function. Using ADMM, the network can solve this optimization problem distributively in a reasonable time at the level of each greenhouse. As an extension to the previous chapters, Appendix A shows with a simulation how the proposed framework in Chapter 5 can work in a P2P network of greenhouses. Finally, Chapter 7 provides a general discussion, and Chapter 8 discusses the limitations and future works.

CHAPTER 2 LITERATURE REVIEW

This chapter presents an overview of the most relevant literature. It will cover the following topics: 1) Smart buildings and demand response programs, 2) energy management systems (EMS), 3) smart agriculture and greenhouses, and 4) optimization methods used in N-MGs.

2.1 Buildings

Around the world, approximately 40% of global energy consumption goes towards buildings where around 75% of this energy is used to control buildings' comfort parameters such as indoor temperature, or ventilation [50]. For this reason, building operators are starting to consider the impacts of their consumption on their carbon footprints and the electrical grid. Therefore, managing the energy consumption of the building while considering the comforts of occupants is a high priority for operators. To this end, buildings are recently evolving toward a new concept called *smart buildings*.

2.1.1 Smart Buildings

Smart buildings are the ones that can efficiently and economically optimize, manage and control their local resources by using various technologies such as Internet of Things (IoT), smart sensors, AI (Artificial Intelligence) and energy management system (EMS).

Some real case studies demonstrate that using appropriate control strategies, especially the predictive ones (e.g., MPC), can remarkably reduce smart buildings' power consumption. Sturzenegger *et al.* in [51] show that applying a model predictive control (MPC) algorithm to an office building located in Swiss can save up to 20% energy while meeting indoor comfort conditions. In [52], authors model a building in Hasselt, Belgium, using identification methods. The application of MPC leads to an energy consumption economy of up to 17%. From recent works, Carli *et al.* propose an MPC-IoT-based architecture for controlling heating, ventilation, and air conditioning (HVAC) systems in smart buildings [53]. Their proposed architecture demonstrates the reduction of building energy consumption by 18%, while increasing occupants' comforts by 20%. Authors in [54] propose a reinforcement learning (RL) approach to control building HVAC systems. Their approach could save energy up to 16.7% while maintaining occupants' comfort.

Although some other works in the literature investigate the performance of different control strategies in buildings [55–58], all of these studies assume that buildings are consumers,

and reducing power consumption without violating occupants' comforts is, therefore, their primary goal. By combining with distributed energy sources, the building's role can be changed from energy consumer to producer, increasing its effectiveness in the main network.

2.1.2 Integration of Distributed Energy Resources in Buildings

Considering smart pricing mechanisms, smart buildings can shift their role from passive consumers to active prosumers. Thanks to recent rapid advances in RES and ESS technologies, buildings can now integrate with distributed energy resources (DER) and generate energy instead of only consuming energy. Buildings can integrate various distributed energy resources such as PV panels, batteries, and EVs. In the following, we discuss each of them.

PV Energy Resources

The integration of PV panels to buildings can change their paradigm. Although PV panels are traditionally installed on the buildings' rooftops, with recent developments, they can be installed on the surface of building facades [59]. Hybrid photovoltaic-thermal panels are also an efficient solution for the use of both solar thermal energy and electricity ([60–64]), although in this work, we only focus on photovoltaic panels and their integration into buildings.

Some feasibility studies in the literature demonstrate the advantages of integrating PV panels to reduce the operation cost of buildings [65–67]. Authors in [68] show that installing PV panels for two different offices could provide annual billing savings up to 58%. Syafii *et al.* in [69] design a rooftop PV system for an office building. Their study shows that the designed system can reduce the energy purchased from the main grid during on-peak times.

The case studies above are institutional and commercial buildings, whose peak load demand time is daytime when PV panels generate the highest PV power. Using PV panels for residential buildings is a challenging task since their peak load demand occurs often at night and in early morning. Using energy storage systems and EVs to store this generated power and use it at peak times is a reasonable solution.

Energy Storage Systems

Energy storage systems (ESS) refer to systems that can store electrical energy in another energy form and convert it back into electricity when needed [70]. One of the most common types of ESS is batteries. Their high initial investment and maintenance costs are their main limitations for the use in large sizes. Therefore, using small to medium-sized batteries in

buildings is more appropriate. Some studies address the sizing problem of ESS and intend to find the best size integrating PV and batteries, given the cost of operation and investment [71–76]. Batteries can store either the excess PV energy or the energy purchased from the main grid at off-peak times [77]. However, the sizing problem is in the design phase and is beyond this thesis's scope. Managing and controlling behaviours of ESS is the task of the energy management system (EMS), which will be discussed later.

Though buildings themselves are not ESS, they can also be used to store energy. According to [78], [79] and [80], to feel comfortable in a typical room, the temperature (depending on the season) should be between 19° and 26° of Celsius when occupied and can be between 5° and 40° when unoccupied. It means that the building can behave like a thermal storage system by changing its temperature. Need to mention here that, given the occupants' comforts, these changes are limited [78]. For example, authors in [81] present the results from a pilot test where the potential of buildings to store thermal energy was tested for residential buildings. The results show that with small changes in the temperature of buildings ($\leq \pm 0.5$°C), a suitable amount of energy (up to 10% depending on different parameters) can be stored.

Although using ESS to store energy seems reasonable, it is not as easy as it sounds. In practice, determining its dis/charging time and amount are challenging. Furthermore, choosing the right strategy to dis/charge ESS is another problem that needs to be appropriately addressed. For example, buildings can store their excess generating power inside the ESS as a strategy. However, if the main grid, especially at peak times, pays a reasonable price for this excess power, the selling strategy to the main grid can be more economical than the storing one. The problem in the N-MGs and in the presence of RES stochastic behaviours becomes even more complicated.

Electric Vehicles

Given the daily growth of electric vehicles (EVs), the grid and the buildings should consider their influences on their power demand. In terms of modelling, the EV can be considered as an electric battery, only available for a certain period and must be charged before departure time. Recently some studies have investigated the effects of EVs in the grid. For example, Sengor *et al.* in [82] propose a new linear programming strategy for maximizing the load factor of an EVs parking lot in the on-peak situation. They model EVs' arrival time and state-of-energy as random variables and then predict and manage them. As a result, significant changes in the load factor are achievable.

In [27], the authors propose a vehicle-to-microgrid framework where EVs can be used to meet the load demand of commercial buildings. In [83], the problem of distributed coordination

of EVs charging with a wind power plant is formulated as a Markov decision process that considers the random characteristics of EVs. The authors then propose a distributed-based policy improvement algorithm to solve the Markov process. Li *et al.* [84], use a similar idea to reformulate the problem as a constrained Markov decision process. They propose a deep neural network-based reinforcement learning method to solve the EVs charge scheduling problem. Although other works studied the effects of EVs in the grid [85–88], but examining the integration of EVs and their benefits for residential buildings has not received enough attention.

Building-Integrated Microgrid

The Building-integrated microgrid (BIMG) refers to a building that uses DERs, such as PV panels or diesel generators, to supply the energy it needs for its load. Among BIMGs, nearly/net-zero energy buildings (NZEBs) are the ones using renewable energy resources to meet almost all of their loads, such as building-integrated photovoltaics (BIPVs). BIPVs can use their stored ESS energy or RES generation capacity to reduce the electricity purchased at peak times. For this reason, they can play an influential role in the power grids while minimizing the environmental impacts.

A significant portion of the building power consumption goes toward HVAC systems for occupants' thermal comfort in residential and commercial sectors. Many studies in the literature investigate the performance of HVAC systems in BIMGs and BIPVs. Yunas and *et al.* in [89] propose a centralized optimization framework for dis/charging of plug-in vehicles in commercial BIMGs. An MPC-based optimization BEMS for controlling indoor temperature and scheduling of building's subsystems is introduced in [90]. Authors in [91] propose an optimal energy management strategy for commercial buildings integrated with DC microgrid. However, according to [92], the complexity of thermal modelling of buildings and their occupants' behaviour alongside uncertainties of RESs are the current challenges of BIMGs, which need to be addressed adequately. Compared to the previously mentioned studies, the methods presented in this dissertation tackle the problems of residential building thermal modelling complexity and the stochastic behaviours of RESs simultaneously.

2.1.3 Demand Response

As previously discussed, loads in MGs can take many forms, such as EVs, buildings and appliances. Traditionally from the grid viewpoint, loads are considered passive, meaning that they are uncontrollable consumers. However, loads can be controllable to some extent and can affect the grid. *Demand response* (DR) programs aim to use these controllable loads

for controlling the demand in the network.

Demand response in the smart grid is defined as: "Changes in electric usage by end-use customers from their normal consumption patterns in response to changes in the price of electricity over time, or to incentive payments designed to induce lower electricity use at times of high wholesale market prices or when system reliability is jeopardized" [93]. Demand response programs provide the opportunity for consumers to influence the grid by shaving or shifting their power consumption in return for financial benefits. For example, a parking lot with EVs can store energy during the off-peak time and can sell it to the main grid or the neighbouring buildings during the on-peak time [82, 94].

In the context of buildings, loads are categorized as controllable and uncontrollable loads. HVAC or lighting systems in a residential building are examples of controllable loads, while fire alarms or surveillance systems are categorized as uncontrollable loads. As previously mentioned, small changes in buildings temperature can end up saving a considerable amount of energy. For this reason, some studies investigate the performance of buildings thermal systems for DR program, such as HVAC [95–98], air handling unit (AHU) [99–101], and heating boilers and pumps [102–104]. These studies show that buildings can support the electrical grid at peak times by participating in the DR programs and reducing their temperature without disturbing occupants' comforts.

Due to uncertainties, the energy management in a building integrated with DER and participating in DR programs is challenging. Authors in [105] formulate the problem of HVAC control in the presence of uncertainties related to solar power and energy prices into a two-stage SOP. Kim *et al.* in [106] present a robust two-stage SOP to achieve the optimal energy management for microgrid. They apply a multi-scenario tree method to generate scenarios. The proposed robust SOP then uses these scenarios to find the optimal values of DER generating power and power purchased from the main grid to minimize the operational cost. Thomas *et al.* in [107] propose a mixed-integer linear programming model which can handle solar uncertainty and stochastic behaviour of EV. They then compare the results of their algorithms with the deterministic approach and show that neglecting the uncertainties related to PV generation can increase the daily cost estimation. Although these works consider buildings with RES, few investigate the effects of RES uncertainties in a network of buildings or N-MGs participating in the demand response program.

2.1.4 Building Energy Management Systems

Buildings need a centralized regulatory control system known as the *building energy management system* (BEMS) to control and manage buildings subsystems such as heating, lighting

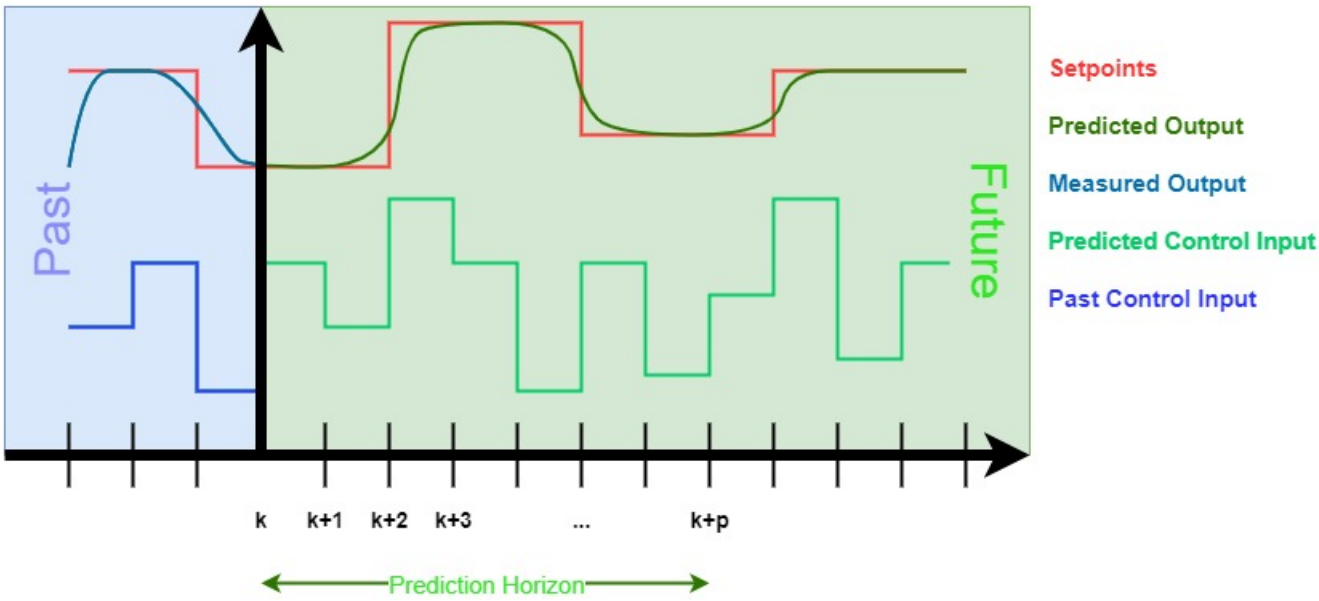

Figure 2.1 Model predictive control (MPC) methodology

and ventilation systems and their participation to DR programs. According to [108], BEMS approaches can be classified into four management strategies: *model predictive control*, *demand side management* (DSM), *optimization*, *diagnosis*. We need to mention here that in practice, BEMS might adopt one or more approaches simultaneously, e.g., MPC, DSM and optimization.

Model predictive control or MPC is an iterative control methodology aiming to optimize an objective function of a process based on the predictions of the process's future states by using its model [109]. Figure 2.1 illustrates this control methodology in general. At the current time-step k, the controller measures the process outputs, models the future of the process's outputs and states using its model for the next p time-steps. Using this information, MPC then solves an optimization problem with a specific objective function (e.g., the tracking error between prediction outputs and setpoints) to find optimal values of the following p time-steps control inputs. Eventually, the first element of the optimal control inputs applies to the process, moving it to its next state.

Due to its foresight ability, using MPC approaches can enhance building performance in terms of energy consumption and comfort levels. In the literature, three modeling methods have been used for MPC: *white-box*, *black-box* and *gray-box*. White-box MPC approaches refer to the MPC approaches that use physics-based modelling methods to explain the energy performance of buildings [110–113]. Data-driven or black-box MPC approaches are using historical collected data of buildings to estimate and manage buildings' energy consumption [114–117].

It is worth mentioning that despite the accuracy of white-box MPC approaches, they are time-consuming due to the integration of many model parameters. Black-box approaches suffer from data shortages, lengthy training processes and lack of interpretability. Merging the advantages of white-box and black-box methods leads to Grey-box methods. These methods are more interpretable than black-box methods, while simpler and more computationally efficient than white-box ones [118–121]. In general, according to [122], the grey-box modelling methods are helpful in the following cases. First, when detailed information about the building is not available for modelling with white-box methods. Secondly, in cases where there is uncertainty in the building's occupants' behaviours that neither white-box nor black-box methods can capture. Finally, grey-box methods are more practical and efficient than black-box ones in cases where the computational power or training datasets are limited. Resistance-capacitance (RC) thermal modelling is a grey-box method, which is of interest in this dissertation for its advantages; we will elaborate more in the next chapters.

DSM refers to a set of actions encouraging consumers to modify their energy use at peak times. *Demand response* (DR) and *energy efficiency* (EE) are the two main approaches of DSM programs. Despite DR programs (described earlier in Chapter 1), EE programs focus on applying different technologies to achieve energy-efficient buildings. Utilizing smart meters [123], estimating thermal load [124, 125], using thermal mass [126] and aggregation of users with a common distribution system [127] are examples of EE programs.

Dealing with different uncertainties such as PV-generated power or real-time prices, the BEMS needs more advanced optimization techniques to enhance buildings performance. The optimization methods used in the literature can be classified into two main groups: *Stochastic optimization* (SO) and *robust optimization* (RO). Works that study SO methods in the BEMS assume the possible future information of uncertainties are known or at least can be evaluated [105, 128–130]. The assumption of RO methods, on the other hand, is that uncertainties are coming from unpredictable sets and by considering a conservative approach, the BEMS applies the same control strategy for all possible cases [106, 131–133].

These studies are mainly focused on non-residential buildings, and the performance of BEMSs in residential buildings needs to be further investigated [108]. Our final approach for the residential BEMS is a stochastic gray-box MPC approach for DR programs, where we assume the RES power generation is stochastic. Therefore, we assume that predictions of RES power generation or its distribution are known beforehand [134–136]. This BEMS is then used in N-MGs where MGs are controlled distributively.

2.2 Smart Greenhouses

As the population grows, the need for more food resources is inevitable, which puts pressure on limited water resources and arable lands [137]. According to the Canadian minister of environment and climate change [138], agricultural activities are responsible for 8.1% of total greenhouse gas emissions in Canada. At the same pace, one-third of global greenhouse gas emissions are due to the food production system [139]. In addition, the COVID-19 pandemic demonstrates that the need for a sustainable, self-reliant food economy is essential. For these reasons, we need to move towards modernized smart agriculture. According to FAO (The Food and Agriculture Organization), climate-smart agriculture (CSA) " is an approach that helps to guide actions needed to transform and reorient agricultural systems to effectively support the development and ensure food security in a changing climate" [140]. Increasing agricultural performance, creating flexible agriculture in the face of climate change, and reducing greenhouse gas emissions are the three main goals of the CSA, of which *greenhouses* are its key components.

Greenhouses are structures with transparent walls and ceilings that can regulate the climatic conditions of their crops. Optimal control of greenhouse climatic conditions leads to an increase in agricultural products and their quality. Furthermore, greenhouse plants can yield at any time during the year. Despite their advantages, greenhouses' power consumption should be controlled; otherwise, they may cause adverse environmental impacts and additional demand peaks.

Each greenhouse usually has several main subsystems to control its climatic conditions; a thermal control system for regulating the indoor temperature, a lighting system for adjusting environmental illumination, a CO_2 generator for controlling CO_2 concentration level, and a ventilation and humidity control system. Crops usually have four growing stages, seed, sprout, seedling and adult plant. Depending on the stage, controlling some of the above parameters have higher priority. For example, controlling indoor temperature is more critical than CO_2 level during the seed stage. The low-priority subsystems have the chance to contribute to the DR program.

Like buildings, greenhouses can play an essential role in the grid by reducing their power consumption. In [141], authors develop a centralized irrigation system that predicts the crop water uptake depth based on soil moisture. The proposed system by rescheduling irrigation times can reduce the energy consumption of the greenhouse. Chen *et al.* in [142] address the non-linear control problem of greenhouse temperature, and propose a two-layer hierarchical control method. The upper layer calculates the optimal setpoints of the thermal subsystem

by minimizing net costs. At the same time, the lower level is responsible for reducing the tracking error between these setpoints and actual temperatures. To optimize the performance and energy consumption of greenhouses' artificial lightening system, Gianluca *et al.* in [143] first introduced a predictive control strategy and then tested their algorithm on an actual greenhouse case study. Their results show that the proposed algorithm can achieve a 19.4% cost saving. However, the main goal of these studies is to reduce energy consumption, and none of them investigate the effects of all greenhouse subsystems directly for the DR program.

Greenhouses can also be integrated with RES. Some studies investigate the performance of RES in greenhouse [144–148], however only a few studies consider their impact in the DR programs. Achour *et al.* in [149] propose an MPC-based approach to control all subsystems of a single greenhouse integrated with wind turbine and PV system. In [150], Ouammi *et al.* present a centralized control approach for a network of smart greenhouses with shared resources such as batteries, PV panels, wind turbines, and a water reservoir, aiming to reduce energy consumption. In a similar study, the author in [151] proposes a cooperative control framework for a network of greenhouses in which electricity can be exchanged in a peer-to-peer manner. However, to the best of the author's knowledge, no works in the literature investigate the distributed control of such networks, where autonomy is given to each greenhouse to control its local climate conditions and distributed resources.

2.3 Optimization Methods in Networks of Microgrids

As discussed in Chapter 1, a network of MGs or N-MGs is a group of interconnected MGs which collaborate to achieve a specific goal. If these MGs are buildings integrated DER, then the network is also known as a network of buildings. Microgrids are willing to participate in N-MGs because of their opportunities, such as blackout emergency backups and financial benefits. In the literature, three different optimization approaches exist for N-MGs: centralized, decentralized and distributed. Fig. 2.2 provides an overview of these approaches. As mentioned earlier, privacy, reliability, computational load and the complexity of the approach for finding the optimal solution are four factors that must be considered when comparing these approaches, Fig. 1.1. In the following, we briefly discuss these approaches and compare them based on these four factors.

2.3.1 Centralized

In centralized methods, all MGs send their information (e.g., thermal models, setpoints and loads) directly to a coordinator, Fig. 2.2a. Then the coordinator solves an optimization

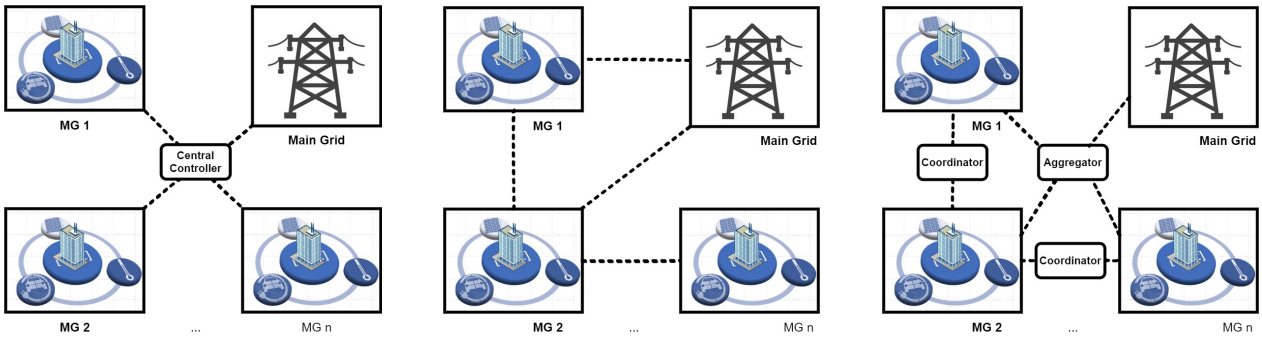

(a) Centralized (b) Decentralized (c) Distributed

Figure 2.2 Different optimization methods used in N-MGs

problem considering MGs, the main grid and the coordinator's constraints and objective functions (known as *general optimization problem*), and then sends back the solutions to MGs [150–154].

In the case of N-MGs, Arefifar *et al.* in [31] present a centralized energy management optimization strategy for a multi-microgrid system to minimize the operational cost. Authors in [32] propose a centralized approach for a network of MGs that aims to minimize the power exchanged between MGs while their local ESS operates around an optimal point. With the same objectives, authors in [155] propose a different centralized optimal power flows control approach based on Pontryagin's minimum principle. In [33], Gupta *et al.* propose a deep reinforcement learning approach for controlling a network of buildings to improve thermal comforts and reduce energy cost. Solving one optimization problem is the main advantage of these approaches. However, the coordinator (central controller) needs considerable computing power to solve this single problem, and this is impossible if there are many MGs in the network. In addition, MGs must share all their data with the coordinator, thus increasing the chances of information disclosure. Finally, the network reliability is as good as its coordinator reliability, and if the coordinator fails, the network can no longer work.

2.3.2 Decentralized

In the decentralized methods, each MG, on the other hand, solves its own optimization problem and makes decisions based on its benefits. The objectives of MGs can be aligned or even opposite. [34–36]. Unlike centralized methods, the decentralized methods can protect the privacy of MGs since they do not need to share their data. Because each MG operates independently of the other networks, decentralized networks are reliable in the case of an

MG failure, Fig. 2.2b. In addition, the computational load is crumbled at the level of each MG.

In N-MGs literature, Wang *et al.* in [156] propose a bi-level decentralized optimization method for networked microgrids, where the first level finds the optimal value for the negotiation penalty factor and the second level is responsible for the coordination of MGs by using this penalty factor. However, they do not consider using predictive methods (e.g., MPC) or participating in the demand response program. Authors in [37] model networks of MGs as teams in which the agents are cooperating to achieve specific goals. A decentralized control approach is then introduced to control the power flows in the network. Similar to previous work, they do not investigate the RES stochastic behaviours or network potential for participating in the DR program. In [157], a game theory approach is utilized to model each agent and its interactions with other MGs. In this study, each MG selfishly tries to maximize its profits, and hence the whole network can work even in the absence of communication. The proposed method uses Karush-Kuhn-Tucker (KKT) conditions to simplify the problem so that the network can participate in the DR program. In general, finding the optimal solution for the decentralized network that participates in the DR program with RES uncertainties is challenging and usually requires intensive computation.

2.3.3 Distributed

The third approach is the distributed methods, which can operate in both hierarchical and P2P networks. In this approach, like the centralized one, the whole network has a general objective function, which needs the cooperation of MGs to optimize; however, different from the centralized approach, each MG shares a limited version of its data with its neighbourhood MGs or the coordinator, Fig. 2.2c. Although the type of information shared depends on the network's distributed method, MGs mainly share their offers to buy or sell the power they need, not their private information. Hence, MGs' privacy is preserved. Unlike the decentralized approach, a third party coordinates the negotiation process between MGs in this approach, ensuring a globally optimal solution.

To this end, decomposition methods are needed to break down the general optimization problem and find the optimal solution. These methods first decompose the general optimization problem at the level of each MG and then find the optimal solution through an iterative process, also known as the negotiation process. This approach is a trade-off between decentralized and centralized ones, and it offers more reliability, more privacy and less computational load than centralized approaches. At the same time, it is more feasible to achieve an optimal global solution in this approach than the decentralized one in a limited

time.

ADMM and dual decomposition are the two most widely used decomposition methods in the N-MGs literature. In [158], authors develop a P2P distributed framework based on dual decomposition for energy trading in a network of islanded MGs. An event-based distributed MPC approach aiming to reduce the negotiation process is presented in [159]. Falsone *et al.* in [160] study the dual decomposition method in a cooperative multi-agent setting, where the agents negotiate with each other over shared resources through a time-varying network. Some other studies use dual decomposition dealing with optimal power flow problems in distributed N-MGs [161, 162].

However, dual methods can successfully decompose an optimization problem, but they suffer from poor convergence properties such as convergence rate and they require a convex objective function [163]. ADMM (alternating direction method of multipliers) is another decomposition method that has better convergence properties compared to dual methods [164, 165]. In the practical cases of N-MGs, the negotiation process between MGs to reach a consensus should be finished within a reasonable time. More specifically, in the networks using MPC methodology, this process should finish before the next time-step, usually in the order of minutes, e.g., 15 minutes. Therefore, the decomposition method used in the network must have a rapid convergence rate feature. ADMM, compared to dual decomposition, converges under much more relaxed conditions while it is more robust and has a fast convergence rate. For these reasons, ADMM methods are considered in this work. Consider the following optimization problem :

$$\begin{aligned} \min_{x,z} \quad & f(x) + g(z) \\ \text{s.t.:} \quad & Ax + Bz = c \end{aligned} \tag{2.1}$$

where x and z are two separate variables set, and f and g are convex functions. Then, using the Gauss-Seidel method, the optimal solution of the above equation can be found by using the following iteration process:

$$\begin{aligned} x^{k+1} &:= \underset{x}{\operatorname{argmin}} \ \Big(f(x) + (\rho/2)\|Ax + Bz^k - c + u^k\|_2^2\Big) \\ z^{k+1} &:= \underset{z}{\operatorname{argmin}} \ \Big(g(z) + (\rho/2)\|Ax^{k+1} + Bz - c + u^k\|_2^2\Big) \\ u^{k+1} &:= u^k + \Big(Ax^{k+1} + Bz^{k+1} - c\Big) \end{aligned} \tag{2.2}$$

where k is the iteration and $\|y\|_2$ represents norm 2 of vector y. We need to mention that the above algorithm in this form is sequential, but it can be adopted to our concept with the

right formulation.

Recently ADMM has received attention in the literature of N-MGs. Braun *et al.* in [44] present an ADMM-based MPC for a network of linear systems that are physically decoupled but coupled in the objective function. However, they assume a linear model for MGs and do not consider the uncertainties of RES. Liu *et al.* in [166] propose a distributed MPC method for frequency regulation in N-MGs with different modes of operation and system topology. A robust distributed energy management method aiming to minimize the total operational cost, which can handle energy exchange and price uncertainties, is developed for N-MGs in [167]. However, none of these studies consider the network in the DR program.

Similarly, Nikmehr in [168] proposes a model for the concept of interconnected energy hubs in N-MGs and controls this network distributively using a robust ADMM approach. Though robust approaches can manage the uncertainty of the network, they result in more conservative decision strategies, meaning in terms of the value of objective function obtained, the stochastic methods usually have better performance. Authors in [25] present a three-layer multi-agent architecture for P2P networked MGs, where frequency/voltage restoration and minimizing power loss are the network's main objectives. Authors in [169] introduce a two-level ADDM-based optimization control framework. At the upper level, the proposed algorithm minimizes the total power generation cost in a distributed manner, while each MG controls its generators at the lower level. Nevertheless, neither of the above studies considers the DR programs.

Some recent studies investigate the performance of distributed N-MGs for DR programs. Authors in [170] investigate the joint coordination of optimal power flow and demand response. Reducing operational costs and controlling the fluctuations of power load are its main objectives. A distributed parallel optimization method for a network of MGs is introduced in [171]. In order to manage energy, the proposed method is then used to decompose coupled constraints of MGs. Liu *et al.* in [172] develop a distributed EMS for a network of residential buildings where residential appliances such as HVAC and ESSs are controlled without participating in the DR program. Given the binary variables defined in their proposed model (e.g., HVAC systems on/off), the objective function is non-convex, so they use ADMM to decompose the optimization problem. In the absence of RES uncertainties, their proposed method can converge to the optimal solution in a reasonable number of iterations. In [173], Zhong *et al.* propose a distributed DR approach for a multi-energy residential network, which surfers incomplete information caused by nonideal communications in a randomly connected network. The proposed approach can be used to plan a day ahead, while it can help consumers buy energy inside the network and at a lower price than the main grid. Although

other works address the problem of DR programs in the distributed N-MGs [174–177], the RES stochastic behaviours in the distributed network of residential buildings have not been well studied in the literature.

This thesis studies the problem of distributive coordination of MGs in the hierarchical and P2P structures. Its novelties are divided into three parts. First, it proposes a real-time energy management system for residential buildings integrated with renewable energy sources and examines their potential to participate in the demand response program. Second, It proposes a novel stochastic ADMM-based decomposition method and proves its convergence mathematically. Finally, this proposed method is used to design an MPC-based framework for controlling the networks of MGs in a distributed manner. The proposed framework can consider the RES uncertainties and work in networks with different topologies, either P2P or hierarchical.

CHAPTER 3 SYNTHESIS OF WORK AS A WHOLE

Fig. 3.1 presents the synthesis of this Ph.D. project. In Chapter 4, the first objective is to model a residential building integrated with RES and EVs. An MPC algorithm is designed to control and manage energy and resources in the building while integrating the RC method for the thermal dynamics of the building. The building energy management system (BEMS) is able to achieve the minimization of the energy consumption in the building without violating occupants' comforts.

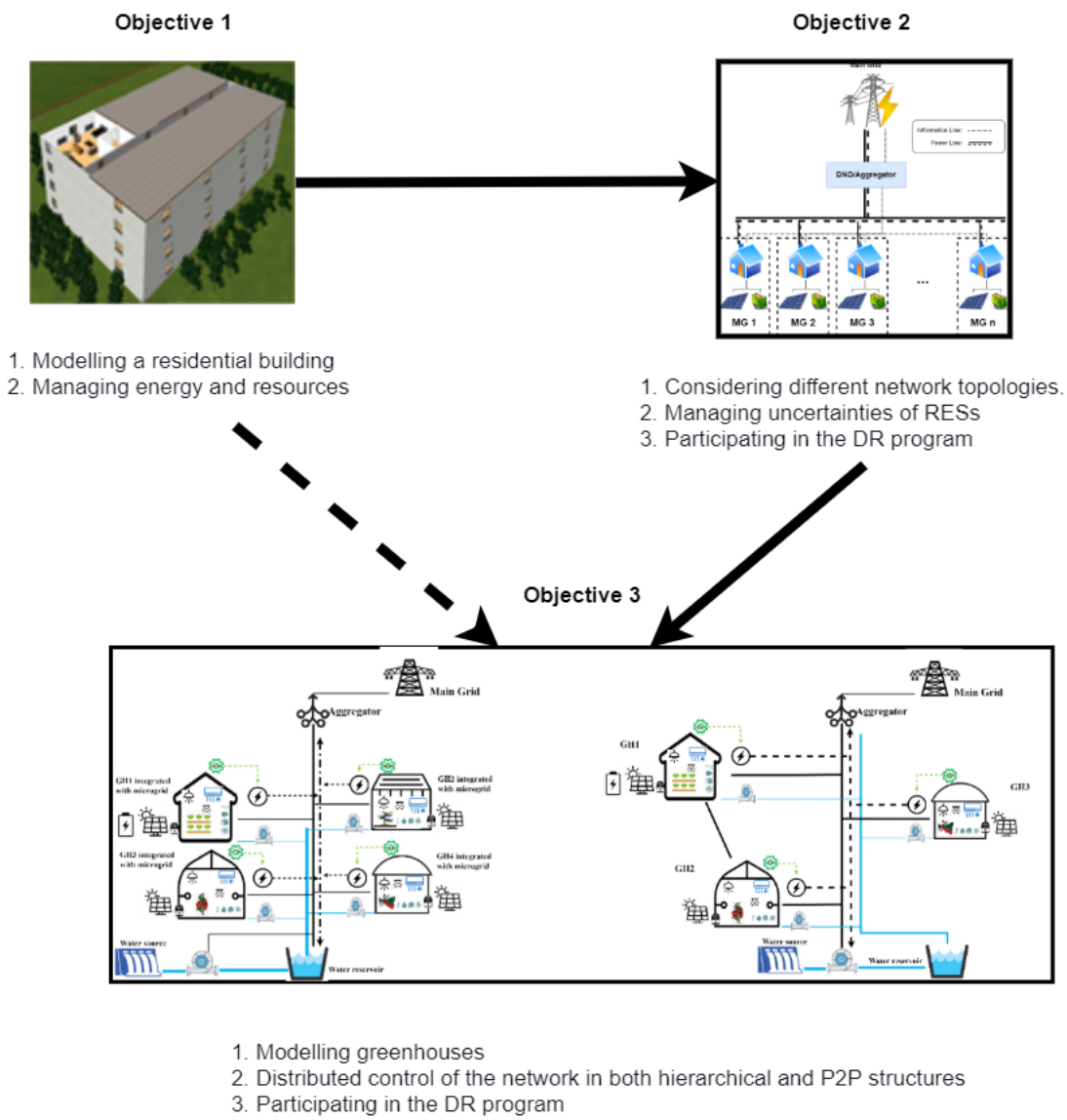

Figure 3.1 Synthesis of the Ph.D. project.

For objective 2, we use the BEMS presented in the previous step to design a stochastic distributed MPC-based framework for networks of BIMGs, where buildings participate in the DR program by controlling their thermal dynamic and battery. The proposed framework can handle the stochastic behaviour of RESs. Furthermore, objective 2 considers different network topologies such as hierarchical and P2P. Hence, it presents a distributed control approach for a network of MGs (mainly residential buildings integrated with RES), in which the uncertainty of RES is considered. The analysis is conducted in Chapter 5.

For objective 3, for the first time in the literature, we propose a distributed MPC-based control method for a network of greenhouses. Compared to the buildings, greenhouses have more subsystems than buildings that can participate in the DR program, such as thermal and CO_2 generation subsystems. In this method, greenhouses are connected to the main grid through an aggregator and participate in the demand response program by utilizing different load shaving and load shifting strategies. The ADMM decomposition method is then adopted to solve the optimization problem with the nonlinear objective function. Chapter 6 analyzes this method.

CHAPTER 4 ARTICLE 1: OPTIMAL REAL-TIME ENERGY MANAGEMENT IN APARTMENT BUILDING INTEGRATING MICROGRIDS WITH MULTIZONE HVAC CONTROL

Authors: Ehsan Rezaei, Hanane Dagdougui
IEEE Transactions on Industrial Informatics, Volume 16, 2020

Abstract: Today, distribution systems are presently transforming from a demand-driven to an active asset driven activity, portrayed by expanding measures of decentralized generation units and an increasing participation of end-users in demand response programs. The role of residential buildings will change to an active player in the power grid, either by integrating distributed energy resources onsite and even by an active orchestration of local demand. This paper presents an effective approach for the modeling and optimization of a multi-unit residential or multiple dwelling units building, integrating a local shared renewable power generation, energy storage system and electric vehicles. We aim to supports decision-making in the context of energy consumption for a multi-unit building through developing a model predictive control able to effectively control the heating, ventilation, and air conditioning (HVAC) system in each apartment of the building in order to reduce the electric bill of the building and improve the matching performance between the local generation and consumption. The problem is solved for a multi-unit apartments building in the Montreal area. The results show the efficiency of proposed method.

Keywords

Energy management, residential building RC model, microgrids, model predictive control, demand response, optimization.

4.1 Introduction

Buildings around the world consume approximately 40% of global energy consumption [178]. In particular, residential buildings are among the buildings sector responsible for high energy consumption. The International Energy Agency (IEA) recommends actions on: improvement of energy efficiency in buildings for the reduction of greenhouse gas (GHG) emissions and introducing the concept of zero-energy buildings (ZEB) [179]. Numerous measures have been taken into account to construct more energy efficient buildings, such as implementing new

effective insulation materials, increasing the utilisation ratio of sunlight, etc. [180]. However, there is also a need for practical solutions to reduce the GHG emissions from the residential and commercial sectors. In particular, the building-integrated microgrid (BIMG) is a prevalent green approach that allows each building to integrate local available Renewable Energy Resources (RES), distribute, and regulate the flow of electricity to consumers using the information and communication technologies, smart meters and building energy management system (BEMS). Particularly, integration of information and communication technologies, and in-building distributed energy resources in each building will allow building manager to communicate, control and coordinate various building devices in order to create the concept of a network of building integrated microgrid. The basic control objectives for a building energy management system are to maintain the high comfort level while reducing total energy consumption and peak of electricity demand. Demand response (DR) is an alternative solution that will allow consumers to reduce and regulate energy consumption and peak loads in response to programs related to electricity prices, or incentive payments [181–183]. With the growth interest of smart grids and the increased use of DR in the residential sector, the number of participating consumers is expected to increase significantly. From the grid perspective, individual residential consumers make only a limited contribution to the overall demand response strategy. However, aggregating consumers' loads become more representative to balance the needs of generation companies and end-users. The rapid increase in urban population and its patterns has led to increase construction of apartment dwellings or multi-unit residential buildings. In Canadian metropolitan areas, the share of dwellings that were apartments was highest in the census metropolitan areas of Montreal, Vancouver and Quebec. Apartment dwellings are attractive target for energy management and demand response, since they aggregate high energy density in one building.

In such type of buildings, HVAC systems are excellent resources for DR participation using temperature adjustments and control in different zones. Majority of works focused on residential buildings from the perspective of an aggregation of consumers or prosumers housing [184–186]. However less works have addressed apartment buildings with consumers or prosumers are connected to the same building, and where thermal multi-zone features also affect the consumption in each apartment.

In BIMG, the intermittent nature of RES, and especially that of solar energy, has led to much concern over the flexibility, stability and reliability of microgrids. Therefore, the BIMG needs to be flexible, and their BEMS needs to respond to real-time fluctuations and uncertainties in energy generation and demand. With the growing popularity of electrical vehicles (EVs) as high fuel economy with low greenhouse gas emissions, their utilization in residential buildings are expected to increase in the near future [187].

From an EV user viewpoint, EVs offer a number of benefits that make them an attractive solution for an increasing number of drivers such as high fuel economy, low operating cost, high performance, low emissions, etc. However, from the building manager viewpoint, the inclusion of EVs' charging load will increase the building loads when vehicles are being charged and can even lead to creating new load peaks in the building. As a result, it is important to implement smart coordination strategies to coordinate the fleet of EVs in the same residential building. The implementation of a BIMG makes it possible to use whenever is possible the additional mobile batteries of EVs as to create the vehicle-to-building (V2B) [188] to contribute to the DR programs by smoothing, dispatching loads and lowering building power consumption.

Consequently, the peak load in apartment building, which occur mostly in nighttime may be avoided using local distributed energy generators, control the temperature set point of each HVAC unit including inter-zonal effects among apartments, but also exploiting the available EVs in the building as a means to enable serving internal loads in the building [189]. In census metropolitan area, such as Montreal, in average, people make about 40 minutes commuting to work [190], and for the rest of the day their cars are mostly parked at parking lots or building garage [191]. While some research works have been recently introduced to investigate the charging and discharging scheduling problem of EVs [192], however, no major research has been reported to study the interaction between EVs and apartments building while considering EVs charging behavior, local residential electric loads, grid interaction and PV systems coupled with stationary storage system. In [193], authors investigated the impact of residential buildings EV charging strategies on grid and buildings themselves. They concluded that for decreasing EV grid impacts, day-time charging is the best solution. In [194], Cristana *et al.* proposed a real-time hardware implementation architecture that aims to control inside temperature by using of electric water heater and Resistance-Capacitance (RC) model of a single three bedrooms [195]. In [196], a new algorithm for allocation and pricing of distributed energy resources (DERs) in apartment houses is proposed to understand the effect of sharing distributed generation, however, no demand response is implemented.

Majority of works focused on residential buildings from the perspective of an aggregations of consumers or prosumers housing [184–186]. In [197], authors presented a nonlinear optimal algorithm to manage energy in smart buildings of a microgrid. This algorithm aims to keep comfort parameters of each building at a suitable range while reducing the operation cost. However, the work did not consider EVs and their impacts. A daily charging and discharging management framework for EVs is investigated in [198]. Also, in [199] a real-time coordination energy management is introduced for an energy-hub. In both works, MPC controller could achieve a better results against uncertainties.

In this paper, we propose an optimization method for the BEMS in an apartment building. The method makes decisions on the operations of local storage system, EVs and controllable HVAC units to take advantages of the available local shared renewable power generation and to minimize the power consumption in the building. So far, a few papers focused on the structure of building to reduce consumption power. In this paper, however, a Grey-box building model is implemented to reduce power consumption while satisfying comfort parameters of each zone in the building. More specifically:

1) We proposed a centralized building energy management system (BEMS) that better control the comfort parameters in each apartment, while considering thermal exchange effect between zones.

2) We use model predictive control to not only control comfort parameters at a satisfied level, but also to prevent power consumption of building excess power subscribed level of building.

3) We study impacts of daytime EVs coordinated charging as a DR tool to response to renewable energy such as solar panels, load and price variations.

The rest of this paper is organized as follows. In Section 4.2, the proposed components of the residential building integrating microgrid are formulated including photovoltaics, energy storage system, electric vehicles and the residential thermal model. In section 4.3, we will define the control method and finally, in section 4.4, the proposed controller has been simulated.

4.2 System Models

4.2.1 Energy management structure

Fig. 4.1 shows the configuration of the proposed microgrid in the residential building. The main distributed energy resources comprise PV array and an energy storage system (ESS) that has the flexibility to be charged by the main grid or power generated from PV pannels. The considered microgrid is connected to parking lot and integrated to an apartment building.

The apartment building may buy/sell electricity from/to the main grid. The BEMS, as shown in Fig. 4.1, is designed to gather and analyze data from various smart meters related to PV generation, energy storage systems, EVs, non-flexible load and HVAC aggregators. In addition, it communicates the optimal control signals to EVs and HVACs through appropriate aggregators. In this paper, we propose a curtailable DR, where customers agree to participate in DR programs defined by the BEMS in response to load dispatching. We consider a scenario

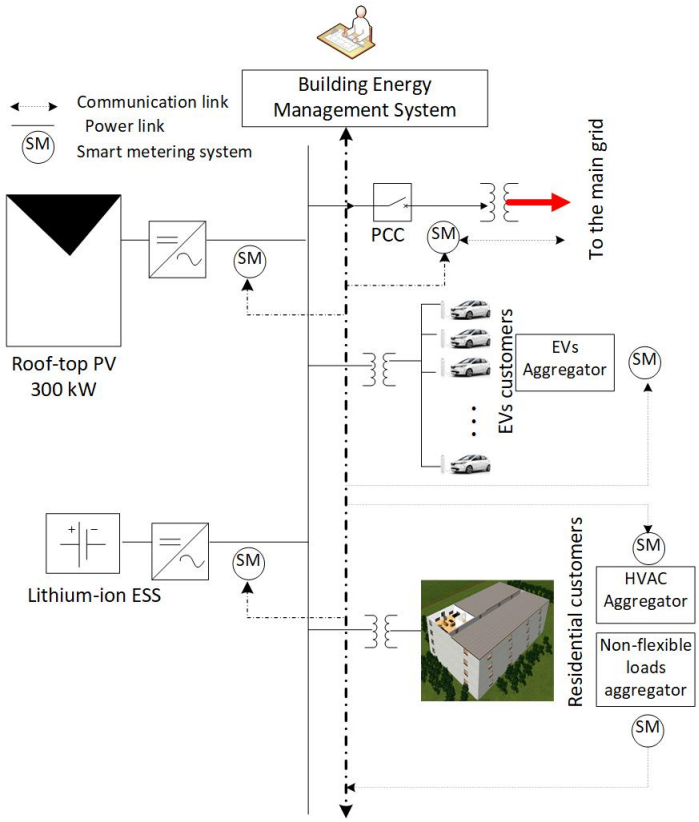

Figure 4.1 Architecture of a building integrated with microgrid.

where a PV generation unit is shared by several apartments. Here it is worth to mention that, two aggregators are acting as intermediate agents to collect and send data to BEMS. The aggregators can also enter into contracts with customers to manage their HVAC units and EVs power consumption in order to participate in the energy market. In all regulation services, the main advantage of having aggregators is to estimate the reserve capacity of population of loads, i.e. the available power that controllable loads could offer in the ancillary service market. This aspect is out of the scope of this paper.

In the following section, elements of this system and their constraints will be modeled. Since we are interested to real-time model predictive control (MPC), the extension form of each element from time step n to $n + n_c$ or $n + n_p$ will be needed. These extension form , later, can be used to solve the real-time optimization problem of MPC.

4.2.2 Model of PV

The output power of the photovoltaic array at the maximum power point (MPP) can be modelled by a linear power source according to the irradiance level. The MPP tracking (MPPT) role is to maximize the power output:

$$P_{pv} = [P_{PV,Rated} \times \frac{G}{1000} \times \eta_{MPPT}] \tag{4.1}$$

where $P_{PV}, P_{PV,Rated}$ are respectively the output power at the MPP and the rated power at the G_T=1000 W/m^2, G_T and η_{MPPT} are respectively the irradiance level and the efficiency of the PV's dc/dc converter and the MPPT system.

4.2.3 Energy storage system model

The BIMG is equipped with an energy storage system (ESS) which provides additional flexibility. Lithium-ion batteries are considered since they provide several advantages and benefits such as no memory effect, and the highest energy density among other types of batteries [200]. It is supposed that the discharged power can be used by apartments or/and for charging the EVs. The battery can be charged by the excess of the PV power generation or/and by the main grid depending on the selected pricing mechanism. The evolution over time of energy stored is supposed to be described by the following state equation:

$$SOC_b[k+1] = SOC_b[k] + (\eta_{b,ch} P_{b,ch}[k] - \frac{P_{b,dch}[k]}{\eta_{b,dch}})\Delta T] \tag{4.2}$$

where $SOC_b[k]$ [kWh] is the state of the energy stored in the ESS, $P_{b,ch}$ (t) and $P_{b,dch}$ are respectively the charged and discharged powers and $\eta_{b,ch}$ and $\eta_{b,dch}$ are respectively the charging and discharging efficiencies.

The power charged/discharged to/from the ESS is bounded by a certain maximum charging/discharging power limits:

$$\begin{aligned} &0 \leq P_{b,ch}[k] \leq P_{b,ch,max} \\ &0 \leq P_{b,dch}[k] \leq P_{b,dch,max} \\ &P_{b,ch}[k] \times P_{b,dch}[k] = 0 \end{aligned} \tag{4.3}$$

Constraint (4.3) is used to avoid charging and discharging the energy storage system at the same time. Furthermore, $SOC_b[k]$ cannot exceed its limitations, which means the battery

state of charge, cannot be more than $SOC_{b,max}$, or less than $SOC_{b,min}$.

$$SOC_{b,min} \leq SOC_b[k] \leq SOC_{b,max} \tag{4.4}$$

Since the $SOC_b[k+n]$ depends on $SOC_b[k]$ and all of $P_{b,ch}[k+i]$ and $P_{b,dch}[k+i]$ for $i \in \{0, 1, \ldots, n-1\}$ we can rewrite $SOC_b[k+n]$ as follows:

$$SOC_b[k+n] = SOC_b[k] + \sum_{i=k}^{k+n-1} (\eta_{b,ch} P_{b,ch}[i] - \frac{P_{b,dch}[i]}{\eta_{b,dch}})\Delta T \tag{4.5}$$

Using model predictive control for a prediction horizon of n_p:

$$\underbrace{\begin{bmatrix} SOC_b[k] \\ SOC_b[k+1] \\ SOC_b[k+2] \\ \vdots \\ SOC_b[k+n_p+1] \end{bmatrix}}_{\mathbf{SOC}_{b,n_p+1}[k]} = \underbrace{\begin{bmatrix} 1 \\ 1 \\ 1 \\ \vdots \\ 1 \end{bmatrix}}_{\mathbf{I}_{(n_p+1)\times 1}} SOC_b[k] +$$

$$+ \underbrace{\begin{bmatrix} 0 & 0 & \cdots & 0 \\ \eta_{b,ch} & 0 & \cdots & 0 \\ \eta_{b,ch} & \eta_{b,ch} & \cdots & 0 \\ \vdots & \vdots & \ddots & \vdots \\ \eta_{b,ch} & \eta_{b,ch} & \cdots & \eta_{b,ch} \end{bmatrix}}_{\mathbf{\Lambda}^{b,ch}_{n_p+1}[k]} \underbrace{\begin{bmatrix} P_{b,ch}[k] \\ P_{b,ch}[k+1] \\ \vdots \\ P_{b,ch}[k+n_p] \end{bmatrix}}_{\mathbf{P}_{b,ch,n_p+1}[k]} - \mathbf{\Lambda}^{b,dch}_{n_p+1}[k] \mathbf{P}_{b,dch,n_p+1}[k] \Rightarrow$$

$$\mathbf{SOC}_{b,n_p+1}[k] = \mathbf{I}_{(n_p+1)\times 1} SOC_b k] + \mathbf{\Lambda}^{b,ch}_{n_p+1}[k] \mathbf{P}_{b,ch,n_p+1}[k] - \mathbf{\Lambda}^{b,dch}_{n_p+1}[k] \mathbf{P}_{b,dch,n_p+1}[k] \tag{4.6}$$

where k can be any time step. Constraints (4.3) and (4.4) can be rewritten as:

$$SOC_{b,min} \times I_{(n_p+2)\times 1} \leq \mathbf{SOC}_{b,n_p+1}[k] \leq SOC_{b,max} \times I_{(n_p+2)\times 1} \tag{4.7}$$

and

$$\begin{aligned}\mathbf{0}_{(n_p+1)\times 1} \leq \mathbf{P}_{b,ch,n_p+1}[k] \leq P_{b,ch,max}(\gamma_{n_p+1} * \mathbf{I}_{(n_p+1)\times 1})\\ \mathbf{0}_{(n_p+1)\times 1} \leq \mathbf{P}_{b,dch,n_p+1}[k] \leq P_{b,dch,max}((1-\gamma_{n_p+1}) * \mathbf{I}_{(n_p+1)\times 1})\end{aligned} \tag{4.8}$$

where $*$ is element-by-element multiplication and $\gamma_{n_p+1} = \begin{bmatrix}\gamma_1 & \gamma_2 & \dots & \gamma_{n_p+1}\end{bmatrix}^T$ is a vector of slacks variables used to avoid problem of charging and discharging at the same time.

4.2.4 EVs Model

The EV can operate under two main modes, in the charging mode, it can be considered as a load, while in the discharging mode, the EV can be regarded as a source of power. This flexibility can participate in enhancing the operation and the power management in the building, especially, during the presence of EVs in the parking garage. Let consider that each EV $j \in N_{ev}$ is equipped with an energy control which enables the vehicle to communicate with the aggregator through a smart metering infrastructure once connected to the charging infrastructure. The EV can transmit data to the EVs aggregator such as battery capacity, the desired charge and the departure time. The state of charge of the *j-th* EV can be expressed as follow:

$$SOC^j_{ev}[k+1] = \beta^j[k](SOC^j_{ev}[k] + (\eta^j_{b,ch}P^j_{b,ch}[k] - \frac{P^j_{b,disch}[k]}{\eta^j_{b,disch}})\Delta T) + \gamma^j[k] \tag{4.9}$$

In this equation, ΔT, $\eta^j_{b,ch}$ and $\eta^j_{b,disch}$ are respectively the sampling time, charging and discharging efficiencies. $\beta^j[k]$ and $\gamma^j[k]$ can be defined for vehicle j as follow:

$$\beta^j[k] = \begin{cases} 1 & k^j_A \leq k \leq k^j_D \\ 0 & otherwise \end{cases}, \gamma^j[k] = \begin{cases} SOC^j_A & T = k^j_A \\ 0 & otherwise \end{cases} \tag{4.10}$$

In this equation, k^j_A and k^j_D are the arrival and the departure time of vehicle j. At the arrival time, vehicle j has the amount of SOC^j_A energy in its battery.

EVs have similar constraints to the ESS, however, they are only valid during the the availability of EVs in the parking garage. Thus, constraints (4.3) and (4.4) can be modified as

follows:

$$
\begin{aligned}
&\beta^j[k]SOC_{ev,min} \leq \beta^j[k]SOC^j_{ev}[k] \leq \beta^j[k]SOC_{ev,max} \\
&0 \leq \beta^j[k]P^j_{ev,ch}[k] \leq \beta^j[k]P^j_{ev,ch,max} \\
&0 \leq \beta^j[k]P^j_{ev,dch}[k] \leq \beta^j[k]P^j_{ev,dch,max} \\
&\beta^j[k]P^j_{ev,ch}[k]P^j_{ev,dch}[k] = 0
\end{aligned} \tag{4.11}
$$

$SOC^j_{ev}[k+n_p+1]$ can be expressed as follow:

$$
\begin{aligned}
SOC^j_{ev}[k+n_p+1] &= (\prod_{i=0}^{n_p} \beta[k+i])SOC^j_{ev}[k] \\
&+ \Bigg[\underbrace{(\prod_{i=0}^{n_p} \beta[k+i])}_{\beta(k,0,n_p)} \delta_c[k] \quad \underbrace{(\prod_{i=1}^{n_p} \beta[k+i])}_{\beta(k,1,n_p)} \delta_c[k+1] \quad \underbrace{\prod_{i=n_p}^{n_p} \beta(k+i)}_{\beta(k,n_p,n_p)} \delta_c[k+n_p] \Bigg] \times \underbrace{\begin{bmatrix} P_c[k] \\ P_c[k+1] \\ \vdots \\ P_c[k+n_p] \end{bmatrix}}_{\mathbf{P}^j_{ev,ch,n_p+1}[k]} \\
&- \begin{bmatrix} \beta(k,0,n_p)\delta_d[k] & \beta(k,1,n_p)\delta_d[k+1] & \beta(k,n_p,n_p)\delta_d[k+n_p] \end{bmatrix} \times \underbrace{\begin{bmatrix} P_d[k] \\ P_d[k+1] \\ \vdots \\ P_d[k+n_p] \end{bmatrix}}_{\mathbf{P}^j_{ev,dch,n_p+1}[k]} \\
&+ \begin{bmatrix} \beta(k,1,n_p) & \beta(k,2,n_p) & \cdots & 1 \end{bmatrix} \underbrace{\begin{bmatrix} \gamma[k] \\ \gamma[k+1] \\ \vdots \\ \gamma[k+n_p] \end{bmatrix}}_{\mathbf{\Gamma}_{n_p+1}[k]} \Rightarrow
\end{aligned}
$$

$$
\begin{aligned}
SOC^j_{ev}[k+n_p+1] &= \beta(k,0,n_p)SOC^j_{ev}[k] \\
&+ \begin{bmatrix}\beta(k,0,n_p) & \beta(k,1,n_p) & \cdots & \beta(k,n_p,n_p)\end{bmatrix} \times \underbrace{\begin{bmatrix}\delta_c[k] & 0 & \cdots & 0 \\ 0 & \delta_c[k+1] & \cdots & 0 \\ \vdots & \vdots & \ddots & \vdots \\ 0 & 0 & \cdots & \delta_c[k+n_p]\end{bmatrix}}_{\mathbf{\Delta}_{c,n_p+1}[k]} \mathbf{P}^j_{ev,ch,n_p+1}[k] \\
&- \begin{bmatrix}\beta(k,0,n_p) & \beta(k,1,n_p) & \cdots & \beta(k,n_p,n_p)\end{bmatrix} \times \mathbf{\Delta}_{d,n_p+1}[k]\mathbf{P}^j_{ev,dch,n_p+1}[k] \\
&+ \begin{bmatrix}\beta(k,0,n_p) & \beta(k,1,n_p) & \cdots & \beta(k,n_p,n_p)\end{bmatrix} \mathbf{\Gamma}_{n_p+1}[k]
\end{aligned}
\tag{4.12}
$$

and finally the model predictive formalization can be written as follow:

$$
\begin{aligned}
\mathbf{SOC}^j_{ev,n_p+1}[k] = \mathbf{\Phi}_{n_p+1}[k]SOC^j[k] &- \mathbf{\Lambda}_{n_p+1}[k]\mathbf{\Delta}_{d,n_p+1}[k]\mathbf{P}^j_{ev,dch,n_p+1}[k] \\
&+ \mathbf{\Lambda}_{n_p+1}[k]\mathbf{\Delta}_{c,n_p+1}[k]\mathbf{P}^j_{ev,ch,n_p+1}[k] + \mathbf{\Lambda}_{0,n_p+1}[k]\mathbf{\Gamma}_{n_p+1}[k]
\end{aligned}
\tag{4.13}
$$

where:

$$
\mathbf{\Phi}_{n_p+1}[k] = \begin{bmatrix}1 \\ \beta(k,0,0) \\ \beta(k,0,1) \\ \vdots \\ \beta(k,0,n_p)\end{bmatrix} \qquad \mathbf{\Lambda}_{0,n_p+1}[k] = \begin{bmatrix}0 & 0 & \cdots & 0 \\ 1 & 0 & \cdots & 0 \\ \beta(k,1,1) & 1 & \cdots & 0 \\ \vdots & \vdots & \ddots & \vdots \\ \beta(k,1,n_p) & \beta(k,2,n_p) & \cdots & 1\end{bmatrix}
$$

$$
\mathbf{\Lambda}_{n_p+1}[k] = \begin{bmatrix}0 & 0 & \cdots & 0 \\ \beta(k,0,0) & 0 & \cdots & 0 \\ \beta(k,0,1) & \beta(k,1,1) & \cdots & 0 \\ \vdots & \vdots & \ddots & \vdots \\ \beta(k,0,n_p) & \beta(k,1,n_p) & \cdots & \beta(k,n_p,n_p)\end{bmatrix}
$$

Therefore, constraint (4.11) will be changed to:

$$
SOC_{ev,min}\mathbf{\Xi}^j_{n_p}[k]\mathbf{I}_{(n_p+1)\times 1} \leq \mathbf{\Xi}^j_{n_p}[k]\mathbf{SOC}_{n_p}[k] \leq SOC_{ev,min}\mathbf{\Xi}^j_{n_p}[k]\mathbf{I}_{(n_p+1)\times 1} \tag{4.14}
$$

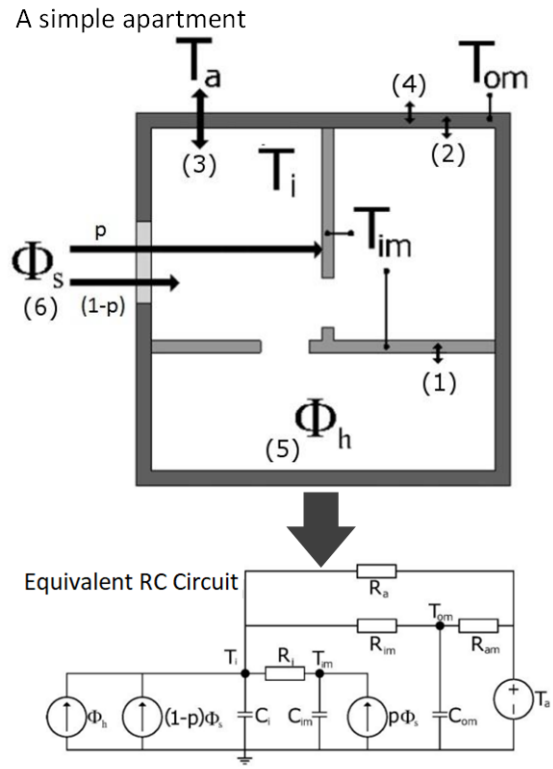

Figure 4.2 An apartment and its equivalent RC circuit (These pictures are adopted from [201]).

where:

$$\Xi^{j}_{n_p}[k] = \begin{bmatrix} \beta[k] & 0 & \cdots & 0 \\ 0 & \beta[k+1] & \cdots & 0 \\ \vdots & \vdots & \ddots & \vdots \\ 0 & 0 & \cdots & \beta[k+n_p] \end{bmatrix} \tag{4.15}$$

Also, there are some other constraints for EVs that must be satisfied:

$$\begin{aligned} \mathbf{0} \leq \mathbf{P}^{j}_{b,ch,n_p+1}[k] \leq P^{j}_{b,ch,max}\Xi^{j}_{n_p}[k](\gamma_{n_p+1} * \mathbf{I}) \\ \mathbf{0} \leq \mathbf{P}^{j}_{b,dch,n_p+1}[k] \leq P^{j}_{b,dch,max}\Xi^{j}_{n_p}[k]((1-\gamma_{n_p+1}) * \mathbf{I}) \end{aligned} \tag{4.16}$$

where in (4.16) matrices $\mathbf{I}$ and $\mathbf{0}$ have appropriate dimensions.

4.2.5 Residential Thermal Model

One of the most significant energy consumption in residential buildings is related to satisfy the thermal comfort of the occupants. From this perspective, the proposed algorithm aims to keep this parameter in a predefined comfort range which means that each apartment requires a specific range of comfort $[T_{min}, T_{max}]$. For achieving this goal, we developed RC-model of an apartment building to control the temperature in each apartment. The RC thermal model is a Grey-Box model that is commonly used to define the thermal dynamics of a building zone. The model uses physics-based models as the structure of the model whose parameters can be estimated using the construction data or estimated from the measured data using a parameter identification technique. Nonlinear least squares, simplex search, and genetic algorithm (GA) are among the widely used identification techniques [202,203]. In this paper, due to the unavailability of data, the parameters of the RC-model have been estimated using EnergyPlus residential building simulation program. More details about the RC-model can be found in [204].

In Fig. 4.2, an example of studio apartment and its equivalent RC model are shown([201]). In this figure, T_i, T_a, T_{om} and T_{im} are interior, ambient, home envelop walls, and inside walls temperatures respectively. ϕ_s is sun radiation on apartment which is divided in two parts: 1) $(1-P)$ percent of sun radiation absorbed by inside air and 2) P percent of sun radiation absorbed by home elements such as inside and outside walls, equipment *etc.* $\phi_h^{z_i}$ is the power that HVAC consumes in apartment z_i to warm it up.

In these study, without loss of generality, we used the map of a given floor which is shown in

Fig. 4.3. For this floor we have :

$$\begin{cases} x[k+1] = A_c x[k] + B_c \underbrace{\begin{bmatrix} \phi_h^{z_1}[k] \\ \phi_h^{z_2}[k] \\ \dots \\ \phi_h^{z_n}[k] \end{bmatrix}}_{u[k]} + E_c \underbrace{\begin{bmatrix} \phi_s[k] \\ T_a[k] \end{bmatrix}}_{v[k]} \\ \underbrace{\begin{bmatrix} T_i^{z_1}[k] \\ T_{im}^{z_1}[k] \\ T_{om}^{z_1}[k] \\ \dots \\ T_i^{z_n}[k] \\ T_{im}^{z_n}[k] \\ T_{om}^{z_n}[k] \end{bmatrix}}_{y[k]} = C_c x[k] + D_c u[k] + F_c v[k] \end{cases}$$

$$\Rightarrow \begin{cases} x[k+1] = A_c x[k] + B_c u[k] + E_c v[k] \\ \\ y[k] = C_c x[k] + D_c u[k] + F_c v[k] \end{cases} \tag{4.17}$$

where (A_c, C_c), (B_c, D_c) and (E_C, F_c) are specific constants matrices related to states, inputs and disturbances values in each apartment. x, u, v and y are states, control inputs, disturbance inputs and zone temperature respectively.

To obtain comfort temperature in each apartment, there are maximum and minimum constraints for inside temperature. However, these limitations depend on different parameters such as walls, floors or ceil of building and even can be changed in presence of occupants. In table 4.1, the comfort standard temperature of a room is shown. Furthermore, power used by HVAC units in each apartment cannot be greater than some specific amount. To conclude, for such building the following constraints can be used:

$$\begin{aligned} &T_{min}^{z_j}[k] \leq T_i^{z_j}[k] \leq T_{max}^{z_j}[k] \\ &0 \leq \phi_h^{z_j}[k] \leq \phi_{max}^{z_j} \end{aligned} \tag{4.18}$$

where $T_{min}^{z_j}$ and $T_{max}^{z_j}$ are minimum and maximum acceptable temperatures in each apartment.

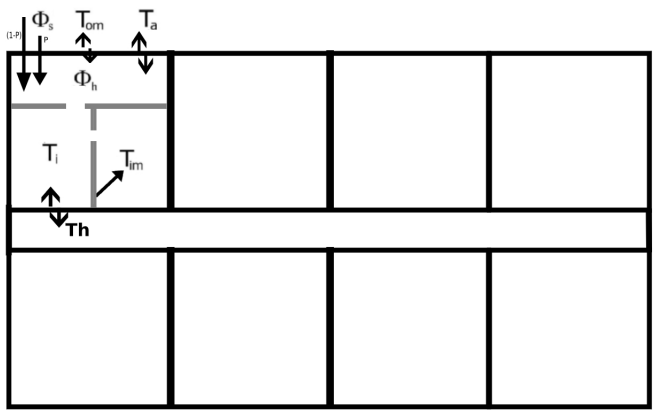

Figure 4.3 Floor map of 8 of studio apartments

Also, $\phi_{max}^{z_j}$ is the maximum power available by heater of each apartment.

$$\underbrace{\begin{bmatrix} x[k] \\ x[k+1] \\ x[k+2] \\ ... \\ x[k+n_p] \end{bmatrix}}_{\mathbf{X}_{n_p}[k]} = \underbrace{\begin{bmatrix} I \\ A \\ A^2 \\ ... \\ A^{n_p} \end{bmatrix}}_{\mathbf{A}_{n_p}} x^{z_j}[k] + \underbrace{\begin{bmatrix} 0 & 0 & ... & 0 & 0 & 0 \\ B & 0 & ... & 0 & 0 & 0 \\ AB & B & ... & 0 & 0 & 0 \\ \vdots & \vdots & \ddots & \vdots & \vdots & \vdots \\ A^{n_p-1}B & A^{n_p-2}B & ... & AB & B & 0 \end{bmatrix}}_{\mathbf{B}_{n_p}} \mathbf{U}_{n_p}^{z_j}[k]$$

$$+ \underbrace{\begin{bmatrix} 0 & 0 & ... & 0 & 0 & 0 \\ E & 0 & ... & 0 & 0 & 0 \\ AE & E & ... & 0 & 0 & 0 \\ \vdots & \vdots & \ddots & \vdots & \vdots & \vdots \\ A^{n_p-1}E & A^{n_p-2}E & ... & AE & E & 0 \end{bmatrix}}_{\mathbf{E}_{n_p}} \mathbf{V}_{n_p}^{z_j}[k]$$

$$\Rightarrow \mathbf{X}_{n_p}^{z_j}[k] = \mathbf{A}_{n_p}^{z_j} x^{z_j}[k] + \mathbf{B}_{n_p}^{z_j} \mathbf{U}_{n_p}^{z_j}[k] + \mathbf{E}_{n_p}^{z_j} \mathbf{V}_{n_p}^{z_j}[k] \tag{4.19}$$

and for outputs:

$$\underbrace{\begin{bmatrix} y[k] \\ y[k+1] \\ \vdots \\ y[k+n_p] \end{bmatrix}}_{\mathbf{Y}_{n_p}^{z_j}[k]} = \mathbf{C}\mathbf{X}_{n_p}^{z_j}[k] + \mathbf{D}\mathbf{U}_{n_p}^{z_j}[k] + \mathbf{F}\mathbf{V}_{n_p}^{z_j}[k]$$

$$\mathbf{C} = \begin{bmatrix} C & \dots & C \end{bmatrix} \quad \mathbf{D} = \begin{bmatrix} D & \dots & D \end{bmatrix} \quad \mathbf{F} = \begin{bmatrix} F & \dots & F \end{bmatrix} \tag{4.20}$$

Now by combining equations (4.19) and (4.20), final form can be obtained:

$$(4.19)\ \&\ (4.20) \Rightarrow \mathbf{Y}_{n_p}^{z_j}[k] = \mathbf{C}\mathbf{A}_{n_p}x[k] + (\mathbf{C}\mathbf{B}_{n_p} + \mathbf{D})\mathbf{U}_{n_p}[k] + (\mathbf{C}\mathbf{E}_{n_p} + \mathbf{F})\mathbf{V}_{n_p}[k] \tag{4.21}$$

and constraint (4.18) changed to:

$$\underbrace{\begin{bmatrix} y_{min}^{z_j}[k] \\ y_{min}^{z_j}[k+1] \\ \vdots \\ y_{min}^{z_j}[k+n_p] \end{bmatrix}}_{\mathbf{Y}_{min}^{z_j}[k]} \leq \mathbf{Y}_{n_p}^{z_j}[k] \leq \underbrace{\begin{bmatrix} y_{max}[k] \\ y_{max}[k+1] \\ \vdots \\ y_{max}[k+n_p] \end{bmatrix}}_{\mathbf{Y}_{max}^{z_j}[k]}$$

$$\begin{bmatrix} 0 \\ 0 \\ \vdots \\ 0 \end{bmatrix} \leq \mathbf{U}_{n_p}^{z_j}[k] \leq \underbrace{\begin{bmatrix} \phi_{max}^{z_j}[k] \\ \phi_{max}^{z_j}[k+1] \\ \vdots \\ \phi_{max}^{z_j}[k+n_p] \end{bmatrix}}_{\mathbf{\Phi}_{max}^{z_j}[k]} \tag{4.22}$$

4.2.6 Demand-Supply Balance Constraint

The power balance constraint can be expressed as follow:

$$P_{buy,G}[k] - P_{sell,G}[k] + P_{PV}[k] - \sum_{i=1}^{N_{apt}} P_{apt}^{i}[k] + \sum_{j=1}^{N_{EVs}} \beta^{j}[k](P_{disch}^{j}[k] - P_{ch}^{j}[k]) + (P_{b,disch} - P_{b,ch}) = 0 \quad \forall k \tag{4.23}$$

In this equation, $P_{buy,G}$ and $P_{sell,G}$ are respectively the amount of power ought from grid and sold to the grid.

4.3 Control Algorithm

In order to control the building, we choose model predictive control because of its capability to consider the future information. The main purpose of the proposed algorithm is to reduce operation costs. Here, we define the objective function as the cost of power buying from the grid minus the cost of poweror selling to grid over a given horizon. Thus, the final form of optimization problem becomes:

$$\begin{aligned}
&\min_{\Theta} \sum_{k=n}^{n+n_p \text{ or } n+n_c} C_{buy}[k]P_{buy,G}[k] - C_{sell}[k]P_{sell,G}[k] \\
&s.t: (4.8) \ \& \ (4.7) \\
&\qquad (4.14) \ \& \ (4.16) \\
&\qquad (4.21) \ \& \ (4.22) \ \& \ (4.23)
\end{aligned} \tag{4.24}$$

where $\Theta = \{u^{z_i}, P_{buy,G}, P_{sell,G}, P^j_{disch}, P^j_{ch}, P_{b,disch}, P_{b,ch} \ |\forall j, i \ \& \ \forall k \in \{n, n+1, ..., n+n_p\}\}$ are the decisional variables which must be found by solving the optimization problem (4.24). In this equation, C_{buy} and C_{sell} are actually refers to purchasing cost and selling cost respectively. This optimization function will be solved at each time step n for times n to $n+n_p$ or $n+n_c$, only the first time step element of Θ will be applied to the system at each time step.

4.4 Simulations

In this section, we illustrate an application of the proposed approach and compare it with the classical PID controller, which is widely used in buildings. We considered a residential building with four floors, each having 8 apartments. The buiding is connected to a parking lot having 20 electric vehicles. The building is connected to the main grid, where a Time-of-use (TOU) pricing is included as a pricing mechanism for power exchange with the grid [205]. For temperature setpoints variations, constraints shown in table 4.1 are considered.

The RC-model of a building including 32 apartments is implemented in *Simulink* to obtain the nonlinear model and then *Linear Analysis Toolbox of MATLAB* was used to obtain the linear state space model. The MPC problem was formulated in *MATLAB* and we used *CPLEX* package for MATLAB to solve the MPC problem at each time step.

The properties of EVs and ESS can be illustrated in table **??**. Besides, we assume that, arrival time, departure time and SOC of each EV at the arrival time can be estimated.

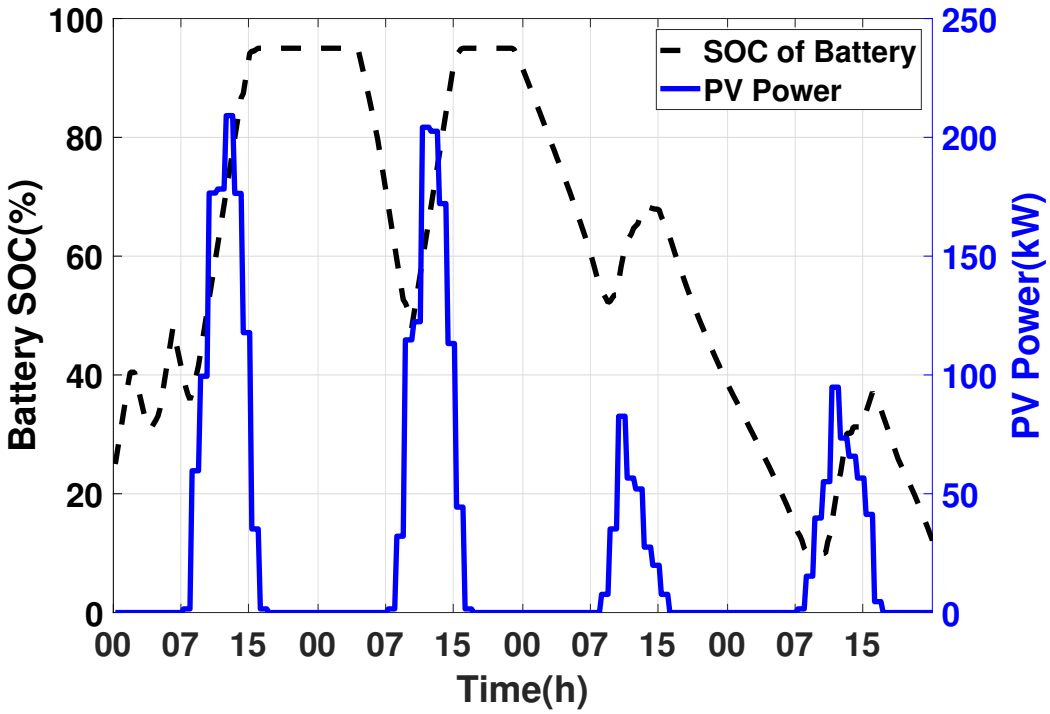

Figure 4.4 PV Power and Battery SOC.

Table 4.1 Standard temperatures to feel comfortable in a room [79].

Parameter	Unit	Occupied
Room temperature	$°C$	$19 \leq T^a_{z_i} \leq 26$
Ceiling surface temp.	$°C$	$15 \leq T^c_{z_i} \leq 27$

The price of C_{buy} is assumed to follow Ontario selling price which depends on time of use (TOU). On the other hand, since power balance (4.23) is used to avoid infeasibility, we decide to choose C_{sell} equals to 2¢ per kWh less than C_{buy} at each time step k. In addition, we assume that the maximum power that can be bought from the grid cannot exceed a certain amount (170kW).

Our sampling time is 15 minute with prediction horizon of $n_p = 4\ days = 4 \times 24 \times 4 = 384\ quarters$ and control horizon of $n_c = 2\ hours = 8\ quarters$. Outside temperature is between [−10°c 1°c] and the rated power generated by the roof-top PV pannels is equal to 300 kW (see Fig. 4.4).

It is assumed that apartments number 4 and 7 require temperature between [20°c 25°c] while

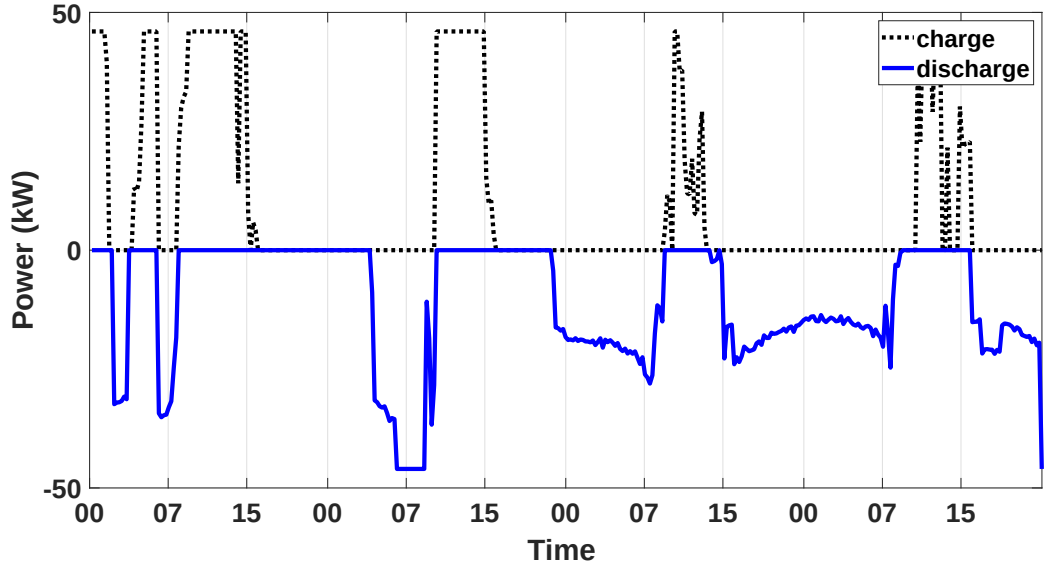

Figure 4.5 Charging and discharging power of ESS

Table 4.2 EVs and Battery Properties

EVs Type	Capacity(kWh)	Charge Rate(kW)
EVs Group 1	24	6.6
EVs Group 2	16	3.6
EVs Group 3	9.2	3.8
EVs Group 4	28	7.6
Battery	5×100	5×9.2

the other apartments define upper and lower bounds temperature equal to 26°c and 19°c respectively. To make simulation more realistic, the building construction materials have been obtained from materials which is used in residential examples of *EnergyPlus* (table **??**).

By solving optimization problem (4.24), the values of u^{z_i}, $P_{buy,G}$, $P_{sell,G}$, P^j_{disch}, P^j_{ch}, $P_{b,disch}$, $P_{b,ch}$ can be found at each time step. In Fig. 4.4, the amount of PV power and SOC of ESS are shown. It must be mentioned that the extra power from PV is saved in ESS and can be used during nighttime period. Fig. 4.5 shows, the status of charging ($P_{b,ch}$) and discharging ($P_{b,disch}$) of the ESS. It seems that ESS stores more energy during the daytime (when PV generates power) and building uses this stored energy during night time. Due to limitation of ESS charging and discharging power, sometimes BEMS suggests whether selling extra power of PV to grid or buying from grid to overcome this limitations. Furthermore, the ESS seems

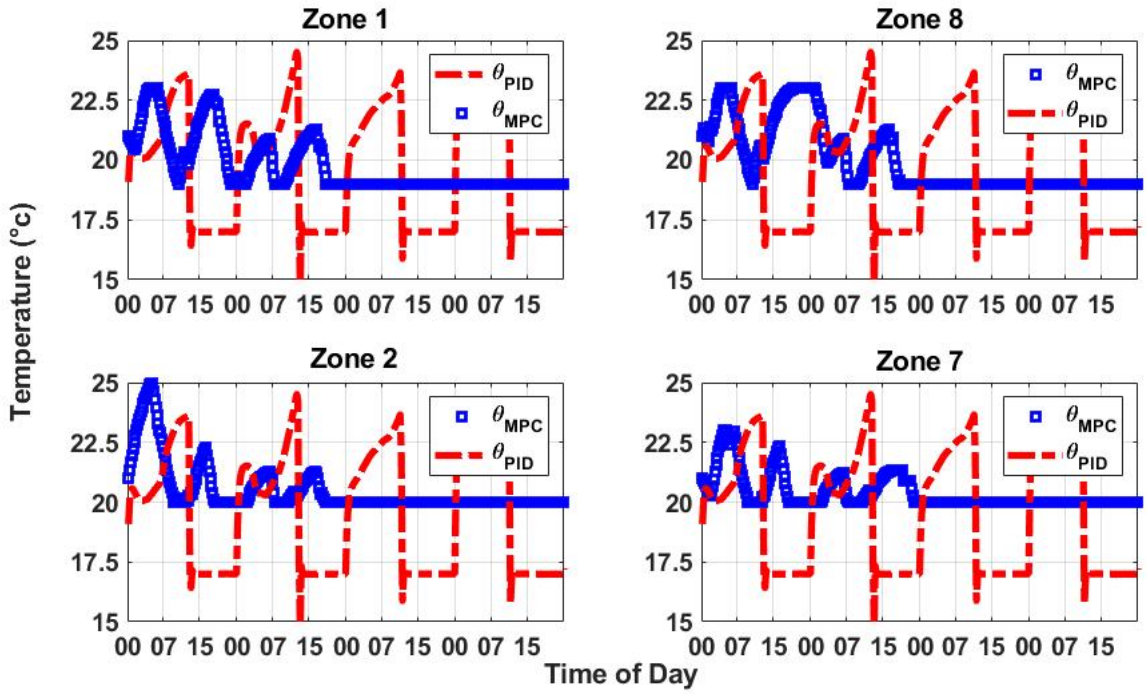

Figure 4.6 Zone temperatures

to be charged and discharged once per day which from the view point of life cycle of batteries, the proposed algorithm follows the normal routine.

As it can be shown in Fig. 4.6, all apartments' temperatures are controlled between desired setpoints by controlling u^{z_i} for each zone z_i. Compared to PID, the proposed approach keeps the temperatures between the minimum and maximum bounds. In figure 4.7, the total amount of power required to keep temperatures of the apartments at desired ranges and the pricing system (TOU) are shown. By comparing Figs. 4.6 and 4.7, it can be depicted that before on-peak time which starts almost at 7am, BEMS tends to warm-up each apartment as much as possible. Thus, in on-peak time, the total consumption of the HVAC units can be reduced. In addition, by comparing results of proposed method with PID, it can be seen that the proposed method tends to consume less power due to the implementation of data prediction. The proposed method avoids high power peak while keeping temperatures at an average values. On other words, the apartment building is considered as a large one-way thermal storage system which can save energy during off-peak time and use it during on-peak time. This implies that, the amount of power which should be bought from grid will be reduced, as can be seen from Fig. 4.9.

Total number of 20 EVs from four types of electrical vehicles have been used in this simulation.

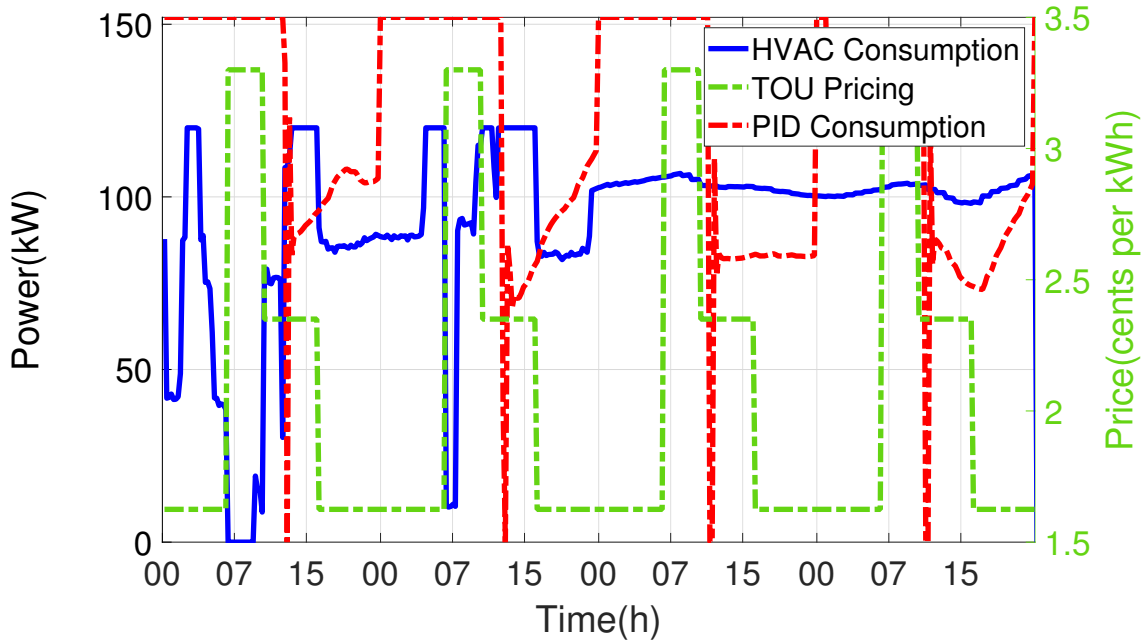

Figure 4.7 The total amount of HVAC power consumption for MPC and PID.

Table 4.3 Building Parameters

Parameter	Value	Parameter	Value
R_i	$50°C/kW$	C_i	$9.7kWh/°C$
R_{im}	$7.14°C/kW$	C_{im}	$0.011kWh/°C$
R_{am}	$0.054°C/kW$	C_{om}	$250.50kWh/°C$
R_a	$8.021°C/kW$		

The time of departure for each vehicle is assumed to follow a normal Gaussian probability distribution function (PDF) with $N \sim (7 \text{ am}, 45 \text{ min})$ and the same PDF for time of arrival, $N \sim (4 \text{ pm}, 45 \text{ min})$ at the same day. Fig. 4.8 shows that, however at the time of the departure each vehicle has the desired SoC, but during time of presence, by controlling P^j_{disch} and P^j_{ch} of each EV, the algorithm uses their batteries to accomplish its objective. For example, at the time of arrival, since it is in an on-peak period, extra power stored in EVs will be used until appropriate amount of PV power is generated or the on-peak period is surpassed.

As can be depicted in Fig. 4.9, othe power purchased from the grid does not exceed the maximum allowable limit of 170kW. Furthermore, during the first 24 hours when high power generation is observed, the excess amount has been used for charging the energy storage

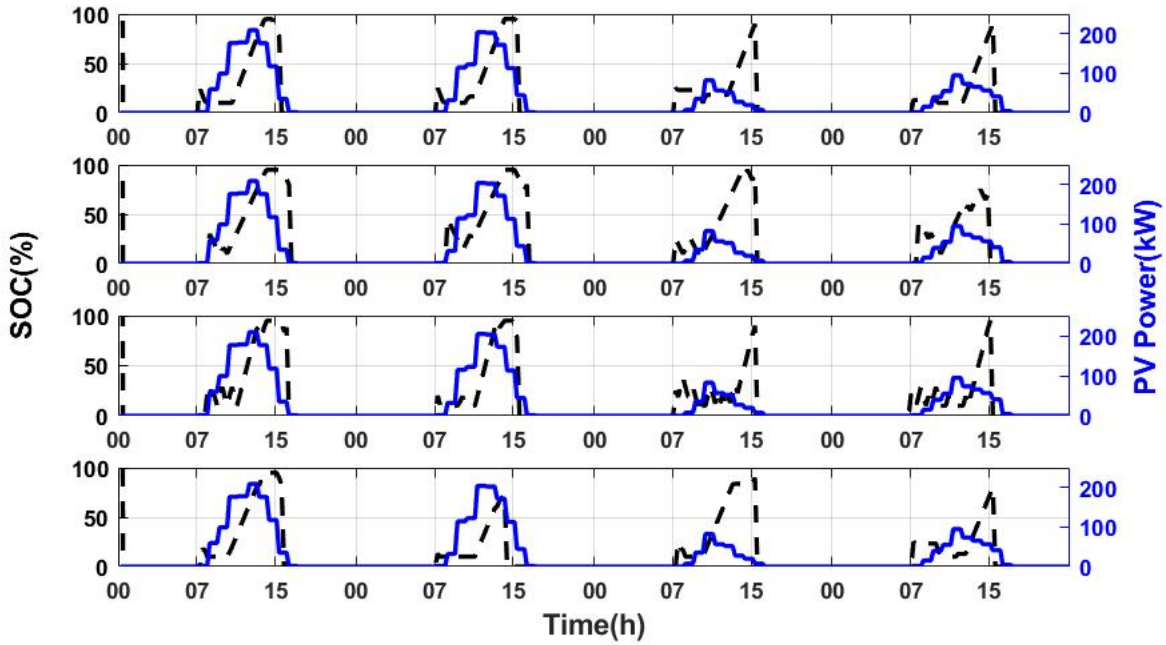

Figure 4.8 State of charge of EVs and power generation from PV.

system and also, sold to the grid.

4.5 Conclusion

In this paper, we proposed a MPC algorithm for energy management in an apartment building integrating microgrid. We aim to present an effective approach for the modeling and optimizing a multi-unit residential building, integrating a local shared renewable power generation, energy storage system and electric vehicles. The proposed algorithm could handle both power consumption and comfort parameters objectives through using MPC while involving HVAC systems in demand response. By applying TOU pricing, results of the algorithm suggested to store extra solar generated power in ESS or sell it to grid to gain more benefits. During off-peak periods, BEMS tried to increase temperature inside building, so in on-peak, which is usually during daytime, less power will be needed. In other words, BEMS is assuming building as a thermal battery and by controlling its temperature, it tries to reduce its power consumption during on-peak periods. Furthermore, through V2B concept, the BEMS uses EVs' batteries to accomplish its goals, charging EVs at off-peak or in case of extra solar power and discharging them in case of on-peak periods.

Future work will investigate the use of stochastic model predictive control for better handling

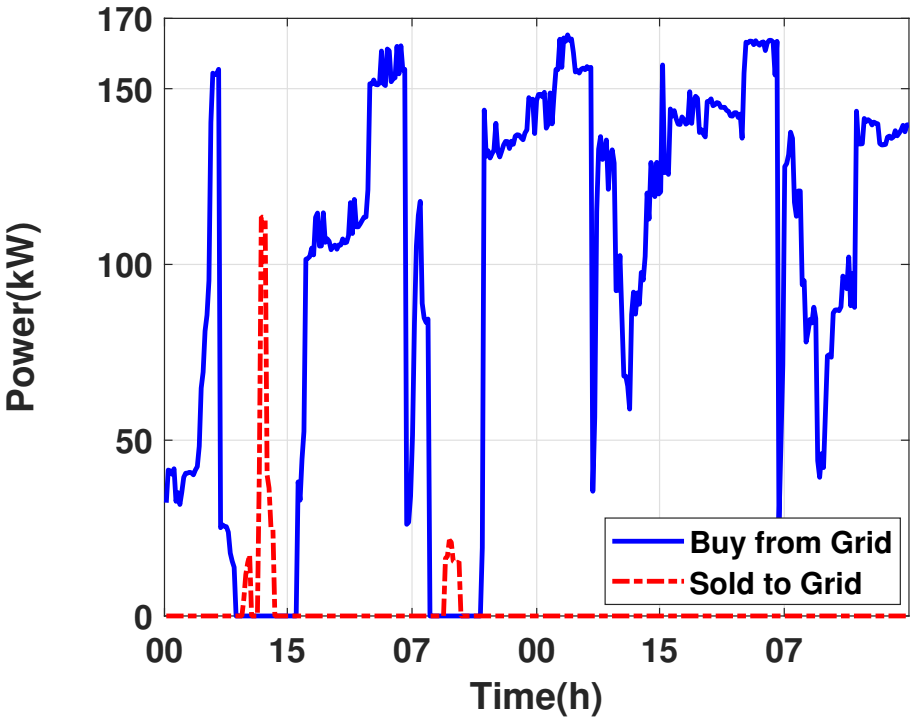

Figure 4.9 red The amount of power exchanged with the grid.

uncertainties related to loads, RESs and electric vehicles. Future work will also aim to implement distributed optimization strategy for a network of residential buildings integrating microgrids, where buildings can cooperate with each other for an overall optimal operation.

CHAPTER 5 ARTICLE 2: DISTRIBUTED STOCHASTIC MODEL PREDICTIVE CONTROL FOR PEAK LOAD LIMITING IN NETWORKED MICROGRIDS WITH BUILDING THERMAL DYNAMICS

Authors: Ehsan Rezaei, Hanane Dagdougui, Mahdi Rezaei
Accepted for publication: IEEE Transactions on Smart Grid, 2021

Abstract: Today's increase in demand for renewable energy resources has attracted a lot of attention towards Microgrids (MGs). Due to their reliability, computation power and performance, a distributed network of MGs seems to be a promising approach to integrate a large number of distributed energy resources, energy storage systems and loads. However, local privacy, the consensus process and the stochastic behaviours of renewable resources are some of the challenges which should be addressed before a wide deployment of such networks. In this paper, we introduce a distributed MGs with buildings, focusing on their ability to provide peak load limiting. The algorithm is formalized as a two-stage stochastic problem, where the first stage variables determine the next time-step buildings' temperatures setpoints in each microgrid, while the second-stage variables define the power exchange decisions for limiting peak load in the network of microgrids. Leveraging by alternating direction method of multipliers (ADMM), the proposed framework can work in a real-time environment as a supervisory controller to coordinate MGs.

Keywords

Network of microgrids, Demand response, Distributed optimization, Stochastic model predictive control, ADMM.

5.1 Nomenclature

i	Index of Microgrid i
$\mathbb{k}_i$	Neighbours of MG i
ΔT	Time-step length
ζ	Scenarios set
ζ_j	Scenario j of scenario set ζ

p_j	Occurrence probability of scenario ζ_j
$\mathbf{v}$	Disturbances vector
Υ	Network adjacency matrix
θ_{out}	Outside temperature
$P_{pv,i}$	Generated PV power
G	Solar irradiation
P^i_{Rated}	Rated power of PV panels
θ^i_{STC}	Standard operation point of PV panels
τ_i	Temperature coefficient of PV panels
$\mathbf{x}^i$	Building state vector
$\mathbf{u}_{l,i}$	Building heating/cooling control vector
$\mathbf{y}^i$	Building measurable temperatures vector
$\mathbf{u}^i_{l,c}$	Maximum power of building cooling system
$\mathbf{u}^i_{l,h}$	Maximum power of building heating system
$\mathbf{y}^i_{des}$	Building desired temperatures (setpoints) vector
$\boldsymbol{\delta}^i$	Vector of small deviation from $\mathbf{y}^i_{des}$
$\Delta\mathbf{u}^i_{max}$	Maximum rate of cooling/heating systems power changes
soc_i	Battery state of charge
$u_{b,c,i}$	Battery charging power
$u_{b,d,i}$	Battery discharging power
$u_{b,i}$	Battery total exchanging power
η^i_{sd}	Battery self-discharging rate
$\eta^i_{b,c}$	Battery charging rate
$\eta^i_{b,d}$	Battery discharging rate
C^i_b	Battery capacitance
$u^i_{max_c}$	Maximum charging power of Battery
$u^i_{max_d}$	Maximum discharging power of Battery
soc^i_{min}	Minimum admissible SOC
soc^i_{max}	Maximum admissible SOC
α_b	Auxiliary Boolean variable
α_p	Price of buying power from main grid per kWh
α_s	Price of selling power to main grid per kWh
α_0	Trade-off level control parameter

$\rho^k_{i,j,\zeta}$	Link $L_{i,j}$ Lagrange multipliers at iteration step k
$\rho^k_{g,i,\zeta}$	Link L_i Lagrange multipliers at iteration step k
$\mathbf{\Phi}_i$	Objective function of MG i
$\mathbf{\Omega}_i$	Constraints of MG i
$\mathbf{\Phi}_g$	Objective function of aggregator
$\mathbf{\Omega}_g$	Independent constraints of aggregator
$\mathbf{\Gamma}_g$	Shared constraints of aggregator
$\mathbf{\Omega}_{l_{i,j}}$	Independent constraints of link $L_{i,j}$
$\mathbf{\Gamma}_{l_{i,j}}$	Shared constraints of link $L_{i,j}$
$P_{g_b,i}$	Bought power from main grid
$P_{g_s,i}$	Sold power to main grid
$P_{j,i}$	Exchange power between MG i and j
P^i_{ncLoad}	Non-controllable load
$P^m_{g,i}$	MG i Maximum exchangeable power with main grid
$P^m_{i,j}$	MG i Maximum exchangeable power with MG j
$\mathbf{\Gamma}_{g,i}$	Link i constraints of link between main grid and MG
$\mathbf{\Gamma}_{i,j}$	Constraints of link between main grid and MG i

5.2 Introduction

Growing energy consumption and meeting environmental targets encourage not only main producers but also consumers to take advantage of renewable energy sources (RESs). Buildings account for 40% of global energy consumption, with 75% of it going toward controlling comfort parameters [50]. Demand response (DR) programs have been considered as a promising solution for utilities and consumers. From a utility perspective, DR helps increase the flexibility in the grid for balancing supply and demand, which may delay investments for new generator units and transmission lines. From the consumer side, DR offers consumers a unique opportunity to increase their participation in grid management while saving money on their energy bills and earning income from the grid.

Due to their potential in energy management, buildings with large thermal dynamic capacitance and distributed renewable energy resources have received much attention in recent years. In [206], a model predictive controller for apartment buildings integrated with RESs and electrical vehicles (EVs) is proposed. The study demonstrated that DR and the proposed controller can successfully overcome on-peak problems using the thermal capacity of apartments, saving energy during off-peak hours and reducing total energy consumption during

on-peak time, without violating occupants' comforts. In [207], the authors extended the previous study to capture uncertainties in electricity price, solar power generation and weather conditions by proposing a two-stage stochastic optimization problem. In [208], a price-based DR framework having the main objectives of minimizing both energy costs and occupants' thermal discomfort is proposed. The author trained a neural network from occupants' votes to find the best thermal preferences. Then the network was estimated with piece-wise linear equations and integrated with DR. An intelligent energy management system for residential buildings, is proposed in [209]. The proposed system schedules the controllable loads to maintain the building's total power consumption below a maximum demand limit (MDL) while considering the dynamic of non-controllable loads and the intermittent behaviour of RESs. In a recent work [210], Yu *et al.* proposed a non-model-based reinforcement learning approach for controlling heating, ventilation, and air conditioning (HVAC) systems in commercial buildings. Although there are some studies investigating the integration of DR in buildings and microgrids (MGs), to the best of the authors' knowledge, coordinating DR actions in a network of building-integrated MGs has not been carefully studied.

A network of MGs consists of several microgrids that can exchange power following a peer-to-peer (P2P) manner or through an aggregator / distribution network operator. Compared to a single MG, a network of microgrids has more potential to influence the main grid. Three different approaches are usually considered to control this type of network: centralized, distributed and decentralized. In [211], a network of building-integrated microgrids coordinated by an aggregator can reduce total consumption below MDL by controlling buildings' temperatures. In [212], the authors developed a supervisory control and data acquisition system and investigating its performance by applying it to a real-scenario case. Despite integrating temperature control in the buildings, both studies implemented a centralized structure, which suffers from heavy computational load, privacy and reliability issues.

To solve the aforementioned problems of centralized networks, distributed methods such as dual decomposition and the alternating direction method of multipliers (ADMM) have been used to decouple the optimization problem to smaller sub-problems at the level of each MG. Parisio *et al.* [213] propose a distributed MPC-based algorithm for network of MGs to manage total exchange power between MGs and the main grid. In [214], a two-level control methodology is presented where the upper-level loop distributively optimizes the generation output of MGs, while optimal settings are tracked in the lower-level loop. Some recent studies consider the electrical aspects of such networks. However, there are some ongoing research investigating or improving its convergence rate (such as [215–217]), but compared to other decomposition optimization methods, ADMM has benefits of practical fast convergence with a reasonable precision, ease to implementation and generalization [165]. In [166], the authors

develop an ADMM-MPC-based algorithm to regulate the frequency of buses while considering their voltage constraints. Zhou *et al.* [218] address unbalanced single- and three-phase MG problems and propose a hierarchical event-based distributed controller that can regulate the power flows of phases. However, none of them consider the stochastic behaviours of RESs or the network of buildings.

In this paper, we present a distributed stochastic model predictive control framework for a network of residential MGs. The problem is formulated as a two-stage stochastic optimization, and the stochastic version of ADMM is introduced. The proposed algorithm can handle uncertainties related to renewable power generation resources while guaranteeing both privacy and reliability of the network. The main contributions of this paper are summarized as follows:

- A novel stochastic distributed framework for a network of MGs is introduced. This framework can handle the stochastic behaviours of renewable energy resources which are modeled as a stochastic process with a dynamic probability distribution function.
- By controlling MGs' HVAC systems and managing their resources, the proposed framework can keep the total purchased power of the network below MDL while satisfying the comfort parameters of buildings' occupants by considering thermal dynamics and multi-zones effects of each building.
- In this framework, aggregators can have their own objectives and optimization problems, which should be solved with respect to their electrical constraints, at each time step.
- Using parallel programming in the simulation section, the performance of proposed framework has been investigated and it is shown that it can be used in real-time applications.

The rest of this paper is organized as follow: Section 5.3 presents mathematical models of MG elements. Section 5.4 first formulates the general optimization problem of a network of MGs and then introduces an ADMM-based distributed stochastic MPC framework for solving the optimization problem. Section 5.5 demonstrates the efficiency of the proposed method through a case study, and finally Section 5.6 concludes the paper.

5.3 Mathematical Modeling

A network of residential building-integrated PV-battery microgrids is a set of N different MGs with PV panels to generate power and a battery to store energy. MGs can exchange

power among themselves or with the main grid in a P2P or hierarchical manner. The network is defined as a directed graph with MGs and the grid / aggregator as its vertexes denoted by $\Psi = \{\text{MG}_n : n \in \{1, 2, \dots n\}\} \cup \{G\}$. Now, Υ can express the network structure as:

$$\Upsilon = \left[\Upsilon_{i,j} | \begin{cases} \Upsilon_{i,j} = 1 & \text{physical link } \overrightarrow{ij} \text{ exists} \\ \Upsilon_{i,j} = 0 & \text{o.w.} \end{cases}\right]_{\forall i,j \in \Psi}$$

Note that the direction of the physical link $\overrightarrow{ij}$ is conventional and obviously, $\Upsilon_{j,i} = 0$ if $\Upsilon_{i,j} = 1$. Moreover, the $L_{i,j}$ represent the link $\overrightarrow{ij}$ if $i, j \in \Psi/\{G\}$, and in case if one of i or j is $\{G\}$, L_i is used to represent the link between MG and main grid.

5.3.1 Thermal Dynamic Model of Buildings

In this work, the thermal behaviour of each building is modeled by its equivalent resistance-capacitance (RC) model. The model obtained from RC method, due to its capabilities in thermal modeling of building's elements and also considering effects of different disturbances, e.g., outside temperature and solar irradiation, has a high accuracy. However, the model is not complex as the white-box models, e.g., 3-D heat equations [219], and so it does not suffer from their problems, mainly needs for high computational power. In the RC modeling method, each element of a building is replaced by its equivalent thermal resistance and heat capacitance. Using the building blueprints, these elements are then connected to each other and, similar to electrical circuits, a thermal network can be designed. The state space equations of this thermal network can now be used to control the temperature of building zones.

According to [204], the discretized version of the RC model obtained from the aforementioned process can be expressed as follows:

$$\forall k : \begin{cases} \mathbf{x}^i[k+1] = A^i\mathbf{x}^i[k] + B^i_u\mathbf{u}_{l,i}[k] + B^i_v\mathbf{v}[k] \\ \qquad + \sum_{j=1}^{n_u}(B^i_{vu,j}\mathbf{v}[k] + B^i_{xu,j}\mathbf{x}^i[k])u_{j,i}[k] \\ \mathbf{y}^i[k] = C^i\mathbf{x}^i[k] \end{cases} \tag{5.1}$$

where $\mathbf{x}^i[k], \mathbf{v}[k]$ and $\mathbf{y}^i[k]$ are the state vector, disturbance vector and output temperature vector, respectively, for a building of MG i. The matrices A^i, B^i_u, B^i_v, C^i, $B^i_{uv,j}$ and $B^i_{xu,j}$ are fixed, and their values can be found either directly from the building's blueprints or using identification methods applied to historical data. Vector $\mathbf{x}^i$ represents temperature of building i's different elements. $\mathbf{u}_{l,i}[k] = \begin{bmatrix} u_{1,i}[k] & u_{2,i}[k] & \dots & u_{n_u,i}[k] \end{bmatrix}^T$ denotes the input control

vector, each $u_{\rho,i}$ represents the output power of a heating / cooling actuator in controllable zone ρ of building i and n_u is the total number of actuators in said building. Usually, the limited number of actuators in the building makes it impossible to control the temperatures of all zones, and so instead of controlling the temperature in all zones, our focus is on controlling the temperature of at most these n_u zones with actuators, temperature vector $\mathbf{y}^i$. Obviously, the vector size of $\mathbf{y}^i$ is less than or equal to n_u (a zone can have more than one actuator). For the sake of simplicity, the superscript notation i is used to distinguish MG i components. The nonlinear summation term $\sum_{j=1}^{n_u}(B^i_{vu,j}\mathbf{v}[k]+B^i_{xu,j}\mathbf{x}[k])u_{j,i}[k]$ models the interaction of inputs-disturbances or inputs-states. For example, blind position (control input) can affect the energy absorbed from sun irradiation through windows (disturbance), and the temperature of ventilated air (control input) can decrease or increase another zone's temperature due to ventilation between different zones (states). A detailed example of applying RC-method to a real case home, used in our case study, is given in Appendix 5.7.1.

According to equation (5.1), the temperature of controllable zones depends on disturbances, control inputs and previous states. To satisfy comfort parameters, we need to keep zone temperatures in an acceptable range near occupants' desired values, setpoints $\mathbf{y}^i_{des}[k]$. Then we have:

$$\forall k : \mathbf{y}^i_{des}[k] - \boldsymbol{\delta}^i \leq \mathbf{y}^i[k] \leq \mathbf{y}^i_{des}[k] + \boldsymbol{\delta}^i \tag{5.2}$$

where $\boldsymbol{\delta}^i$ is a small acceptable deviation from $\mathbf{y}^i_{des}[k]$, which should not violate occupants' comforts. Due to its thermal retention characteristic, a building behaves like a large thermal battery. Defining $\boldsymbol{\delta}^i$ can guarantee the feasibility of the final optimization problem. Also, buildings can act as thermal storage systems using this small deviation and their slow thermal dynamic feature, providing additional flexibility to the related MGs and to the network.

The maximum power consumption of actuators can be guaranteed by:

$$\forall k : -\mathbf{u}^i_{l,c} \leq \mathbf{u}_{l,i}[k] \leq \mathbf{u}^i_{l,h} \tag{5.3}$$

where $\mathbf{u}^i_{l,c}$ and $\mathbf{u}^i_{l,h}$ show the maximum cooling and heating power, respectively. Obviously, in cooling (warming) seasons, the value of $\mathbf{u}^i_{l,c}$ ($\mathbf{u}^i_{l,h}$) should be set to zero. Furthermore, for avoiding any damage to building's thermal systems , the rate of $\mathbf{u}_{l,i}[k]$ changes should be limited:

$$\forall k : -\Delta\mathbf{u}^i_{max} \leq \mathbf{u}_{l,i}[k] - \mathbf{u}_{l,i}[k-1] \leq \Delta\mathbf{u}^i_{max} \tag{5.4}$$

Note that $\Delta\mathbf{u}^i_{max}$ is a function of cooling/heating mode of thermal systems and time-step ΔT

used for discretization of RC-model (5.1). Although the response time of building's thermal systems is not modeled explicitly, but choosing a big enough time-step ΔT can cover their response time delay.

5.3.2 PV Panels

In this study, the PV panels are assumed to work at their maximum power, and the model (5.5) is therefore considered to estimate generated power $P_{pv,i,\zeta}$ from solar irradiation G_ζ:

$$\forall k, \zeta : P_{pv,i,\zeta}[k] = P^i_{Rated} \frac{G_\zeta[k]}{1000} [1 + \tau_i(\theta_{out} - \theta^i_{STC})] \tag{5.5}$$

where P^i_{Rated}, θ^i_{STC} and τ_i are the rated power, the temperature of the standard operation point and temperature coefficient of solar panels, respectively and θ_{out} denotes outside temperature. At time step k, solar irradiation $G_\zeta[k]$ depends on a random process ζ at each time step k, which its probability density function (pdf) $p(\zeta[k])$ can be found by analyzing solar irradiance data from previous years [220]. Using a continues form of $p(\zeta[k])$ in practice, needs considerable computational power and time, and hence using a reduced and discrete form of an ensemble realizations of $p(\zeta[k])$, is necessary. Deploying scenario tree method to discretize $\zeta[k]$ to different n-value $\zeta_1[k], \zeta_2[k], \ldots, \zeta_n[k]$ with occurrence probabilities of $p_1[k], p_2[k], \ldots, p_n[k]$ at time k, is a reasonable and yet efficient way to decrease its complexity, where p_is are defined as follow:

$$\begin{aligned} \forall k : p_j[k] &= \begin{cases} \int_0^{\gamma_1} p(\zeta[k])\, d\zeta & j = 1 \\ \int_{\gamma_{j-1}}^{\gamma_j} p(\zeta[k])\, d\zeta & o.w. \end{cases} \\ \gamma_j &= \frac{\zeta_j + \zeta_{j+1}}{2} \end{aligned} \tag{5.6}$$

Besides, as we will explain later in part 5.3.4, due to power flow constraints, almost all decision variables have stochastic behaviours and therefore, for rest of this paper, we use subscript ζ to show the dependency of a variable on ζ.

5.3.3 Electrical Storage System

Usually, PV panels come with batteries to save their extra generated energy. In this study, each MG has its own energy storage system, mainly batteries. If $soc_i[k]$ denotes the state of

charge of the MG i battery at time step k, the battery can be modeled for all k and ζ as:

$$soc_{i,\zeta}[k+1] = \eta^i_{sd} soc_{i,\zeta}[k] + \frac{1}{C^i_b}\left(\eta^i_{b,c} u_{b,c,i,\zeta}[k] - \frac{1}{\eta^i_{b,d}} u_{b,d,i,\zeta}[k]\right) \tag{5.7}$$

$$\begin{cases} 0 \leq u_{b,c,i,\zeta}[k] \leq u^i_{max_c} \\ 0 \leq u_{b,d,i,\zeta}[k] \leq u^i_{max_d} \end{cases} \tag{5.8}$$

$$\begin{cases} 0 \leq u_{b,c,i,\zeta}[k] \leq \alpha_b[k] u^i_{max_c} \\ 0 \leq u_{b,d,i,\zeta}[k] \leq (1-\alpha_b[k]) u^i_{max_d} \end{cases}, \alpha_b[k] \in \{0,1\} \tag{5.9}$$

$$soc^i_{min} \leq soc_{i,\zeta}[k] \leq soc^i_{max} \tag{5.10}$$

where in (5.7), η^i_{sd}, $\eta^i_{b,c}$ and $\eta^i_{b,d}$ respectively denote the self-discharging, charging and discharging rates of battery with capacitance C^i_b. Equations set (5.8) limits the charging and discharging power of battery $u_{b,c,i,\zeta}$ and $u_{b,d,i,\zeta}$, by their maximum values $u^i_{max_c}$ and $u^i_{max_d}$, while equations set (5.9) by defining binary variables $\alpha_b[k]$ prevents battery's charging and discharging mode activate at the same time. Also by limiting its *soc* between maximum and minimum admissible soc^i_{min} and soc^i_{max}, equation (5.10) guarantees safety of battery from being fully charged or discharged. The auxiliary variable $u_{b,i,\zeta}$ defined as

$$u_{b,i,\zeta}[k] = u_{b,c,i,\zeta}[k] - u_{b,d,i,\zeta}[k], \qquad \forall i, \zeta, k, \tag{5.11}$$

will help us to consider effects of battery's charging and discharging power together. Obviously when the battery is in charging (discharging) mode, the sign of $u_{b,i,\zeta}[k]$ is positive (negative).

5.3.4 Power Balance

In a hierarchical structure, each MG can buy power $P_{g_b,i}$ from or sell power $P_{g_s,i}$ to the main grid through the aggregator. In a P2P structure, on the other hand, MGs can exchange power with either the main grid or their neighbours. Considering the adjacency matrix Υ, if $\Upsilon_{i,j}$ is non-zero, then there is a link $L_{i,j}$ between two MGs i and j and they can therefore exchange power $P_{i,j}$. To solve the optimization problem, for all time steps k, power exchange $P_{j,i}[k]$ should be equaled to $-P_{i,j}[k]$, otherwise the optimization becomes infeasible. Depending on the network structure, we can have two different power balance equations for each MG

$i, \forall k, \zeta$:

Hierarchical structure:

$$P_{pv,i,\zeta}[k] + u_{b,i,\zeta}[k] + P_{g_b,i,\zeta}[k] - P_{g_s,i,\zeta}[k] \\ - \sum_{j=1}^{n_u} |u_{j,i,\zeta}[k]| - P^i_{ncLoad}[k] = 0 \tag{5.12a}$$

P2P structure:

$$P_{pv,i,\zeta}[k] + u_{b,i,\zeta}[k] + P_{g_b,i,\zeta}[k] + \sum_{j \in \mathbb{k}_i} P_{j,i,\zeta}[k] \\ - P_{g_s,i,\zeta}[k] - \sum_{j=1}^{n_u} |u_{j,i,\zeta}[k]| - P^i_{ncLoad}[k] = 0 \tag{5.12b}$$

where $P^i_{ncLoad}[k]$ is the non-controllable consumption of MG i at time step k. Also, in reality, to avoid physical damage to the power transmission cables, each power line (link) has a maximum capacity defined by, $\forall \zeta, i, k, j \in \mathbb{k}_i$:

$$\begin{cases} \mathbf{\Gamma}_{g,i}(\mathbf{P}_{g_{s,b},i}) : \begin{cases} 0 \leq P_{g_b,i,\zeta}[k], P_{g_s,i,\zeta}[k] \leq P^m_{g,i} \\ P_{g_b,i,\zeta}[k] P_{g_s,i,\zeta}[k] = 0 \end{cases} \\ \mathbf{\Gamma}_{i,j}(P_{i,j}, P_{j,i}) : -P^m_{i,j} \leq P_{i,j,\zeta}[k] = -P_{j,i,\zeta}[k] \leq P^m_{i,j} \end{cases} \tag{5.13}$$

where $\mathbf{P}_{g_{s,b},i} = \begin{bmatrix} P_{g_b,i} & P_{g_s,i} \end{bmatrix}^T$.

5.4 Distributed Optimization

5.4.1 Single MG Optimization Problem

Each MG is minimizing its energy consumption cost while keeping constantly a comfortable temperature for occupants, for all controllable zones of a building:

$$\mathbb{E}_\zeta \left[\alpha_0 \|\mathbf{y}^i[k] - \mathbf{y}^i_{desi}[k]\|_2^2 + \boldsymbol{\alpha}_1 \mathbf{P}_{g_{s,b},i,\zeta}[k] \right] \tag{5.14}$$

where $\| \cdot \|_2$ represents norm 2 of the matrix, $\boldsymbol{\alpha}_1 = \begin{bmatrix} \alpha_p & -\alpha_s \end{bmatrix}$ is the matrix of prices for exchanging with (buying from and selling to) the main grid and α_0 is a control parameter, set by each MG to adjust the trade-off level between building temperature comforts and its

exchange power with the main grid. Obviously, α_s should be less than α_p, otherwise the optimization problem will be infeasible, since buying power from the main grid and selling it back right after is an optimal solution that can maximize objective function (5.14).

The stochastic behaviour of PV-generated power influences all variables in (5.14) through power balance equations (5.12b or 5.12a), and so these variables can all have stochastic behaviours. However, standing at time step $t-1$, the MG i should find optimal values for zones' temperatures $\mathbf{y}^i$ and set these temperatures during the next time step t. As a result, $\mathbf{y}^i$ and the total power consumption of the building can be seen as first-stage variables that should be decided at the beginning of time step t and are independent of ζ. In this case, $P_{g_s,i,\zeta}$ and $P_{g_b,i,\zeta}$, selling and buying power, respectively, are second-stage variables. Therefore, the optimization problem of each MG over prediction horizon n_p can be reformulated as:

$$\begin{aligned} &\min_{\mathbf{x}_i} \sum_{k=t+1}^{t+n_p} \overbrace{\alpha_0 \|\mathbf{y}^i[k] - \mathbf{y}^i_{desi}[k]\|_2^2 + \mathbb{E}_\zeta\Big[\boldsymbol{\alpha}_1 \mathbf{P}_{g,i,\zeta}[k]\Big]}^{\boldsymbol{\Phi}_i(\mathbf{x}_i[k])} \\ &\text{s.t.: } \boldsymbol{\Omega}_i \end{aligned} \tag{5.15}$$

where $\mathbf{x}_i$ represents the vector of all optimization variables, such as $P_{g_b,i,\zeta}$, $P_{g_s,i,\zeta}$ and $u_{b,i,\zeta}$, and $\boldsymbol{\Omega}_i$ is the set of all constraints of MG i, (5.7) to (5.13).

5.4.2 Aggregator Optimization Problem

In hierarchical coordination, the aggregator has the opportunity to offer flexibility services to the distribution system operators. In this case, an objective function ($\boldsymbol{\Phi}_g$) defines the energy scheduling:

$$\begin{aligned} &\min_{agg.\ vars} \sum_{k=t+1}^{t+n_p} \boldsymbol{\Phi}_g[k]\Big(\text{or } \boldsymbol{\Phi}_{L_{i,j}}[k]\Big) \\ &s.t.\ \forall \zeta, k \in [t+1, t+n_p] : \begin{cases} \boldsymbol{\Gamma}_g\Big(\text{or } \boldsymbol{\Gamma}_{l_{i,j}}\Big) \\ \boldsymbol{\Omega}_g\Big(\text{or } \boldsymbol{\Omega}_{l_{i,j}}\Big) \end{cases} \end{aligned} \tag{5.16}$$

where the aggregator and link $L_{i,j}$ have independent constraints $\boldsymbol{\Omega}_g$ and $\boldsymbol{\Omega}_{L_{i,j}}$ and shared constraints $\boldsymbol{\Gamma}_g$ and $\boldsymbol{\Gamma}_{L_{i,j}}$, respectively.

The peak load limiting strategy can be achieved by assuming all MGs are connected to the grid through the same transformer or substation that may impose power limits sometimes. At the level of the aggregator, the objective of the scheduling problem is to control the total

net power exchange to achieve better grid stability and high network performance during on-peak time and to keep the power generated by the main grid at a reasonable level. As a result, the shared constraint $\mathbf{\Gamma}_g$ can be broken down to keep the total net power consumption of the MGs around a desired MDL level c_{desi}, and also a group of constraints $\mathbf{\Gamma}_{g,i}(P_{g,i,\eta})$, related to both MG i and the aggregator / main grid:

$$\min_{c,\ agg.\ vars} \sum_{k=t+1}^{t+n_p} \mathbb{E}_\zeta[(c_\zeta[k] - c_{desi}[k])^2] + \mathbf{\Phi}_g[k] \tag{5.17}$$

$$s.t.\ \forall \zeta, k \in [t+1, t+n_p] : \begin{cases} \mathbf{\Omega}_g \\ \mathbf{\Gamma}_{g,i}(P_{g,i,\zeta}) \\ \sum_i P_{g,i,\zeta}[k] = c_\zeta[k] \end{cases}$$

where $c_\zeta[k]$ is a decisional variable denoting the total net power consumption of scenario ζ at time step k. Note that the first group of constraints in equation (5.17), $\mathbf{\Omega}_g$, expresses the constraints of the aggregator itself such as voltage regulation and line capacitance constraints. The role of the link, on the other hand, is to coordinate the power exchange among the MGs through the consensus process. So it can be assumed $\mathbf{\Phi}_{L_{i,j}}[k] = 0$. The optimization problem of the links will be given later, in Section 6.3.2.

5.4.3 ADMM Introduction

In the network of MGs introduced in section 5.4.1, individual MG prefers conservative approaches for sharing their information with third party or other MGs, especially when they have different stakeholders. On the other hand, the network main goal is to keep its total purchased power under MDL and therefore, a distributed communication way is needed. ADMM-based distributed optimization due to its practical speed and convergence properties, can be used in favor of both MGs privacy policy and network MDL objective, [165].Therefore, the ADMM decomposition method is implemented to solve the problem in a distributed fashion. In this work, a stochastic version of ADMM is proposed to handle the stochastic variables.

Theorem 1 *Assume ζ is a random variable that comes from a known distribution $\boldsymbol{P}$, and is discretized to $\zeta_i s$, using a discretization method. In this case, a solution to the optimization*

problem

$$\begin{aligned} &\min_{x,\boldsymbol{z}} f(x) + \mathbb{E}_\zeta[g(z_\zeta)] \\ &s.t.: Ax + Bz_{\zeta_i} = c_{\zeta_i} \quad \forall \zeta_i \in \zeta \end{aligned} \tag{5.18}$$

can be found by using following iteration method:

$$\begin{aligned} \boldsymbol{z}^{k+1} &= \underset{\boldsymbol{z}}{\operatorname{argmin}} \left(\mathbb{E}_\zeta \left[g(z_\zeta) + \frac{\rho}{2} \|D(Ax^k + Bz_\zeta - c_\zeta + u_\zeta^k)\|_2^2 \right] \right) \\ x^{k+1} &= \underset{x}{\operatorname{argmin}} \left(f(x) + \frac{\rho}{2} \mathbb{E}_\zeta \left[\|D(Ax + Bz_\zeta^{k+1} - c_\zeta + u_\zeta^k)\|_2^2 \right) \right. \\ u_{\zeta_i}^{k+1} &= u_{\zeta_i}^k + (Ax^{k+1} + Bz_{\zeta_i}^{k+1} - c_{\zeta_i}) \quad \forall \zeta_i \in \zeta \end{aligned} \tag{5.19}$$

Its convergence proof is given in Appendix 5.7.2. In the next section, we use this theorem to propose an ADMM-based distributed stochastic MPC (SMPC) algorithm for networks of MGs.

5.4.4 ADMM-based Distributed SMPC

Model predictive control (MPC) is a well-known control methodology that is widely used and shows high performance due to its model consideration and prediction properties. SMPC proposes a stochastic version of MPC that can deal with stochastic variables in the model, such as solar irradiation.

According to equation (5.5), the probability density function of sun irradiation $p(\zeta[k])$ is needed to find the optimal solution. For this reason, we assume the location of the MGs is known to both the aggregator and the links and they therefore know the $p(\zeta_i)$ of MG i at each time step. The algorithm can be extended to different $p(\zeta_i)$, but without loss of generality and for the rest of the paper, we assume that all MGs are located in the same geographical location (e.g., city) and therefore have similar $p(\zeta_i)$. The general objective function can be

now expressed as follows:

$$\min_{x_i,c} \text{ Tobj} = \sum_{k=t+1}^{t+n_p} \Big[\mathbb{E}_\zeta[(c_\zeta[k]-c_d[k])^2] + \mathbf{\Phi}_g[k] + \sum_i \mathbf{\Phi}_i(x_i[k])\Big]$$
$$s.t.: \forall i,k,\zeta,j \in \mathbb{k}_i \begin{cases} \text{MG cons:} & \mathbf{\Omega}_i \\ \text{Link cons:} & \mathbf{\Gamma}_{L_{i,j}}(P_{i,j,\zeta}, P_{j,i,\zeta}) \\ \text{Grid cons:} & \begin{cases} \mathbf{\Omega}_g \\ \mathbf{\Gamma}_{g,i}(P_{g,i,\zeta}) \\ \sum_i P_{g,i,\zeta}[k] = c[k] \end{cases} \end{cases} \tag{5.20}$$

Notice that the links' constraints $\mathbf{\Gamma}_{L_{i,j}}$ and total net exchange power are coupled among MGs. For decoupling, we need to define the following auxiliary variables $\bar{P}_{g,i,\zeta} = P_{g,i,\zeta}$ and $\bar{P}_{i,j,\zeta} = P_{i,j,\zeta}$:

$$\min_{x_i,c} \text{ Tobj}$$
$$s.t.: \forall i,k,\zeta,j \in \mathbb{k}_i \begin{cases} \text{MG cons:} & \mathbf{\Omega}_i \\ \text{Grid cons:} & \begin{cases} \mathbf{\Omega}_g \\ \mathbf{\Gamma}_{g,i}(\bar{P}_{g,i,\zeta}) \\ \sum_i \bar{P}_{g,i,\zeta}[k] = c[k] \end{cases} \\ \text{Link cons:} & \mathbf{\Gamma}_{i,j}(\bar{P}_{i,j,\zeta}, \bar{P}_{j,i,\zeta}) \\ \text{Coupled cons:} & \begin{cases} \bar{P}_{g,i,\zeta} = P_{g,i,\zeta} \\ \bar{P}_{i,j,\zeta} = P_{i,j,\zeta} \end{cases} \end{cases} \tag{5.21}$$

Now according to [165], the dual function of (5.21) with respect to coupled constraints can

be expressed as:

$$\text{Tobjnew} = \sum_{k=t+1}^{t+n_p} \Bigg(\mathbb{E}_\zeta[(c_\zeta[k] - c_d[k])^2] \tag{5.22a}$$

$$+ \sum_i \frac{\rho^k_{g,i,\zeta}}{2} \mathbb{E}_\zeta \Big[\|\bar{P}_{g,i,\zeta}[k] - P_{g,i,\zeta}[k] + v_{i,\zeta}[k]\|_2^2 \Big] \tag{5.22b}$$

$$+ \sum_i \mathbf{\Phi}_i(x_i[k]) + \frac{\rho^k_{g,i,\zeta}}{2} \mathbb{E}_\zeta \Big[\|\bar{P}_{g,i,\zeta}[k] - P_{g,i,\zeta}[k] + v_{i,\zeta}[k]\|_2^2 \Big] \tag{5.22c}$$

$$+ \sum_i \sum_{j \in \mathbb{k}_i} \frac{\rho^k_{i,j,\zeta}}{2} \mathbb{E}_\zeta \Big[\|\bar{P}_{i,j,\zeta}[k] - P_{i,j,\zeta}[k] + w_{i,j,\zeta}[k]\|_2^2 \Big] \tag{5.22d}$$

$$+ \sum_i \sum_{j \in \mathbb{k}_i} \frac{\rho^k_{i,j,\zeta}}{2} \mathbb{E}_\zeta \Big[\|\bar{P}_{i,j,\zeta}[k] - P_{i,j,\zeta}[k] + w_{i,j,\zeta}[k]\|_2^2 \Big] + \dots \Bigg) \tag{5.22e}$$

where $\rho^k_{i,j,\zeta}$ and $\rho^k_{g,i,\zeta}$ are corresponding Lagrange multipliers, and $v_{i,\zeta}$ and $w_{i,j,\zeta}$ are optimization control parameters that will be used to coordinate and guarantee the convergence of ADMM. Also, there are some constant terms that do not affect the optimization problem (for more information, see [165]). In objective function (5.22), the first and second terms are related to the main grid / aggregator, the third and fourth terms can be handled by each MG, and the last term will be optimized in the corresponding link $L_{i,j}$. For simplicity, a time-dependent variable without time index denotes the vector of all its values between time steps $[t+1, t+n_p]$. Now, a new objective function can be defined for each part:

- Main Grid:

$$\text{obj}_g(c, \mathbf{v}, \bar{\mathbf{P}}_g, \mathbf{P}_g) = (5.22a) + (5.22b) \tag{5.23}$$

  where $\mathbf{v}, \bar{\mathbf{P}}_g$ and $\mathbf{P}_g$ denote all values of $v_{i,\zeta}, \bar{P}_{g,i,\zeta}$ and $P_{g,i,\zeta}$, respectively.

- MG i:

$$\text{obj}_i^{MG}(v_i, \mathbf{u}_i, \bar{P}_{g,i}, P_{g,i}, \bar{\mathbf{P}}_i, \mathbf{P}_i) = (5.22c) + (5.22d) \tag{5.24}$$

  where $\mathbf{u}_i, \bar{\mathbf{P}}_i$ and $\mathbf{P}_i$ are all values of $u_{i,j,\zeta}[k], \bar{P}_{i,j,\zeta}[k]$ and $P_{i,j,\zeta}[k]$, respectively.

- Link $L_{i,j}$ (where $j \in \mathbb{k}_i$):

$$\text{obj}_{L_{i,j}}(u_{i,j}, \bar{P}_{i,j}, P_{i,j}) = (5.22e) \tag{5.25}$$

The proposed ADMM-based distributed SMPC algorithm is given in Algo. 1. The variables $v^0_{i,\zeta}$, $w^0_{i,j,\zeta}$, $\bar{P}^0_{g,i,\zeta}$ and $\bar{P}^0_{i,j,\zeta}$ are initialized at each time step t (line 1). Considering the location of each MG, the main grid / aggregator can calculate the pdf of solar irradiation $p(\zeta)$ and broadcast pair $(\zeta, p(\zeta))$ to the corresponding MG (line 2). By starting the consensus process (lines 4-11), the main grid / aggregator and links will send $v^n_{i,\zeta}, w^n_{i,j,\zeta}, \bar{P}^n_{g,i,\zeta}$ and $\bar{P}^n_{i,j,\zeta}$ values to the corresponding MG (lines 5 and 6).

Considering the proposed powers of the aggregator and links at iteration n, MG i should solve its optimization problem (5.26) and find the values of $P^{n+1}_{g,i,\zeta}$ and $\mathbf{P}^{n+1}_i$ (line 7). These values represent MG i's new suggestions for its energy requirements during the next consensus iteration $n+1$. Obviously, MG i tries to make a trade-off between its own goals and the tracking powers proposed by aggregator and links, without violating its constraints.

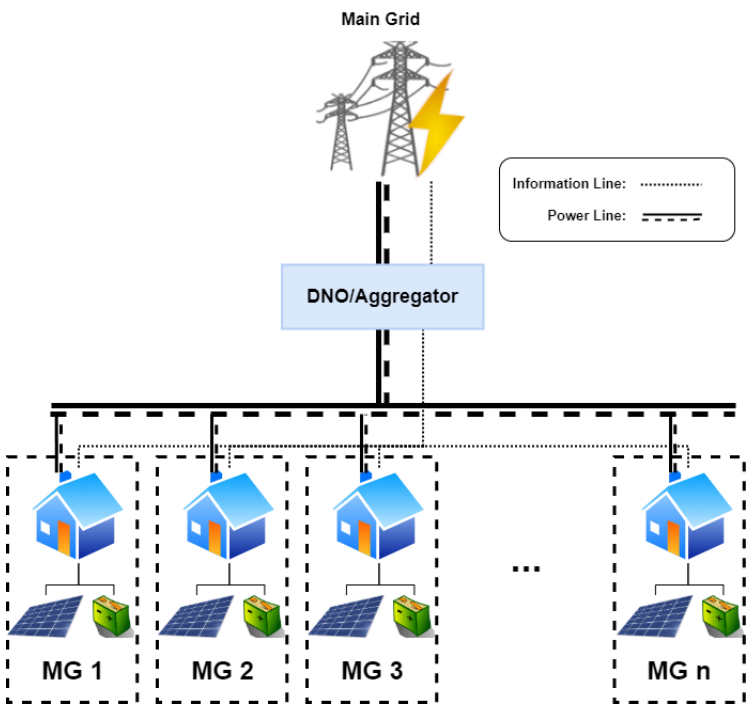

Figure 5.1 Example of MGs trading energy with the main grid

This information is then sent to the aggregator and the corresponding link $L_{i,j}$ (line 8). In the next step, considering the MGs' power requirement suggestions, the main grid / aggregator and each link $L_{i,j}$ can solve their own optimization problems (5.27) and (5.28) (lines 9 and

Algorithm 1: DMPC algorithm via ADMM

for *Time step* $t = 1, 2, \ldots$ **do**

Initialize $v^0_{i,\zeta}$, $w^0_{i,j,\zeta}$, $\bar{P}^0_{g,i,\zeta}$ and $\bar{P}^0_{i,j,\zeta}$, $\forall \zeta, i, j \in \Bbbk_i$;

Main grid/aggregator should broadcast $(\zeta, p(\zeta))$;

Set $n = -1$;

repeat

$n \leftarrow n + 1$;

for $\forall i, j \in \Bbbk_i$ *(in parallel)* **do**

Main grid/aggregator broadcasts $v^n_{i,\zeta}$ and $\bar{P}^n_{g,i,\zeta}$ to MG i;

Link $L_{i,j}$ broadcasts $w^n_{i,j,\zeta}$ and $\bar{P}^n_{i,j,\zeta}$ to MG i;

MG i should find values of $P^{n+1}_{g,i,\zeta}$ and $\mathbf{P}^{n+1}_i$:

$$P^{n+1}_{g,i,\zeta}, \mathbf{P}^{n+1}_i = \text{argmin} \quad \text{obj}^{MG}_i \qquad \text{s.t.:} \quad \mathbf{\Omega}_i \tag{5.26}$$

MG i should send $P^{n+1}_{g,i,\zeta}$ to main grid and $P^{n+1}_{i,j,\zeta}$ to link L_{ijl}, for all ζ and each $j \in \Bbbk_i$;

end

aggregator should find values of $\bar{\mathbf{P}}^{t+1}_g$:

$$c^{n+1}, \bar{\mathbf{P}}^{n+1}_g = \text{argmin} \ \text{obj}_g \tag{5.27}$$

$$\text{s.t.:} \quad \begin{cases} \mathbf{\Omega}_g \\ \mathbf{\Gamma}_{g,i}(\bar{P}_{g,i,\zeta}) \\ \sum_i \bar{P}_{g,i,\zeta}[k] = c[k] \end{cases}$$

for $\forall i, j \in \Bbbk_i$ **do**

Link $L_{i,j}$ should find values of $\bar{P}^{n+1}_{i,j,\zeta}$s and $\bar{P}^{n+1}_{j,i,\zeta}$:

$$\bar{P}^{n+1}_{j,i,\zeta}, \bar{P}^{n+1}_{i,j,\zeta} = \text{argmin} \ \text{obj}_{L_{i,j}} + \text{obj}_{L_{j,i}} \qquad \text{s.t.}: \begin{cases} \mathbf{\Gamma}_{i,j}(x_i, x_j) \\ \bar{P}_{i,j,\zeta} = -\bar{P}_{j,i,\zeta} \end{cases} \tag{5.28}$$

end

Main grid and links should update $v^{n+1}_{i,\zeta}[k]$ and $w^{n+1}_{i,j,\zeta}[k]$, for all $\zeta, i, k \in [t+1, t+n_p]$ and $j \in \Bbbk_i$;

$$\begin{cases} v^{n+1}_{i,\zeta}[k] = v^n_{i,\zeta}[k] + (\bar{P}^{n+1}_{g,i,\zeta}[k] - P^{n+1}_{g,i,\zeta}[k]) \\ w^{n+1}_{i,j,\zeta}[k] = w^n_{i,j,\zeta}[k] + (\bar{P}^{n+1}_{i,j,\zeta}[k] - P^{n+1}_{i,j,\zeta}[k]) \end{cases} \tag{5.29}$$

until $\sum_{i,\zeta} \|v^{n+1}_{i,\zeta} - v^n_{i,\zeta}\|^2_2 + \sum_{\zeta,i,j} \|w^{n+1}_{i,j,\zeta} - w^n_{i,j,\zeta}\|^2_2 \leq \epsilon$ *or maxItr*;

Apply $P^{n+1}_{g,i}[t+1]$ and $P^{n+1}_{i,j}[t+1]$ for all $i, j \in \Bbbk_i$;

$t \leftarrow t + 1$

end

10, respectively). Solving these optimization problems makes it possible to determine the values of c^{n+1}, $\bar{\mathbf{P}}_g^{n+1}$ and $\bar{P}_{i,j}^{n+1}$, which are the aggregator's and links' new proposed powers after considering the MGs' suggestions. Also, the coordination values $\mathbf{v}$ and $\mathbf{w}_i$ are updated at the level of the main grid / aggregator and links (line 11). These values are updated in the direction that the aggregator's and links' proposed powers become as close as possible to those proposed by the MGs. The consensus process is finished if the difference in proposed powers is less than a fixed threshold or the maximum number of iterations, $maxItr$, is reached.

Finally, after the consensus process is finished,the MGs should set their buildings' setpoints at $\mathbf{y}^i[t+1]$ and should wait until the value of $\zeta_i[t+1]$ is reached, and the corresponding scenario can be applied based on that. Meanwhile, the algorithm can go to the next time step by setting $t \leftarrow t+1$ and starting over from line 1. In the case of P2P, the value of $\mathbb{E}_\zeta\left[\rho_{i,j,\zeta}^{t+1} w_{i,j,\zeta}^{n+1}[t+1]\right]$ can be used as the MG clearing price, the power exchange price among MGs in market equilibrium [214].

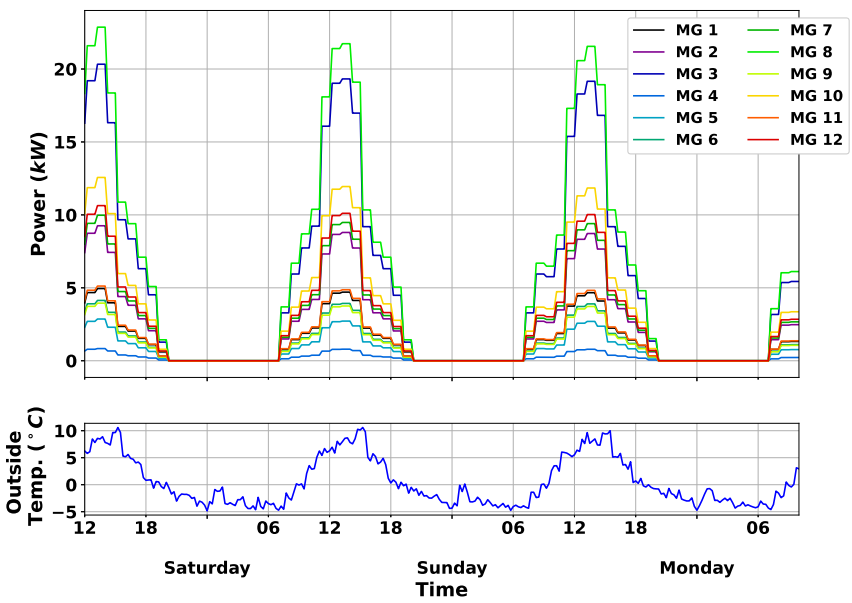

Figure 5.2 Generated PV power of MGs (top) and outside temperature (bottom)

5.5 Case Study

In order to demonstrate the performance of the proposed distributed algorithm, the algorithm is applied to a single line IEEE 12-bus network of buildings integrated with PV panels and a battery. We define the network adjacency matrix, which expresses the network, as follows:

$$\Upsilon = \Big[\upsilon_{i,j} | \upsilon_{i,g} = 1, \upsilon_{i,j} = 0, \forall i, j \in \Psi\Big]$$

Fig. 5.1 illustrates the aforementioned network structure. To consider various roof-top PV installed capacities, different sizes of PV panels are used: 1kW, 2.5kw, 5kW (for 4 houses), 10kw (for 3 houses), 12kw and 22kW (for 2 houses) PV panels are assumed to be installed. At each time step, MGs can either buy energy from or sell it to the main grid through the aggregator. It is assumed that all MGs are located in the same geographical area and so the difference between the MGs' probability density function (pdf) is negligible. The thermal satisfaction of building occupants, the zones temperatures in each MG's building are randomly set between 19° and 23° Celsius during the daytime (from 7_{AM} to 10_{PM}), and are changed daily. During nighttime (from 10_{PM} to 7_{AM}) and for saving energy purpose, however, these set-points are set to their minimum admissible limit, 19°C. For this case study, a hierarchical structure is assumed for the network where the proposed algorithm is used as a high-level controller to manage the power exchanging among MGs and main grid. Therefore, a 15-minute time-step is chosen for ΔT and the same time-step is used both for discretizing building's RC-model and MPC time-step. Furthermore, to handle the variations of PV and other resources which are usually less than 15 minutes, it is assumed that primary and secondary control levels are available in each microgrid and can manage those variations.

A fixed price scheme as the one used in Quebec [221], is used for exchanging power with the main grid; MGs can buy energy from the main grid at a price of \$0.07/kWh or sell energy to it at a price of \$0.056/kWh. Also, we consider a total subscribed power (c_{desi}) of 9.5kW for 12 buildings. According to (5.17), by solving this optimization problem, the aggregator will decide the value of $c[k]$ at each time step; however, choosing a different value than $c_{desi}[k]$ will come at a heavy price in terms of $(c[k] - c_{desi}[k])^2$. To maintain the accuracy of the solar irradiation predictions, a 90-minutes prediction horizon with time-step of 15 minutes ($np = 6$) is chosen for MPC. Besides, as mentioned in Section 5.3.2, due to computational limitations, the probability density function $p(\zeta[k])$ should be discretized to scenarios. In this simulation, we consider three different scenarios for irradiation ζ at time step k;

- similar sun irradiation $\zeta_n[k]$ as the predictions, with probability of $p(\zeta_n[k]) = 0.7$
- a lower level of sun irradiation $\zeta_l[k]$ than the predictions, 15% lower than normal ($\zeta_l[k] = 0.85\zeta_n[k]$), with probability of $p(\zeta_l[k]) = 0.2$
- a higher level of sun irradiation $\zeta_u[k]$ than the predictions, 10% higher than normal

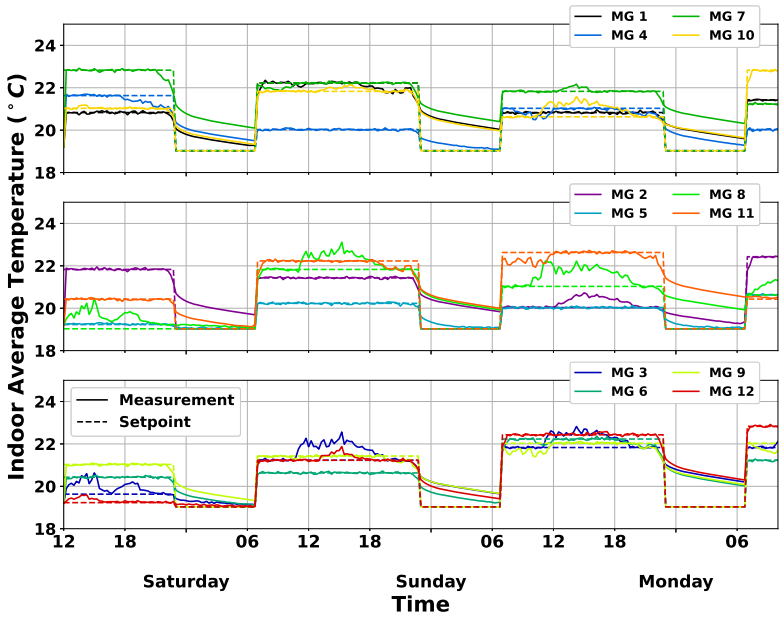

Figure 5.3 Buildings' average temperatures and setpoints

$(\zeta_u[k] = 1.1\zeta_n[k])$, with probability $p(\zeta_l[k]) = 0.1$.

Therefore, at the beginning of each time step, the prediction horizon times the number of different scenarios (6×3) for both $\zeta_m[k]$ and $p(\zeta_m[k])$ $(m \in \{n, l, u\}$ and so a total of 36 numbers) should be calculated and broadcast to all MGs to help them solve their optimization problem.

Fig. 5.2 shows the generated PV power of each MG. Although the generated power varies between 0 and 12kW, it was expected because the small-sized MGs 4 and 12 produce less and MGs 3 and 8 produce more PV power compared to the other MGs. In this simulation and for simplicity, we assume just solar irradiation has a stochastic behaviour, and the outside temperature is deterministic and can be predicted at least for the prediction time horizon.

Each simulated building has 13 different zones, 9 of which have access to HVAC. One of the MGs' objectives is to control these zones' temperature around desired setpoints. The average temperature of the MGs' buildings and their power consumptions are shown in Fig. 5.3 and Fig. 5.4, respectively. In the early hours of the simulation, depending on the difference between its initial and desired temperatures, each MG needs different amount of power to satisfy its comfort objectives; MGs with lower temperature setpoints such as No. 3, 5, 8 and 12 require less amount compare to the others. This behaviour, however, becomes more

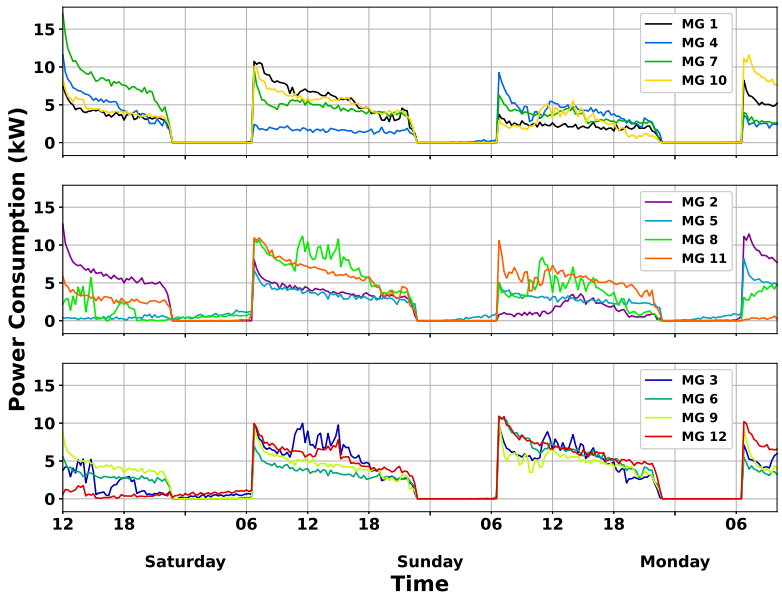

Figure 5.4 Buildings' power consumption

reasonable in the days that follow. According to Fig. 5.3, due to their nighttime lower setpoints (19°C), other MGs except the four mentioned above, reduce their temperatures and so their power consumption, near the end of the daytime 10_{PM}, Fig. 5.4. This behaviour arises from the looking ahead characteristic of MPC and the trade-off property of the objective function (5.14), which encourages MGs to lower their temperatures in advance to reduce the amount of purchased power from the grid. MGs No. 3, 5, 8 and 12, on the other hand, have almost the same setpoints during first day and night times, and so they do not need to reduce their consumption, anymore. In fact, in order to preserve their occupants' comfort during nighttime, they need to increase their power consumption, otherwise due to lower outside temperature (Fig. 5.2), their indoor temperatures will drop below admissible minimum limit. The same pattern can be found in MG No. 5 behaviour during next days nighttime, when they increase their consumption to preserve their comforts.

Figs. 5.5 and 5.6 show the state of charge and charging/discharging power of the batteries, respectively. As it can be seen in Fig. 5.5, almost all MGs try to store extra electrical power generated by the PV panels during the day and use that energy later. Using the thermal capacitance of the building is another way of saving this extra energy. This effect can be seen obviously in MGs No. 3 and 8, and during the third day in MGs No. 2 and 10 when, due to the physical constraints of the batteries (either maximum charging rate or SOC), MGs

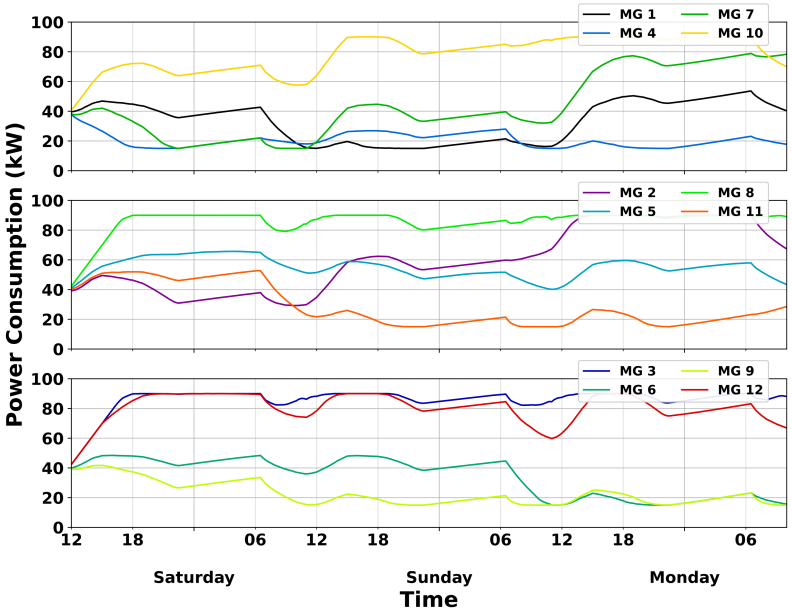

Figure 5.5 State of charge (SOC) of MGs' batteries

can save extra energy by preheating their buildings to increase inside temperatures. Fig. 5.7 shows, although MGs No. 3 and 8 use preheating method to store PV generated power, but their temperatures are kept in their comfort zone.

Behaviours of MGs during nighttime are also of interest, when despite their consumption profiles, they receive the same amount of power from main grid unless they have some limitations (e.g., soc limitations) to store it.

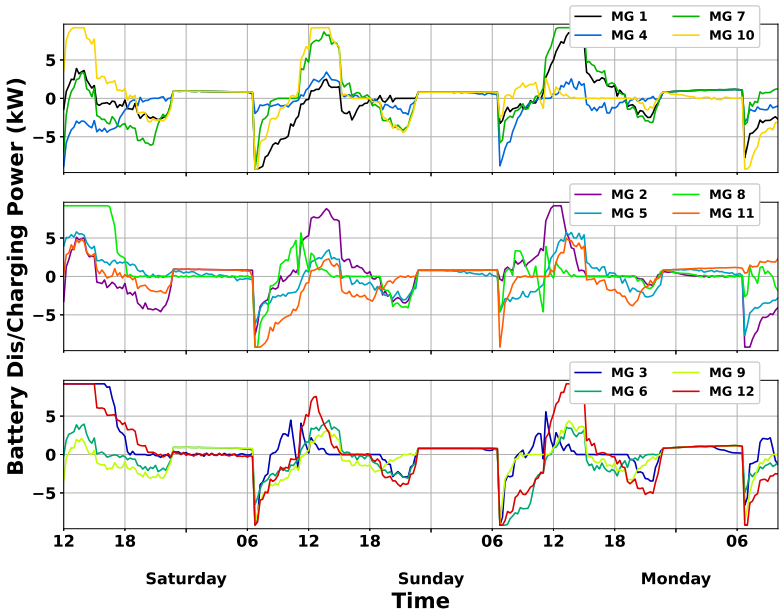

Figure 5.6 Charging and discharging status of MGs' batteries

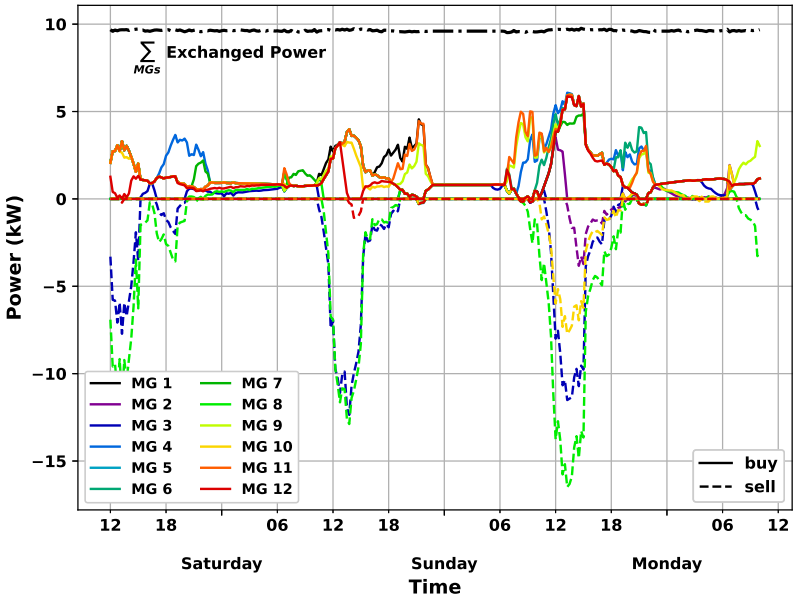

Figure 5.8 Total of exchanged power (dashed-dot line) and power exchanged between MGs and main grid (solid lines and dash lines).

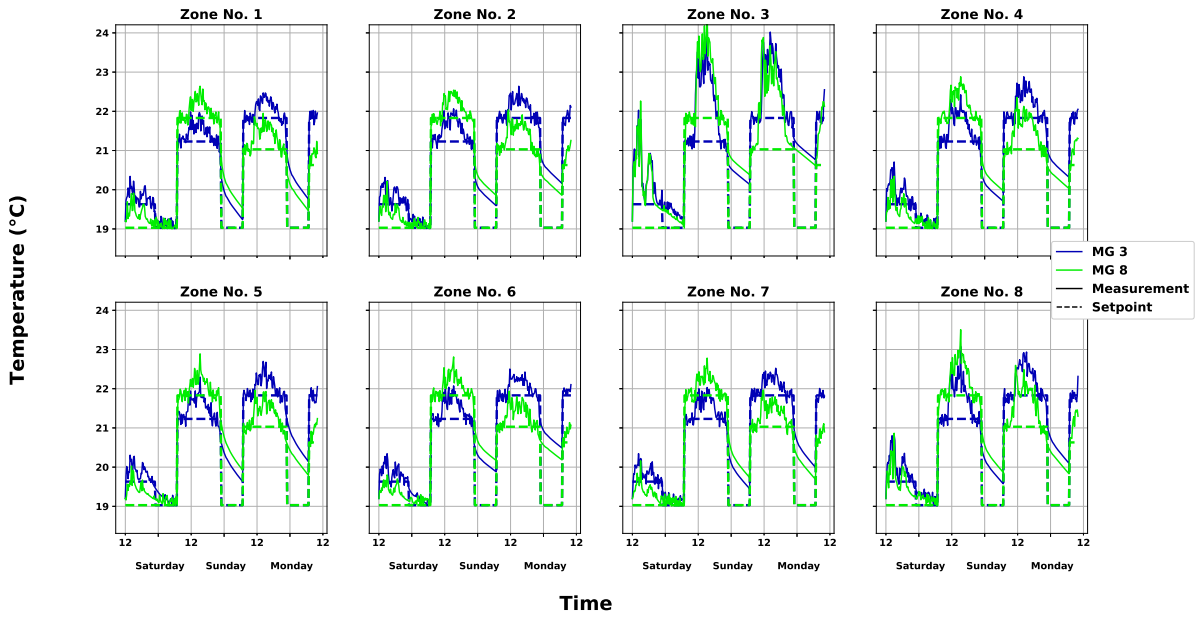

Figure 5.7 Indoor temperatures of two MGs for each zone.

The power exchanged between the MGs and main grid through the aggregator is illustrated in Fig. 5.8. As mentioned before, subscribed power for this network is set exactly to 9.6kW. The black dashed-dot line in the figure shows the total power exchanged (power bought minus power sold) and, as it is shown, this value is almost fixed around 9.5kW, which is the main objective of peak load limiting. The following table gives more details about the results:

desired MDL	average	min	max
9.6kw	$\simeq$9.626kw	$\simeq$ 9.514kw	$\simeq$9.76kw

As can be seen, with a small deviation (maximum 150 W), the MGs' total power consumption is limited around MDL. To achieve this goal, collaboration between the MGs is needed. For example, during the second day, MGs No. 3 and 8 sell part of their PV-generated power to the main grid and store the rest of that power either by preheating the building and increasing building temperatures without violating occupants' comfort or store it in their battery. This strategy will later let them sell more of their generated power to the main grid, to keep total exchange power at a fixed level.

From practical viewpoint, we simulated three days of this network on an Intel Core i7-7700@3.60 GHz laptop, using IBM ILOG CPLEX Optimization Studio API for python (docplex) to solve the optimization problems. Leveraging by parallel programming, six cores out

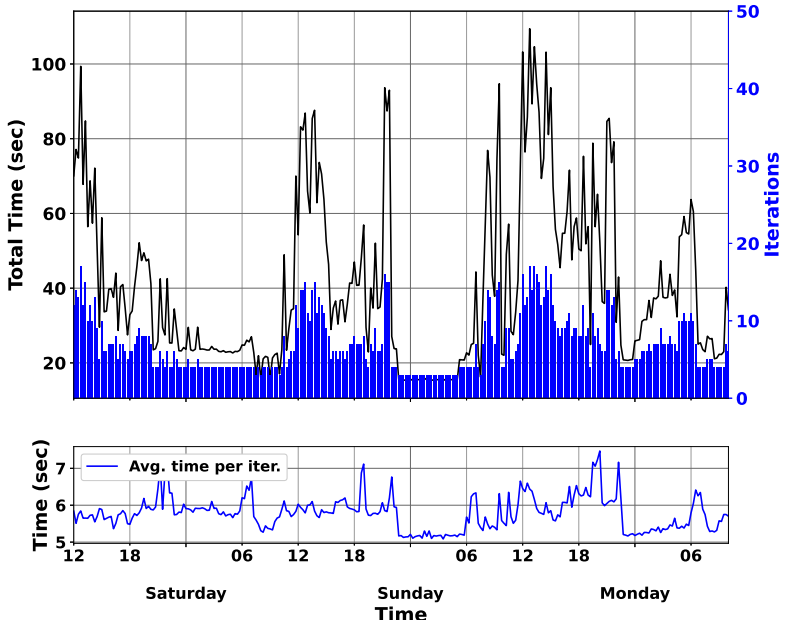

Figure 5.9 Iterations information; top) Number of iterations (blue bars) and total consumed time (red line) to reach a consensus per each step. bottom) Average time per each iteration.

of laptop's 8 cores were used to run lines 5 to 8 of algorithm 1 in parallel and the operation time was then recorded for each iteration. It means, to simulate 12 MGs, these 6 cores should be deployed twice and the real operation time of each iteration is so half of the recorded ones. Fig. 5.9 illustrates the performance of consensus process. As it can be seen in the top figure, the necessary time and iterations for MGs and aggregator to find the optimal solution are reasonably small, less than 100 seconds and 20 iterations. Although, in some steps, more iterations and time are required, on average, 40 seconds and 8 iterations are needed for the consensus process. Note that choosing a reasonable 15-minutes time step not only guarantees the feasibility of algorithm in time steps where more iterations and time are needed, but also can handle other unseen delays such as communication or response time of HVACs. This makes the algorithm suitable for real-time applications.

5.6 Conclusion

In this paper, we propose an ADMM-based distributed stochastic model predictive control framework for a network of building-integrated microgrids. The problem is formulated in the form of a two-stage stochastic optimization problem. The first-stage variables are related to buildings' zone temperatures, while the second-stage variables are exchanged power and

the charging/discharging of the batteries. This formulation makes it possible for networks to capture the uncertainties of renewable resources by exchanging as little information as possible, such as the location of MGs for finding the value of $p(\zeta_i)$. Thanks to ADMM, the privacy and reliability of the network is preserved and the convergence of the consensus process is guaranteed. Simulation results prove the performance of the proposed method in such networks, and due to its fast convergence, it can be used in real-time control. For future works, considering the uncertainties of loads with unknown distribution, investigating the effects of other types of loads such as EVs and EWH, and moving towards more intelligent methods can be considered.

5.7 Appendices

5.7.1 Appendix A: Details of Building RC Model

In this project, We modeled a real triplex home Fig. 5.10, using real data of home. This home has three floors with 15 rooms and closets, of which 9 have access to HVAC systems and so only their temperatures are controllable. Vector $\mathbf{u}^i$ and $\mathbf{y}^i$ in equation (5.1) denote these rooms HVACs' powers and temperatures. It is also assumed that each floor ceiling is thermal-proof and according to its blueprints two different types of walls are used in this building: Internal walls and external walls. Obviously, external walls are more resistant against thermal conduction. Detailed information of building such as materials, thickness, density, thermal resistance and capacitance are shown in table 5.1 which can easily be found from building's blueprints. For the windows, we consider the same material with the same thermal parameters but different area.

Table 5.1 Wall types and their materials; Thermal resistance and heat capacitance units are (m°K/W) and (J/kg°K) respectively.

Wall Type	**Materials (Thickness cm)**	
ExtWall	EP(0.01),MI(0.1),C(0.15),IP(0.01)	
IntWall	IPP(0.015),RW(0.07),IPP(0.015)	
Identifier	**Description (Density kg/m^3)**	**Thermal Res.& Cap.**
IPP	Interior Panel Plasterboard (700)	1000 & 4.8
EP	External Plaster (1600)	1000 1.2
IP	Internal Plaster (1400)	1000 1.4
RW	RockWool (90)	612 27.8
MI	Mineral Insulation StoTherm (90)	830 27.8
C	Concrete (2000)	1000 0.6

Figure 5.10 The model of studied triplex home(This figure is plotted by [222]).

In the next step, each element of building will be replaced by its equivalent thermal values and using the map of building, they can then be connected together to build a electrical circuit network. Fig. 5.11 show the equivalent electrical circuit of thermal network of 3rd floor of the mentioned home. In this circuit, each node represents temperature of an element inside the building, e.g. first layer of third floor south ExtWall. Vector $\mathbf{x}^i$ in equation (5.1) represents these temperatures. Since, the ceilings are assumed to be heat-proof, the same method can be applied to other floors to obtain their models. Finally, effects of 6 different types of disturbance are consider for this building; outside temperature, ground temperature and 4 directions of sun irradiation. These disturbances are shown in equation (5.1) by $\mathbf{v}^i$.

After providing these information, and also a map of the building, a MATLAB toolbox, proposed in [223], was deployed to generate equivalent electrical circuits. Choosing a 15 minutes time-step, this continuous model was then discretized to a discrete model which is represented in equation (5.1).

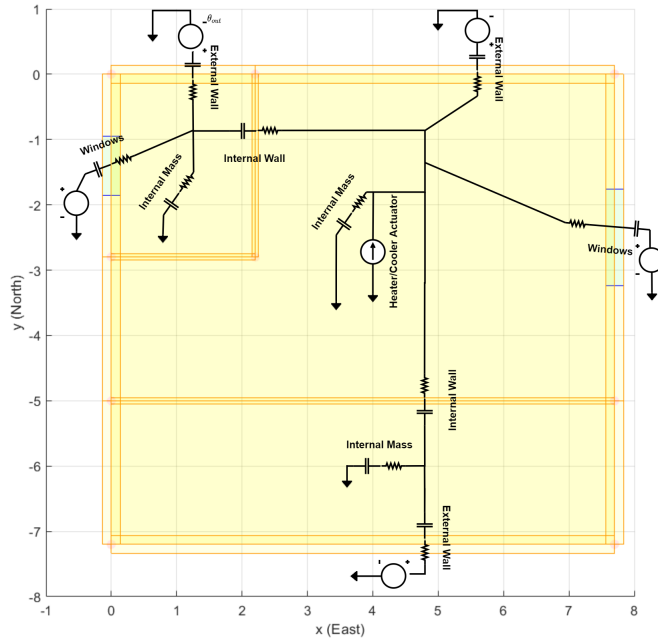

Figure 5.11 An example of thermal network of 3rd floor of mentioned home.

5.7.2 Appendix B: Proof of Theorem 1

First we show that if matrix D has a diagonal form with positive elements, then a solution to optimization problem

$$\min_{x,z} f(x) + g(z) \quad s.t. : Ax + Bz = c \tag{5.30}$$

where f and g are convex functions, can be found by following iterative method:

$$\begin{aligned} x^{k+1} &:= \underset{x}{\operatorname{argmin}}(f(x) + (\rho/2)\|D(Ax + Bz^k - c + u^k)\|_2^2) \\ z^{k+1} &:= \underset{z}{\operatorname{argmin}}(g(z) + (\rho/2)\|D(Ax^{k+1} + Bz - c + u^k)\|_2^2) \\ u^{k+1} &= u^k + (Ax^{k+1} + Bz^{k+1} - c) \end{aligned} \tag{5.31}$$

Note that, since matrix D is a positive definite matrix, it can be multiplied to both side of problem (5.30) constraint. Now if we rewrite the augmented Lagrangian with quadratic

penalty term, we have:

$$
\begin{aligned}
t := Ax+Bz-c=0 \Leftrightarrow Dt=0 \Rightarrow \\
L(x,z,y) &= f(x)+g(z)+y^T Dt+\frac{1}{2}\|Dt\|_2^2 \\
&= f(x)+g(z)+\frac{1}{2}(2y+Dt)^T Dt \\
&= f(x)+g(z)+\frac{1}{2}(y+Dt+y)^T(y+Dt-y) \\
&= f(x)+g(z)+\frac{1}{2}\|y+Dt\|_2^2-\frac{1}{2}\|y\|_2^2
\end{aligned}
$$

D is invertible (D^{-1} exists) and is also positive definite. So $y = Du$ is a bijection map between u and y spaces and as a result, we can define new variable u such that $u = D^{-1}y$:

$$
\begin{aligned}
&L(x,z,u) = \\
&\qquad f(x)+g(z)+\frac{1}{2}\|D(Ax+Bz-c+u)\|_2^2-\frac{1}{2}\|Du\|_2^2
\end{aligned}
$$

Finally, by applying Gauss-Seidel iteration method, the same update rules as (5.31) can be found for x^{k+1} and z^{k+1}. For variable y, we have:

$$
\begin{aligned}
y^{k+1} &= y^k + Dt^{k+1} \\
&= y^k + D(Ax^{k+1}+Bz^{k+1}-c) \xRightarrow[D^{-1}\text{exist}]{y=Du} \\
u^{k+1} &= u^k + (Ax^{k+1}+Bz^{k+1}-c)
\end{aligned}
$$

Now just by setting $D \leftarrow \sqrt{\mathbf{p}(\boldsymbol{\zeta})}D$, we have:

$$
\begin{aligned}
&\|\sqrt{\mathbf{p}(\boldsymbol{\zeta})}D(Ax^k+Bz_\zeta-c_\zeta+u_\zeta^k)\|_2^2 \\
&\qquad = \sum_\zeta p(\zeta)\|d_\zeta(Ax^k+Bz_\zeta-c_\zeta+u_\zeta^k)\|_2^2 \\
&\qquad = \mathbb{E}_\zeta\Big[\|D(Ax^k+Bz_\zeta-c_\zeta+u_\zeta^k)\|_2^2\Big]
\end{aligned}
$$

and update rules (5.19) can be found easily and it completes our proof.

CHAPTER 6 ARTICLE 3: HIERARCHICAL DISTRIBUTED ENERGY MANAGEMENT FRAMEWORK FOR MULTIPLE GREENHOUSE CONSIDERING DEMAND RESPONSE

Authors: Ehsan Rezaei, Hanane Dagdougui, Kianoosh Ojand
Accepted for publication: IEEE Transactions on Sustainable Energy, 2022

Abstract: Greenhouses are a key component of modernised agriculture, aiming for producing high-quality crops and plants. Furthermore, a network of greenhouses has enormous potential as part of demand response program. Saving energy during off-peak time, reducing power consumption and delaying the start time of subsystems during on-peak time are some strategies that can be used to limit power exchanged with the main grid. In this work, a hierarchical distributed alternating direction method of multipliers-based model predictive control framework is proposed that has two main objectives: 1) providing appropriate conditions for greenhouses' crops and plants to grow, and 2) limiting the total power exchanged with the main grid. At each time step in the framework, an aggregator coordinates the greenhouses to reach a consensus and limit the total electric power exchanged while managing shared resources, e.g., reservoir water. The proposed framework's performance is investigated through a case study.

Keywords

distributed control, demand response, network of greenhouses, load shifting, load shaving

6.1 Introduction

International economic development, predicted population growth, the expansion of cities and extreme weather patterns put considerable pressure on the restricted water resources and arable lands of the earth [137]. Therefore, using traditional agriculture is an inadequate strategy to cover the growing needs of the population and alleviate food security concerns [224]. Based on a report published by Canada's Minister of Environment and Climate Change, approximately 10% of annual greenhouse gas emissions in Canada are due to agricultural activities. At the current values, one-third of global greenhouse gas emissions are due to the food production system [139]. The COVID-19 pandemic has had various impacts on agriculture activities; it has accentuated the need for sustainable self-reliant food economies [225].

Sustainable greenhouse systems present a strong opportunity to increase the productivity and efficiency of the modern agriculture sector. However, if greenhouse energy consumption is not controlled, it may cause adverse environmental impacts and increase peak demand. Hence, it is vital to develop a sustainable and reliable energy management system to control commercial greenhouses. Using a distributed energy management system for greenhouses can lead to several benefits. It can increase the penetration of distributed energy resources, reduce greenhouse gas emissions along with the greenhouses' dependency on non-renewable energy sources and create additional income for the farmer through bidirectional energy exchange with the grid. Microgrid systems can be designed to support greenhouses. With their potential flexibility, they can offer myriad benefits including a reliable and resilient energy supply, peak load reduction and increased penetration of renewable energy resources. These systems can be optimised to provide the energy required for ideal growing conditions. Recently, research activities demonstrating the benefits of demand response have been widely developed for the residential and commercial sectors. The potential of demand response for agricultural consumers is still challenging and deserves careful attention.

In the literature, there are several studies that have investigated various methods to reduce energy consumption in greenhouses. Some examples of these methods include enhancing the efficiency of the energy production equipment including water irrigation systems [141], upgrading the structure of greenhouses [226], and controlling indoor climate conditions [227].

In [228], the authors propose an idea to integrate smart agriculture with clean energy. In fact, they conduct a comprehensive review in order to depict a road map for integrating smart agriculture with clean energy. They also summarise the recent technologies, advantages and bottlenecks. In their approach they suggest using extra clean energy to help agricultural production. In addition, when following their approach, smart agriculture can support the main grid through the penetration of clean energy. A model for an internet of things(IoT)-based based agricultural greenhouse system is investigated in [229]. The proposed greenhouse management system aims to enhance crop production by utilising automated detection, controlling important greenhouse climate factors and decreasing human intervention. A cooperative control mechanism for a cluster of microgrids consisting of multiple smart greenhouses is proposed in [151]. It uses a centralised model predictive control (MPC) to manage the performance of microgrids and reach a net-zero framework.

Energy management systems for individual greenhouses are addressed in several studies. The authors of [230] use NSGA-II (a multi-objective evolutionary algorithm) as well as a combined microclimate crop yield model to develop a model to increase crops' production yield by applying a microclimate control setpoints strategy. In [231], two problems are addressed for

a single greenhouse. First, the authors solve a sizing problem to find the optimal number of renewable energy and storage units. Afterwards, they propose a scenario-based robust optimisation approach to maximise income in grid-connected mode and minimise costs in islanded mode. Their results show that the lowest objective function value is reached when the investment in combined heat and power systems is half of the investment in solar power and 4 times that in energy storage systems. A stochastic multi-timescale energy management system for greenhouses considering a photovoltaic (PV) system, a combined heat and power unit and an energy management system is introduced in [232]. In this study, the uncertainties of renewable energy sources (RES) and weather conditions are considered by formulating the problem as a multi-timescale Markov decision process. A climate control problem for a single greenhouse is addressed in [233]. To solve this problem, an indirect adaptive fuzzy control scheme is suggested for a multi-input multi-output non-affine nonlinear system with unknown conditions and dynamics. In [234], a model-based predictive controller assisted by heater and ventilation windows is designed to adjust the indoor temperature of a greenhouse in order to reach setpoint tracking and reduce cost. In [149], a greenhouse environment controller using MPC is proposed. This controller aims to maintain the artificial lighting level, CO_2 rate, indoor greenhouse temperature and humidity within acceptable boundaries.

The intensification of greenhouse agriculture is now a growing reality around the world to meet the nutritional needs of humans. The clustered coordination of greenhouses integrating distributed energy resources is a new opportunity to better manage electricity consumption, increase agricultural demand-side flexibility to reduce peak demand and generate new revenue streams for farmers. To the best of the authors' knowledge, no studies have focused on developing a comprehensive distributed energy management system for a network of greenhouses, and if there are any, they contribute to centralised energy management systems, which impose vital data sharing with the controller [150].

In this work, we present an alternating direction method of multipliers (ADMM)-based MPC framework to manage a network of greenhouses in a distributed manner. The main contributions of this paper are:

- A hierarchical distributed framework to control a network of greenhouses that participate in the demand response programs. This framework helps the network to provide benefits to the electricity grid while reducing its energy costs.
- A mathematical model to control temperature, CO_2, lighting and irrigation subsystems that enables the framework to consider both load shaving and shifting for demand response programs.

- In the proposed framework, the aggregator is responsible for not only the coordination of greenhouses to limit the network's total power exchange with the main grid, but also managing shared resources, e.g., reservoir water. Therefore, the network can further contribute to the demand response program by controlling its subsystems (e.g., pumping system).
- Due to its fast convergence rate, the proposed framework can be used for practical projects. The simulation results show that the algorithm response time is less than 1 minute, which makes it suitable for real-time applications.

The rest of this paper is organised as follow: mathematical models of greenhouse subsystems with their objectives and constraints are presented in Section 6.2. In Section 6.3, the optimisation problems of each greenhouse and the aggregator are formulated, and the proposed framework is then introduced. The efficiency and performance of the proposed framework are demonstrated by a case study in Section 6.4 and finally, future work and the conclusion are discussed in Section 6.5.

6.2 Mathematical Modelling

Fig. 6.1 shows a network of greenhouses. As it is illustrated, each greenhouse has its own renewable energy resource (mostly PV panels), energy storage system (battery), temperature control, lighting, CO_2 and water subsystems. The greenhouses can exchange energy with the main grid through the aggregator, which also controls the shared resources such as the reservoir water. In the following subsections, mathematical models of the greenhouses' subsystems and the aggregator are presented and their constraints are discussed.

6.2.1 Modelling of Greenhouse Components

In each greenhouse, artificial lighting, CO_2 generation, HVAC (heating, ventilation and air conditioning) and water pumping subsystems are needed for microclimate control to achieve maximum plant growth and yield. These subsystems are modeled below with their constraints.

PV Panels

Each greenhouse is equipped with PV panels that generate power that can be used to cover greenhouse's energy needs or be either sold to the main grid or stored in the energy storage system. It is assumed that the PV panels work at their maximum power point when connected

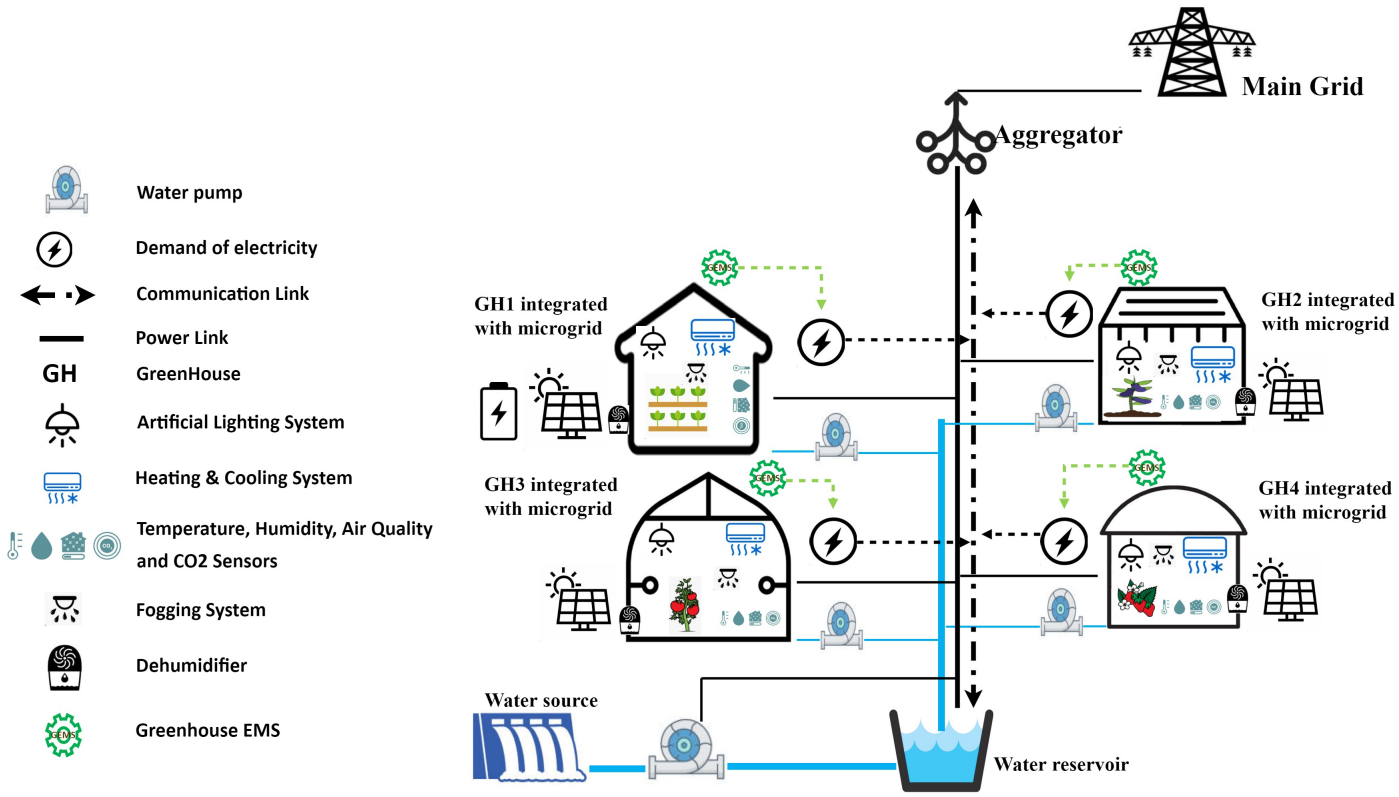

Figure 6.1 Conceptual model of the proposed network of greenhouses

to the main grid and generate the maximum possible PV power. The following model can then express the power generated by the PV panels:

$$u_{pv,i}[k] = A_{pv,i}\eta_{pv,i}P_{f,i}G[k] \tag{6.1}$$

where $A_{pv,i}$, $\eta_{pv,i}$ and $P_{f,i}$ are the PV panels' area, efficiency and packing factor, respectively, and their values depend on the panels technology of greenhouse i. The generated PV power $u_{pv,i}[k]$ depends also on the solar irradiation G at time step k, which is assumed to be the same for all greenhouses.

Energy Storage System (ESS)

Stored energy can be either used by the greenhouses or sold to the main grid. The ESS has an important role in the greenhouse demand response program; it can support load shifting

and shaving at peak times. The dynamic of a battery can be expressed as follows:

$$
\begin{aligned}
soc_i[k+1] &= \alpha soc_i[k] + (\beta_{ch,i} u_{ch,i}[k] - \frac{1}{\beta_{dch,i}} u_{dch,i}[k])\Delta T \\
\forall k: &\quad \begin{cases} 0 \leq u_{ch,i}[k] \leq u_{ch}^{max} \\ 0 \leq u_{dch,i}[k] \leq u_{dch}^{max} \\ soc_i^{min} \leq soc_i[k] \leq soc_i^{max} \end{cases} \\
\forall k, \beta_k \in \{0,1\}: &\quad \begin{cases} 0 \leq u_{ch,i}[k] \leq \beta_k u_{ch}^{max} \\ 0 \leq u_{dch,i}[k] \leq (1-\beta_k) u_{dch}^{max} \end{cases}
\end{aligned} \tag{6.2}
$$

where soc_i denotes the state of charge (SOC) of greenhouse i's battery, $u_{ch,i}$ and $u_{dch,i}$ represent its charging and discharging power, respectively, and $\alpha, \beta_{ch,i}$ and $\beta_{dch,i}$ are the self-discharging, charging and discharging efficiencies of the battery, respectively. The first group of constraints in (6.2) ensures the safety of the battery, and the second group makes sure that the battery does not charge and discharge at the same time.

Thermal Dynamic

Resistance-capacitance (RC) modelling is capable of capturing the thermal behavior of a greenhouse. Using an RC model requires the equivalent thermal capacitance and resistance models of the greenhouse's elements including the walls, roof and floor. These equivalent RC models are then combined to form an electrical circuit of the greenhouse and the greenhouse's thermal dynamic can then be expressed as:

$$
\begin{cases} \mathbf{x}_i[k+1] = A_i \mathbf{x}_i[k] + B_{u,i} \mathbf{u}_{G,i}[k] + B_{v,i} \mathbf{v}[k] + f_i(\mathbf{x}_i, \mathbf{u}_{G,i}) + g_i(\mathbf{x}_i, \mathbf{v}) \\ \mathbf{y}_i[k] = C \mathbf{x}_i[k] \end{cases} \tag{6.3}
$$

where $A_i, B_{u,i}, B_{v,i}$ and C are constant matrices depending on the construction materials of greenhouse i, and $\mathbf{u}_{G,i}$ and $\mathbf{v}$ are the HVAC power vectors and outside disturbances, respectively. Variable $\mathbf{x}_i[k]$ represents the temperature vector of the elements inside the greenhouse at time step k. Practically, it is not possible to measure all the values of temperature vector $\mathbf{x}_i$ directly, so the temperature vector $\mathbf{y}_i$ is introduced to represent the measurable temperatures, such as the indoor temperature. Functions f_i and g_i are modelling the nonlinear effects of $\mathbf{u}_{G,i}$ and $\mathbf{v}$ on $\mathbf{x}_i$. To simplify this model, two assumptions can be considered:

- The greenhouse is using an artificial ventilation system. In other words, the CO_2 system is also responsible for ventilation inside the greenhouse and has its own temperature

control loop that adjusts the temperature of the air injected into the greenhouse.

- Considering the model's accuracy, a time step ΔT bigger than the response time of the ventilation process is chosen. By choosing this ΔT, the dynamic of the ventilation system can be neglected.

As a result of these assumptions, the nonlinear terms f_i and g_i in equation (6.3) can be neglected and the thermal equivalent circuit of the greenhouse can be simplified as in Fig. 6.2. Also, to reduce the effects of model uncertainties and consider the impacts of the current control signal on the future of the system, the MPC methodology is used.

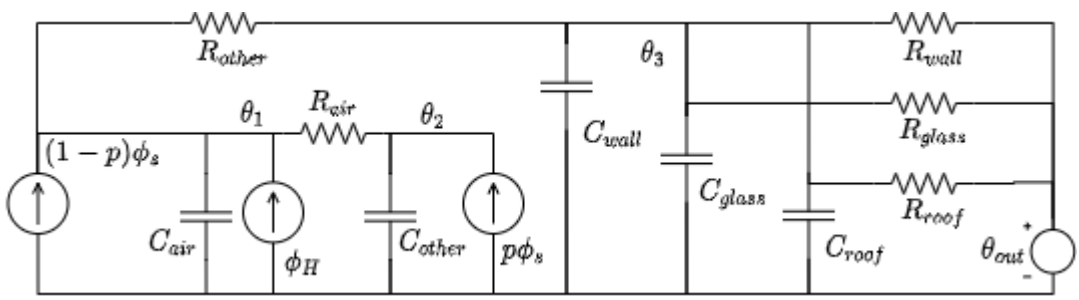

Figure 6.2 Thermal equivalent circuit of the greenhouse

The following greenhouse elements are modeled:

- *Walls, glass and roof*: Assuming walls, glass and roof are in thermal equilibrium at all times, their temperatures are denoted by θ_3.
- *Air*: The indoor air can also store thermal energy and needs to be considered. Due to HVAC and CO_2 generation activities, the indoor air is homogeneous; and the same temperature θ_1 can therefore be assumed for air at each point inside the greenhouse.
- *Other*: A major portion of the space in a greenhouse is occupied by the plants, which carry a huge portion of water, hence their thermal capacitance cannot be neglected and should be included in the modelling. It is worth mentioning that thermal capacitance and resistance are different for each type of crop. Crops' temperatures are expressed by θ_2.

If the vector $\begin{bmatrix}\theta_1[k+1] & \theta_2[k+1] & \theta_3[k+1]\end{bmatrix}^T$ is denoted by $\mathbf{x}[k+1]$, the state space equations of the circuit presented in Fig. 6.2 for greenhouse i can be reformulated as:

$$\mathbf{x}_i[k+1] = \underbrace{\begin{bmatrix} -a_i & a_i & 0 \\ a_i & a_i & 0 \\ \frac{r^i_{eq}}{e_i} & 0 & \frac{r^i_{eq}+R^i_{other}}{-e_i} \end{bmatrix}}_{A_i} \mathbf{x}_i[k] + \underbrace{\begin{bmatrix} \frac{1}{C^i_{air}} \\ 0 \\ 0 \end{bmatrix}}_{Bu,i} \mathbf{u}_{G,i}[k] + \underbrace{\begin{bmatrix} 0 & \frac{1}{C^i_{air}}(1-p_i) \\ 0 & \frac{1}{C^i_{air}}(p_i) \\ \frac{R^i_{other}}{e_i} & 0 \end{bmatrix}}_{B_{v,i}} \underbrace{\begin{bmatrix} T_a[k] \\ \phi_s[k] \end{bmatrix}}_{\mathbf{v}[k]}$$

$$\Rightarrow \mathbf{x}_i[k+1] = A_i\mathbf{x}_i[k] + B_{u,i}\mathbf{u}_{G,i}[k] + B_{v,i}\mathbf{v}[k] \tag{6.4}$$

where:

$$\begin{cases} a_i = 1/(C^i_{air}R^i_{air}) \\ e_i = c^i_{eq}r^i_{eq}R^i_{other} \\ c^i_{eq} = C^i_{wall} + C^i_{glass} + C^i_{roof} \\ \frac{1}{r^i_{eq}} = \frac{1}{R^i_{wall}} + \frac{1}{R^i_{roof}} + \frac{1}{R^i_{glass}} \end{cases}$$

In these equations, the thermal resistance of the roof, glasses, walls, indoor air and other elements are denoted by R_{roof}, R_{glass}, R_{wall}, R_{air}, and R_{other}, respectively. The constant values C_{roof}, C_{glass}, C_{wall}, C_{other} and C_{air} refer to the thermal capacitance of the roof, glass, walls, other elements and inside air, respectively. The power of solar irradiation at time k is shown by $\phi_s[k]$ with its $1-p_i$ portion absorbed by indoor air, making the indoor temperature increases compared to the outside temperature $T_a[k]$, whereas θ_1 shows the indoor (measurable) temperature:

$$\mathbf{y}_i[k] = \theta^i_1 = \underbrace{\begin{bmatrix} 1 & 0 & 0 \end{bmatrix}}_{C} \begin{bmatrix} \theta^i_1[k] \\ \theta^i_2[k] \\ \theta^i_3[k] \end{bmatrix} \Rightarrow \mathbf{y}_i[k] = C\mathbf{x}_i[k] \tag{6.5}$$

And so we have:

$$\begin{cases} \mathbf{x}_i[k+1] = A_i\mathbf{x}_i[k] + B_{u,i}\mathbf{u}_{G,i}[k] + B_{v,i}\mathbf{v}[k] \\ \mathbf{y}_i[k] = C\mathbf{x}_i[k] \end{cases} \tag{6.6}$$

Due to the actuators' limitations, the values of $\mathbf{u}_{G,i}$ should be restricted by $\mathbf{u}^i_{max\ cool}$ and $\mathbf{u}^i_{max\ heat}$ that express the actuators' maximum cooling and heating power vectors, respectively. In this case, the actuators' power vector constraint can be written as follows:

$$-\mathbf{u}^i_{max\ cool}[k] \leq \mathbf{u}_{G,i}[k] \leq \mathbf{u}^i_{max\ heat}[k] \tag{6.7}$$

During cooling (heating) periods, the value of $\mathbf{u}^i_{max\ cool}$ ($\mathbf{u}^i_{max\ heat}$) should be set to zero. On the other hand, the value of the indoor temperature θ^i_1 should also be limited at each time step to avoid damaging the plants:

$$\begin{aligned} &\theta^i_{min}[k] \leq \theta^i_1[k] \leq \theta^i_{max}[k] \\ \Rightarrow &\theta^i_{min}[k] \leq \mathbf{y}_i[k] \leq \theta^i_{max}[k] \end{aligned} \tag{6.8}$$

CO_2 Generator

The control of the CO_2 concentration level inside a greenhouse plays an important role in different phases of plant growth. The dynamic model described in [235] is used to model the CO_2 variation level:

$$c_i[k] = c_i[k-1] + \beta^i_1 p_i[k] + \beta^i_2(c_{out}[k] - c_i[k]) + \beta^i_3 \mathbf{y}_i[k] + \beta^i_4 I_i[k] + \beta^i_5 \tag{6.9}$$

where $c_i[k]$ and $p_i[k]$ denote the indoor CO_2 level and the pressure of CO_2 injected by the generator of greenhouse i at time k. The outside CO_2 level is represented by $c_{out}[k]$, whereas the β_js are constant variables that depend on various factors of greenhouse i such as its sizes, the crop type(s) and the ventilation system.

In the linearized equation (6.9), the second and third terms model the CO_2 injected into the greenhouse by the generator and the ventilation system, respectively. The fourth and fifth terms show the amount of CO_2 generated by the plants themselves and depend directly on the indoor temperature and lighting intensity. Due to the generator's fast response compared to time-step ΔT, its consumption power can be expressed as a linear relationship:

$$\begin{aligned} &u_{C,i}[k] = \alpha^i_C \times p_i[k] \\ &0 \leq u_{C,i}[k] \leq u^i_{max\ CO_2} \\ &c^i_{min}[k] \leq c_i[k] \leq c^i_{max}[k] \end{aligned} \tag{6.10}$$

where α^i_C represents the efficiency of the generator, while $u_{C,i}[k]$ is its power consumption. The first equation in (6.10) expresses the relationship between its power consumption and injected CO_2 pressure $p_i[k]$. The second equation limits the value of $u_{C,i}$, and last one ensures that the CO_2 level is limited to an appropriate range. For higher productivity, the indoor CO_2 level is usually kept higher than that outside. In other words, decreasing the indoor CO_2 level is usually done through the ventilation system, the third term on the right-hand side of equation (6.9).

Artificial Lighting

Due to the fast response of the artificial lighting system compared to other subsystems, its dynamic can be considered a linear relationship between its generated illumination $I_i[k]$ and power consumption $u_{I,i}[k]$ at each time step k:

$$u_{I,i}[k] = \alpha_L^i \times I_i[k] \tag{6.11}$$

where coefficient α_L^i is a constant value representing the efficiency of greenhouse i's lighting system. The crop growing process depends on the light, but providing the necessary artificial light at specific periods does not have high priority. In other words, inside a greenhouse, lights can be turned on with delay without a loss of productivity or quality, so the greenhouse can contribute even more to the demand response program:

$$\forall k: \quad \begin{cases} 0 \leq u_{I,i}[k] \leq u_{I,i}^{max} \\ \beta_I[k](I_{sp,i}[k] - \sigma I_i) \leq I_i[k] \leq \beta_I[k](I_{sp,i}[k] + \sigma I_i) \\ \beta_I[k] \in \begin{cases} \{0,1\} & \text{if } k - k_{sp,i}^I \leq \Delta k_{I,i} \\ \{1\} & o.w. \end{cases} \end{cases} \tag{6.12}$$

In this equation, $u_{I,i}^{max}$, $I_{sp,i}$ and σI_i denote the maximum power of the lighting system, the illumination setpoint and admissible tolerance from the illumination setpoint, respectively. $\beta_I[k]$ is a binary decision variable that depends on the turn-on delay $(k - k_{sp,i}^I)$ of the lighting system. If the delay is more than an acceptable delay $\Delta k_{I,i}$, then by setting $\beta_I[k] = 1$, the value of $I_i[k]$ is forced to be nonzero and limited to a specific range, and the lighting system can therefore participate in the peak load shaving only during peak periods. On the other hand, if the delay is less than $\Delta k_{I,i}$, then $\beta_I[k]$ can be either zero or one, resulting in a zero or nonzero $I_i[k]$. As a result, this subsystem can participate in both peak load shaving and peak load shifting during on-peak times.

Water Pump

Each greenhouse has access to a water pump installed at a fixed height. This system can be modeled as follows:

$$u_{W,i}[k] = \alpha_w^i \times q_{w,i}[k] \tag{6.13}$$

where $u_{W,i}$ and $q_{w,i}$ are the power consumption of the pump and the flow of injected water, respectively, and α_w^i denotes the efficiency of the water pump times ΔT. Similarly to the artificial lighting system, the water system can also participate in both the load shaving and the load shifting of the demand response program. In this case, by defining u_W^{max}, $q_{sp}, \sigma q, k_{sp,i}^W$ and Δk_W as the maximum admissible pump power, the water flow setpoint, the admissible tolerance of the water flow, the start time setpoint and the admissible delay time of the water pump, a similar set of constraints can be defined, $\forall k$:

$$\begin{cases} 0 \leq u_{W,i} \leq u_{W,i}^{max} \\ \beta_W[k](q_{sp,i}[k] - \sigma q_i) \leq q_{w,i}[k] \leq \beta_W[k](q_{sp,i}[k] + \sigma q_i) \\ \beta_W[k] \in \begin{cases} \{0,1\} & \text{if } k - k_{sp,i}^W \leq \Delta k_{W,i} \\ \{1\} & o.w. \end{cases} \end{cases} \tag{6.14}$$

Grid Interactions

Greenhouses are also connected to the main grid through an aggregator. In the event of insufficient PV power generation, they can buy the power they need from the main grid. The following equation expresses the power balance constraint of each greenhouse for all k:

$$\mathbf{u}_{G,i}[k] + u_{C,i}[k] + u_{I,i}[k] + u_{W,i}[k] + u_{ch,i}[k] - u_{dch,i}[k] - u_{pv,i}[k] = u_{grid,i}[k] \tag{6.15}$$

where u_{grid} represents the power exchanged with the main grid. Obviously, the sign of u_{grid} is positive if a greenhouse buys power from the main grid and negative if it sells power to the grid.

6.2.2 Modelling of Aggregator Components

In this work, the aggregator has two main objectives. First, it controls the aggregated power consumption of all greenhouses while keeping it below a maximum demand limit (MDL). Second, it controls the shared reservoir's water level by controlling its input water pump. These components are modeled below.

Water Reservoir

As shown in Fig. 6.1, greenhouses use the water stored in the reservoir for plant irrigation. The reservoir model can be described as:

$$v_R[k] = v_R[k-1] + \left(\delta_Q Q_w[k] - \sum_i \delta_i q_{w,i}[k]\right)\Delta T. \tag{6.16}$$

In this equation, v_R denotes the volume of water stored in the reservoir. At each time step, the water flow Q_w is pumped into the reservoir and $\sum_i q_{w,i}$ is pumped out. Depending on the properties of the input water pump (δ_Q), the greenhouses' pumps (δ_i) and time step ΔT, the water level can be increased or decreased. For safety and redundancy, the level of water in the reservoir should be maintained between a minimum v_{min} and a maximum v_{max}:

$$\forall k : v_{min} \leq v_R[k] \leq v_{max} \tag{6.17}$$

Similarly to the greenhouses' pumps, the following model and constraints can be used for the input water pump:

$$\text{Model:} \qquad u_R[k] = \alpha_R \times Q_w[k] \tag{6.18}$$

$$\text{Constraint:} \qquad 0 \leq u_R[k] \leq u_R^{max} \tag{6.19}$$

where α_R denotes the efficiency of the input water pump and u_R^{max} is the pump's maximum power.

Maximum Demand Limit

The aggregator's main goal is to keep the total power consumption under or near the MDL level which can be expressed as the following constraint:

$$\forall k : u_R[k] + \sum_i u_{grid,i}[k] \lesssim P_{MDL}[k] \tag{6.20}$$

where P_{MDL} is the MDL, and its value is set by the main grid.

6.3 Optimisation Problems

6.3.1 Greenhouse and Aggregator Optimisation Problems

The greenhouses' main goals are to provide suitable conditions for crops and plants growth, and reduce the amount of power purchased from the main grid. These two objectives can sometimes not be aligned in the same direction. Therefore, the objective function of greenhouse i can be defined as:

$$\begin{aligned}\min_{\mathbf{X}_i} \Phi_i(\mathbf{X}_i) = \sum_{k=t}^{t+n_p} \Big(& \gamma_y(\mathbf{y}_i[k] - \mathbf{y}_{sp,i}[k])^2 + \gamma_c(c_i[k] - c_{sp,i}[k])^2 + \gamma_I(I_i[k] - I_{sp,i}[k])^2 \\ & + \gamma_W(q_{w,i}[k] - q_{sp,i}[k])^2 + \gamma_g u_{grid,i}[k] \Big) \\ s.t. : \Omega_i = \Big\{ & \text{Constraints (6.1)-(6.2) and (6.6)-(6.15)}, \forall k \Big\}\end{aligned} \tag{6.21}$$

where t is the current time step, n_p is the prediction horizon and $\mathbf{X}_i$ is the set of decision variables of greenhouse i. Control parameters $\gamma_g, \gamma_y, \gamma_c, \gamma_I$ and γ_W are used to make a trade-off between different components of this objective function.

On the other hand, the optimization problem of the aggregator can be described as:

$$\begin{aligned}\min_{\mathbf{X}_g} \Phi_g(\mathbf{X}_g) &= \sum_{k=t}^{t+n_p} (p[k] - P_{MDL}[k])^2 \\ s.t. : \Omega_g &= \left\{ \forall k \begin{cases} u_R[k] + \sum_i u_{grid,i}[k] = p[k] \\ \text{Constraints: (6.16)-(6.19)} \end{cases} \right\}\end{aligned} \tag{6.22}$$

where $\mathbf{X}_g$ is the set of aggregator decision variables.

6.3.2 Optimization Problem Decomposition

In this paper, ADMM is used to decouple the main optimization problem. This decomposition approach ensures a general optimal solution is found while preserving the local information of each greenhouse and increasing the reliability of the network. To satisfy the objectives of the greenhouses and the aggregator, the general objective function of the network can be defined as a summation of all the objectives:

$$\begin{aligned}&\min_{\mathbf{X}_i, \mathbf{X}_g} \Phi(\mathbf{X}_g) + \sum_i \Phi(\mathbf{X}_i) \\ &s.t. : \Omega_g \cup \{\forall i : \Omega_i\}\end{aligned} \tag{6.23}$$

To solve this optimization problem in a distributed manner, only constraints (6.16) and (6.20) need information from all greenhouses and the aggregator; the rest of constraints can be assigned either to each greenhouse or the aggregator. To handle these constraints, first some auxiliary variables need to be defined:

$$\bar{q}_i = q_{w,i}, \qquad \bar{u}_i = u_{grid,i} \tag{6.24}$$

The variables with the bar can be interpreted as duplicates of the original variables that are going to be optimised and broadcasted by the aggregator. Now, constraints (6.16) and (6.20) change to the following format:

$$\bar{\Omega}_g = \left\{ \forall k : \begin{cases} v_R[k] = v_R[k-1] + \left(\delta_Q Q_w[k] - \sum_i \delta_i \bar{q}_i[k]\right)\Delta T \\ u_R[k] + \sum_i \bar{u}_i[k] \lesssim P_{MDL}[k] \\ \text{Constraints: (6.17)-(6.19)} \end{cases} \right\}$$

and the optimization problem (6.23) then changes to:

$$\begin{aligned} &\min_{\mathbf{X}_i, \mathbf{X}_g} \Phi(\mathbf{X}_g) + \sum_i \Phi(\mathbf{X}_i) \\ &s.t. : \{\bar{\Omega}_g\} \cup \{\forall i : \Omega_i, \bar{q}_i = q_{w,i}, \bar{u}_i = u_{grid,i}\} \end{aligned} \tag{6.25}$$

Note that in this current structure, the variables in (6.24) are the only coupled ones. Now, by applying the ADMM process, the optimization problem of each entity can be expressed as follows:

for greenhouse i:

$$\begin{aligned} &\min_{\mathbf{X}_i} \bar{\Phi}_i(\bar{\mathbf{q}}_i, \bar{\mathbf{u}}_i, \mathbf{v}_i, \mathbf{w}_i) = \Phi_i + |\mathbf{q}_{w,i} - \bar{\mathbf{q}}_i + \mathbf{v}_i\|_2^2 + \|\mathbf{u}_{grid,i} - \bar{\mathbf{u}}_i + \mathbf{w}_i|_2^2 \\ &s.t. : \Omega_i \end{aligned} \tag{6.26}$$

where the bold notation is used to represent the time aspect of variables; for example, $\bar{\mathbf{u}}_i = \left[\bar{u}_i[t], \ldots \bar{u}_i[t+n_p]\right]^T$.

and for the aggregator:

$$\begin{aligned} &\min_{\mathbf{X}_g, \bar{\mathbf{q}}_i, \bar{\mathbf{u}}_i} \bar{\Phi}_g(\mathbf{q}_{w,i}, \mathbf{u}_{grid,i}, \mathbf{v}_i, \mathbf{w}_i) = \Phi_g + \sum_i \left(\|\mathbf{q}_{w,i} - \bar{\mathbf{q}}_i + \mathbf{v}_i\|_2^2 + \|\mathbf{u}_{grid,i} - \bar{\mathbf{u}}_i + \mathbf{w}_i\|_2^2 \right) \\ &s.t. : \bar{\Omega}_g \end{aligned} \tag{6.27}$$

Algorithm 2: ADMM-based DMPC algorithm

H **for** *Time step* $t = 1, 2, \ldots$ **do**

1 Initialise $\mathbf{u}_i^0$, $\mathbf{w}_i^0$, $\bar{\mathbf{q}}_i^0, \bar{\mathbf{u}}_i^0$;

2 Set $n = -1$;

repeat

3 $n \leftarrow n + 1$;

for $\forall i$ *(in parallel)* **do**

4 Aggregator broadcasts $\mathbf{u}_i^n.\mathbf{w}_i^n, \bar{\mathbf{q}}_i^n$ and $\bar{\mathbf{u}}_i^n$ to greenhouse i;

5 greenhouse i finds values of $\mathbf{u}_{grid,i}^{n+1}$ and $\mathbf{q}_{w,i}^{n+1}$:

$$\mathbf{u}_{grid,i}^{n+1}, \mathbf{q}_{w,i}^{n+1} = \text{argmin}\, \bar{\Phi}_i(\bar{\mathbf{q}}_i^n, \bar{\mathbf{u}}_i^n, \mathbf{v}_i^n, \mathbf{w}_i^n)$$
$$s.t. : \Omega_i$$

6 $\mathbf{u}_{grid,i}^{n+1}$ and $\mathbf{q}_{w,i}^{n+1}$ are sent to aggregator;

end

7 Aggregator finds values of $\bar{\mathbf{q}}_i^{n+1}$ and $\bar{\mathbf{u}}_i^{n+1}$:

$$\forall i : \bar{\mathbf{u}}_i^{n+1}, \bar{\mathbf{q}}_i^{n+1} = \text{argmin}\, \bar{\Phi}_g(\mathbf{q}_{w,i}^{n+1}, \mathbf{u}_{grid,i}^{n+1}, \mathbf{v}_i^n, \mathbf{w}_i^n)$$
$$s.t. : \bar{\Omega}_g$$

8 Aggregator updates $\mathbf{v}_i^{n+1}$ and $\mathbf{w}_i^{n+1}$, for all i;

$$\begin{cases} \mathbf{v}_i^{n+1} = \mathbf{v}_i^n + (\mathbf{q}_{w,i}^{n+1} - \bar{\mathbf{q}}_i^{n+1}) \\ \mathbf{w}_i^{n+1} = \mathbf{w}_i^n + (\mathbf{u}_{grid,i}^{n+1} - \bar{\mathbf{u}}_i^{n+1}) \end{cases}$$

until $\sum_i \|\boldsymbol{v}_i^{n+1} - \boldsymbol{v}_i^n\|_2^2 + \|\boldsymbol{w}_i^{n+1} - \boldsymbol{w}_i^n\|_2^2 \leq \epsilon$ *or maxItr*;

9 Apply first elements of $\mathbf{u}_{grid,i}^{n+1}$ and $\mathbf{q}_{w,i}^{n+1}$ for all i;

10 $t \leftarrow t + 1$

end

Algorithm 2 presents the proposed ADMM-based distributed model predictive control (DMPC) for the network of greenhouses. At the beginning of each time step t, the values of $\mathbf{u}_i^0, \mathbf{w}_i^0, \bar{\mathbf{q}}_i^0$ and $\bar{\mathbf{u}}_i^0$ should be initialised (line 1). After the initialization step and at the start of the iteration process, the aggregator broadcasts the values of $\mathbf{u}_i^n.\mathbf{w}_i^n, \bar{\mathbf{q}}_i^n$ and $\bar{\mathbf{u}}_i^n$ to the corresponding greenhouse (line 4). After solving their optimization problems (line 5), the greenhouses send the values of $\mathbf{u}_{grid,i}^{n+1}$ and $\mathbf{q}_{w,i}^{n+1}$ to the aggregator (line 6). After receiving these values from all the greenhouses, the aggregator finds $\bar{\mathbf{q}}_i^{n+1}$ and $\bar{\mathbf{u}}_i^{n+1}$ using the received information and solves its optimization problem (line 7). Using gradient ascent, the aggregator updates the values of $\mathbf{v}_i^{n+1}$ and $\mathbf{w}_i^{n+1}$ as the final step in each iteration (line 8). The iteration process is finished whenever these values converge to the optimal point or n reaches its maximum

iteration value $maxItr$. Finally, as the MPC methodology proposes, each greenhouse applies the first element of $\mathbf{u}_{grid,i}^{n+1}$ and $\mathbf{q}_{w,i}^{n+1}$ (line 9), and the whole network moves to the next time step (line 10).

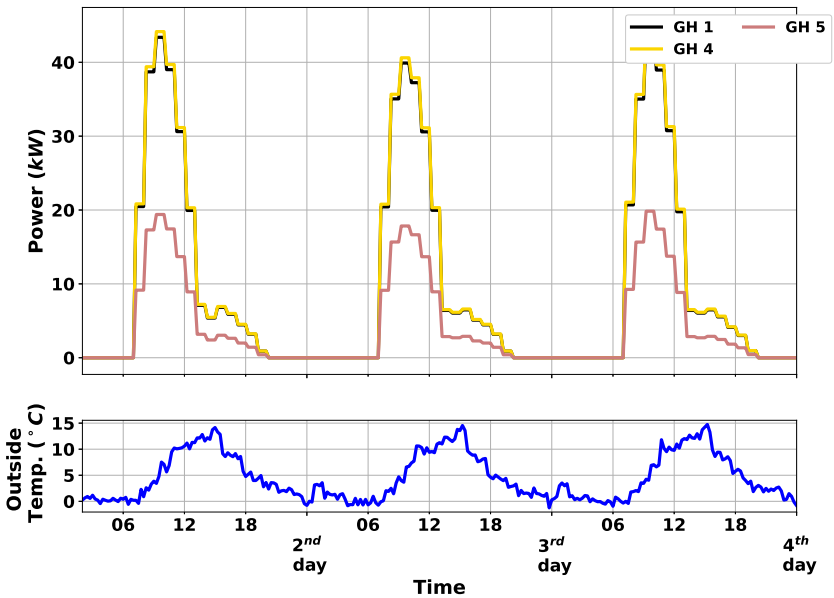

Figure 6.3 Top: PV generated power of each greenhouse. Bottom: Outside temperature.

6.4 Case Study

For the case study, a network of five greenhouses with different crops is simulated for three days. Although each greenhouse has its own energy storage system, only three of them have PV panels. Two have a 40kW panel, and the third has a 15 kW panel. We assume that all the greenhouses are located in a limited geographical area, therefore, similar outside temperature and disturbances are used for the simulation. The greenhouses' generated PV power and the outside temperature are shown in Fig. 6.3. The simulation time step ΔT is 15 minutes, and the prediction horizon is 90 minutes.

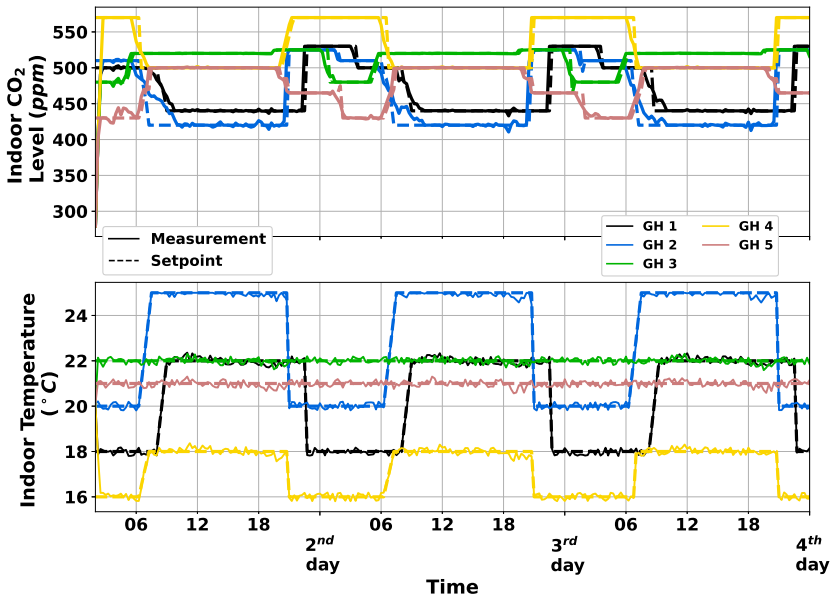

Figure 6.4 Top: Indoor CO_2 level. Bottom: Indoor temperature.

In each of the four stages of crop growth (seed, sprout, seedling and adult plant), some of the environmental parameters have a higher impact on the quality of the final product. For example, in the seed stage, controlling indoor temperature using the HVAC subsystem is more important than controlling the CO_2 level. To control the importance of each subsystem, controlling parameters γ are introduced in the equation (6.21). For the simulation, the following table is used to set the values of γ:

Table 6.1 Control parameters values.

	Parameter	Values
1	γ_y	$20000\gamma_g$
2	γ_c	$100\gamma_g$
3	γ_I	$30\gamma_g$
4	γ_W	$50\gamma_g$
5	γ_g	$9.502¢/kWh \simeq 2.5¢/kW\Delta T$

Furthermore, according to [236], two time periods are considered for each day: the diurnal period, which starts around 07:00AM and ends at 10:30PM, and the nocturnal period. Fig 6.4 presents the greenhouses' indoor CO_2 level (top) and temperature (bottom), where the dashed and solid lines are the setpoints and measurements, respectively. The temperature

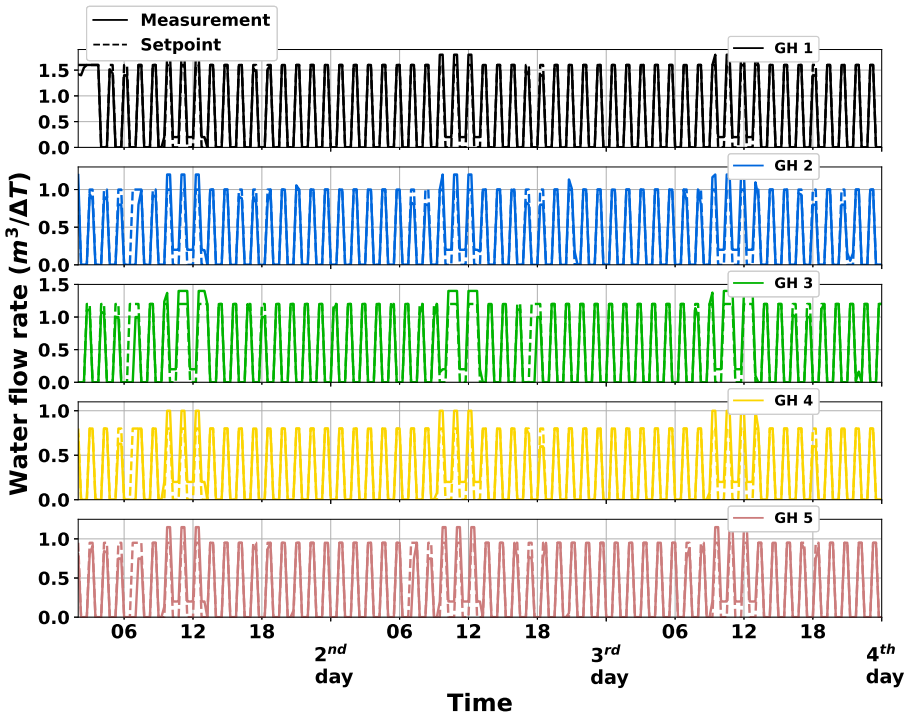

Figure 6.5 Greenhouse watering plot

setpoints of greenhouses No. 1, 2 and 4 vary during the diurnal and nocturnal periods, whereas a constant diurnal temperature is required for the crops in greenhouses No. 3 and 5. The CO_2 level setpoints also vary. Greenhouses No. 3 and 5 need a higher level of CO_2 during the diurnal period, whereas, greenhouses No. 1, 2 and 4 need it during the nocturnal period. According to Table 6.1, as expected, high values of γ_y and γ_c ensure acceptable temperature and CO_2 level tracking performance for all greenhouses except for greenhouse No. 2, where it is challenging to achieve perfect tracking of CO_2 setpoints due to its slow CO_2 evacuation dynamic. Greenhouses should irrigate crops usually once per hour for a duration of 15 minutes. This process, however, can be delayed up to 40 minutes and therefore, the greenhouse can contribute even more to the demand response program. As it is illustrated in Fig. 6.5, due to constraints (6.14) and a lower value of γ_W, greenhouse watering subsystems have more flexibility in the demand response program than the HVAC and CO_2 subsystems, as both the irrigation time and rate can be optimised. It can be noted that on the 1st day at around 06:00AM all greenhouses except greenhouse No. 1 not only postpone the activation of the watering process (load shifting), but also reduce their required water (load shaving). The same behaviour can be observed in greenhouse No. 3 during the evening of the 2nd day. On the other hand, near noon when greenhouses have surplus PV energy, they are asked to

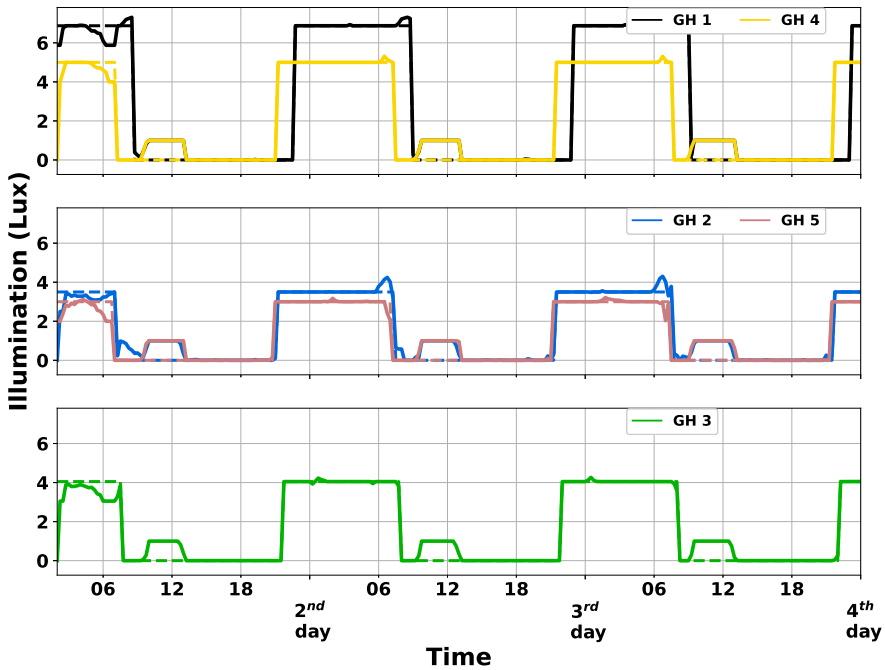

Figure 6.6 Greenhouse illumination

consume more energy so the total power exchanged with the main grid can still respect the MDL.

To maximise plants productivity, greenhouse illumination should always be kept at a specific level during diurnal periods: sunlight during the daytime and artificial light during the nighttime. Fig 6.6 shows the setpoints and behaviours of the greenhouses' lighting subsystems. During the surplus energy time (around 12:00PM), since the greenhouses' batteries are either fully charged (greenhouses No. 1 and 4 in Fig. 6.7 bottom) or are charging at their maximum admissible power (greenhouses No. 2, 3 and 5 in Fig. 6.7 top), lighting systems are turned on to consume a portion of the surplus energy. It should also be mentioned here that due to crops' sensitivity to indoor temperature increases, the high value of γ_y requires that a preheating strategy be avoided for energy saving purposes.

Fig. 6.8 illustrates a) the energy exchanged between the greenhouses and the main grid (top), and b) the main pump consumption and reservoir capacity (bottom). The red dash-dot line shows the MDL power dynamic. The MDL power is set to a total of 110kW (average 22kW per greenhouse) during the on-peak time (from 09:00AM to 06:00PM) and to 350kW (average 70kW/greenhouse) during the off-peak period (from 06:00PM to 09:00AM). Also, the Quebec

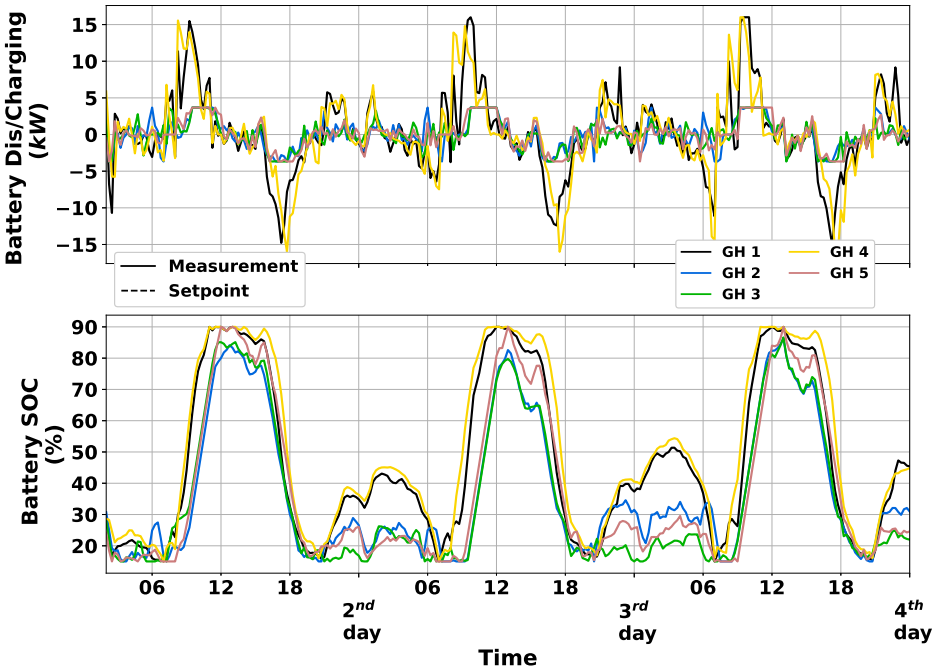

Figure 6.7 Top: Battery dis/charging power. Bottom: Battery SOC

Rate D flat price mentioned in Table 6.1 (9.502¢/kWh) [237] is used for energy exchanged with the main grid. The solutions obtained using Algorithm 2 try to follow the MDL, but due to the dynamic of the greenhouses and the discontinuity of MDL, these solutions are not as practical and efficient as expected. To overcome this issue, the MDL should have a continuous form (for example a ramp) and consider the average response time of each greenhouse. With a prediction horizon of 90 minutes, considering a 2-hour ramp seems appropriate:

$$P_{MDL}[k] = \begin{cases} 350 & 20\text{PM} \leq k \leq 07\text{AM} \\ 350 - 30(k - 7\text{AM}) & 07\text{AM} \leq k \leq 09\text{AM} \\ 110 & 09\text{AM} \leq k \leq 18\text{PM} \\ 110 + 30(k - 18\text{PM}) & 18\text{PM} \leq k \leq 20\text{PM} \end{cases} \tag{6.28}$$

As it is presented in Fig. 6.8 top, the total power consumption of the greenhouses (black dash-dot line) usually follows the MDL, except around the middle of the day when greenhouses No. 1 and 4 generate excess PV energy. The batteries of the other greenhouses can then

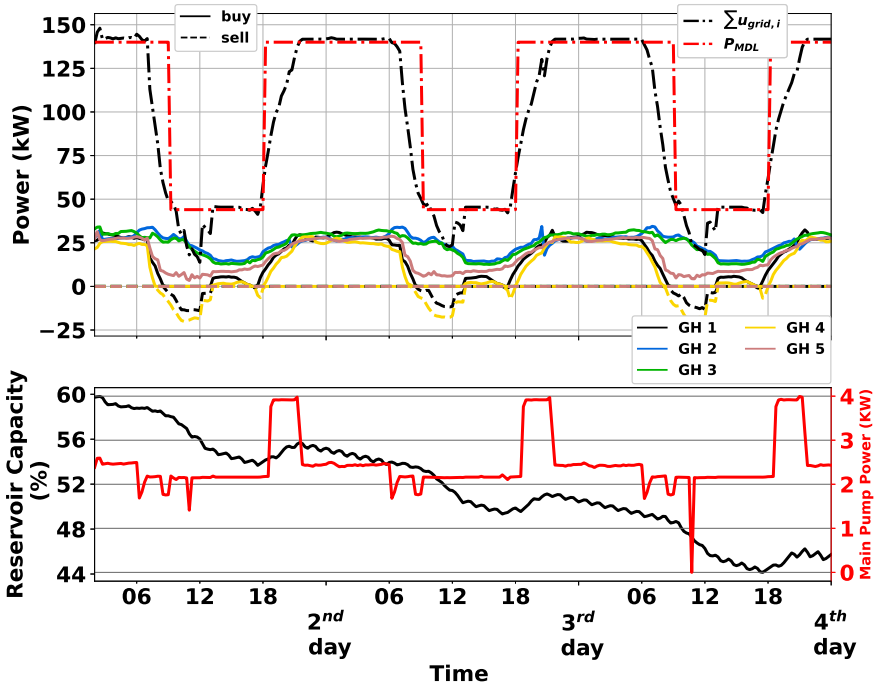

Figure 6.8 Top: Greenhouse exchanged power. Bottom: Main pump power and reservoir capacity

store this energy until reaching their maximum state of charge and the remaining energy is sold to the main grid. For example, around 12:00AM, the batteries of greenhouses No. 2, 3 and 5 charge at their maximum charging power until the maximum admissible SOC. Later on, in the evening, this stored energy is used to satisfy the greenhouses' energy needs. The cooperation between greenhouses to limit the total buying of power from the main grid can be seen in the evening and at the end of on-peak time, when greenhouses No. 1 and 4 sell their stored energy to other greenhouses. Together with load shifting and load sharing strategies, this cooperation can limit the total power consumption of the network during on-peak time.

During the night and off-peak time, by setting a higher level of MDL, the aggregator encourages greenhouses to use and store more energy. As a result, the batteries start to charge during the night, as shown in Fig. 6.7. Furthermore, during the nighttime, the aggregrator also uses this higher level of MDL to fill up the reservoir at a faster rate using the main pump (see Fig. 6.8 bottom). According to the objective function (6.26), around noon, the greenhouses and aggregator prefer to sell their surplus energy to the main grid so the main pump doesn't work at full capacity at that time.

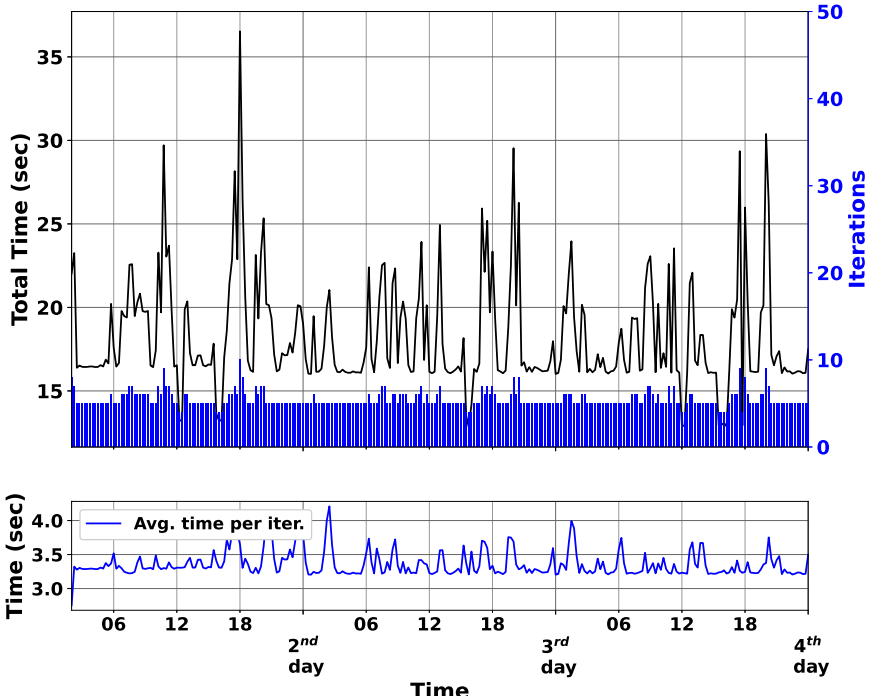

Figure 6.9 Number of iterations, total time and average time of each step

From a practical view point, the network was simulated on an Intel Core i7-8565u@1.80GHz and 1.99GHz laptop using IBM ILOG CPLEX Optimization Studio API for python (docplex) to solve the optimisation problems. To measure the speed and performance of the proposed algorithm, parallel programming was leveraged and each core of the laptop was assigned to a separate greenhouse. In other words, the optimisation problem of each greenhouse was solved in a core so lines (5) to (7) of Algorithm 2 were computed in parallel. The results are illustrated in Fig. 6.9. Note, however, that the *maxItr* was set to 50, but the consensus process was usually finished before 10 iterations and the total time per step was between 15 and 35 seconds (average time per iteration is 3.5 seconds). These results show that the proposed algorithm suits the real-time applications.

6.5 Conclusion

In this paper, a distributed optimisation method is introduced for a network of greenhouses having access to distributed energy resources. The proposed ADMM-based algorithm can increase the performance of greenhouses while implementing demand response strategies such as load shifting and load shaving. A hierarchical coordination scheme is implemented through

an aggregator to keep the total power exchanged with the main grid below or around the MDL level. This power limitation does not affect the quality of the greenhouses' crops, however. Depending on the crops' growing stage, the proposed algorithm makes more effort to control the subsystems that are most important for crop growth, while other subsystems can participate in the demand response program. The proposed algorithm's performance has been proven by the case study, and its fast convergence rate means it can be used for real-time scenarios. In future work, we would like to investigate a distributed peer-to-peer network scheme that considers uncertainties related to renewable energy resources and energy prices.

CHAPTER 7 GENERAL DISCUSSION

In this dissertation, we study the problem of distributed energy management in N-MGs, which include residential buildings or greenhouses integrated with renewable energy resources.

As the first objective of this dissertation, we present an effective way to model a multi-unit residential building integrated with PV panels, an energy storage system and electric vehicles. We first propose a mathematical model for the thermal dynamics of the building by using the RC modelling method and then integrate it with the building's battery and EVs models. Then, we present an MPC approach for the BEMS, which uses the proposed model to reformulate the building's energy consumption problem to an optimization problem. Reducing the building's operational cost while satisfying occupants' comfort is the objective of the optimization problem. The simulation results show that the BEMS uses the building preheating method alongside its battery and available EVs' to store energy during off-peak periods. Later on, the battery's stored energy is used to satisfy the building's comfort parameters during on-peak periods. Furthermore, the BEMS successfully charges EVs to the desired SOC before the departure time.

In the second objective, we design a stochastic distributed MPC-based framework for the networks of MGs. The proposed framework addresses the RES stochastic behaviours problem in both hierarchical and P2P structures. The P2P structures do not integrate an aggregator, so it becomes challenging to find the optimal solution. The general optimization problem of N-MGs is reformulated as a two-stage SOP, and a novel ADMM-based decomposition method is then introduced to decompose the two-stage SOP. In the proposed framework, the coordinators calculate the next time-step RES scenarios along with their probabilities and broadcast this data to all MGs. Each MG solves a two-stage SOP; The first stage variables are the building's indoor temperatures, while the second stage variables are PV generated power, battery dis/charging power, and power exchanged with the main grid or neighbours. The negotiation process starts when MGs send their proposed power exchanges to neighbouring MGs and ends when all parties agree on the amount of power. The efficiency of the proposed framework is demonstrated through the case study, and due to the fast convergence rate of the proposed method, the framework can be used in real-time applications.

As the third objective of this dissertation, for the first time to the best of the author's knowledge, we introduce a hierarchical distributed approach for a network of greenhouses integrated with RESs and batteries. The proposed approach is an ADMM-based MPC approach where the aggregator coordinates the greenhouses and manages the shared resources such as water

reservoirs. Limiting the power exchanged with the power grid at the MDL level and controlling indoor climatic conditions for plant growth are the main goals of the network. In this approach, the aggregator limits the power problem while each greenhouse solves a local optimization problem to reach optimal indoor conditions. The network can contribute to the DR programs through various DR strategies such as load shifting and shaving by using the proposed approach.

CHAPTER 8 CONCLUSION AND RECOMMENDATIONS

8.1 Concluding Remarks

This dissertation introduces a model predictive control approach for minimizing the power consumption of residential buildings integrated with renewable energy resources and EVs. The suggested method can limit the total power consumption of the building to a maximum demand limit indicated by the main grid, while maintaining occupants' comfort.

This control approach is then used to propose an ADMM-based distributed framework for a network of microgrids, which considers the stochastic behaviours of RESs. The proposed framework can work with different network topologies such as peer-to-peer or hierarchical. In hierarchical networks, the aggregator plays an interface role between the MGs and the main grid. The aggregator coordinate the shared resources and is responsible to limit the total power demand in the network. In the peer-to-peer networks, MGs can exchange their required power directly with each other, while limiting the total power exchange with the main grid can be done by the main grid or an aggregator.

With different simulations on the network of MGs (residential buildings and greenhouses), the performance of the proposed framework is evaluated. In a well-designed network, the framework can drive the negotiation process between the MGs to the optimal point reasonably fast, in both peer-to-peer and hierarchical structures. Hence, it can be used in real-life applications.

8.2 Limitations

In terms of work's limitations, while the author tried to simulate the proposed algorithms and frameworks with the real-world data, for the validation purposes, they need to be tested and validated in real-world applications. Validating the proposed methods in the real-world scenarios is the first limitation of this dissertation.

We use the RC method to model buildings with different applications. This method usually requires a lot of information about a building, such as its blueprints or building materials. Sometimes, and especially for old buildings, this data is either missing or not shareable. In this case, the efficiency of the RC method is questionable, which is the next limitation of this work.

Finally, the number of MGs in each network is another limitation which needs to be investi-

gated. Due to computational power limitation, MGs number in the simulations was limited, however in a real-life applications, we can have more MGs in a network.

8.3 Future Work

Although the RC modelling method showed an acceptable performance in the simulations, it requires a high volume of information from the building. Moving toward data-driven approaches such as model-free and model-based reinforcement learning approaches can be a good research direction [33, 84, 114, 115, 210].

So far in the literature of N-MGs, networks of homogeneous-type microgrids were mainly considered, e.g., a network of residential buildings or a network of greenhouses. Inhomogeneous networks with various types of MGs need to be investigated more, so they are a good direction for future considerations.

In this work, we assumed that the scenarios for the prediction horizon were known beforehand, and we did not discuss how they could be generated in real-life applications. Forecasting scenarios by using generative adversarial networks or GANs are also engaging for future works.

Finally, improving the convergence rate of the proposed framework and methods can help them to be used for real-life applications.

REFERENCES

[1] S. Wu, J. B. Rendall, M. J. Smith, S. Zhu, J. Xu, H. Wang, Q. Yang, and P. Qin, "Survey on prediction algorithms in smart homes," *IEEE Internet of Things Journal*, vol. 4, no. 3, pp. 636–644, 2017.

[2] I. G. Energy, "Co2 status report 2017. international energy agency. 2017c," 2018.

[3] M. Lombardi, K. Panerali, S. Rousselet, and J. Scalise, "Electric vehicles for smarter cities: the future of energy and mobility," in *World Economic Forum. http://www3. weforum. org/docs/WEF_2018_% 20Electric_For_Smarter_Cities. pdf*, 2018.

[4] N. Hatziargyriou, H. Asano, R. Iravani, and C. Marnay, "Microgrids. ieee power energy mag 5 (4): 78–94," 2007.

[5] "[a,b] "microgrid", *Electropedia*, International Electrotechnical Commission (IEC)„" https://www.electropedia.org/iev/iev.nsf/display?openform&ievref=617-04-22, 2017-12-15. Retrieved 2020-10-06.

[6] P. Sreedharan, J. Farbes, E. Cutter, C.-K. Woo, and J. Wang, "Microgrid and renewable generation integration: University of california, san diego," *Applied energy*, vol. 169, pp. 709–720, 2016.

[7] J. L. Martinez-Ramos, A. Marano-Marcolini, F. P. Garcia-Lopez, F. Almagro-Yravedra, A. Onen, Y. Yoldas, M. Khiat, L. Ghomri, and N. Fragale, "Provision of ancillary services by a smart microgrid: An OPF approach." IEEE, sep 2018.

[8] Z. Shuai, Y. Sun, Z. J. Shen, W. Tian, C. Tu, Y. Li, and X. Yin, "Microgrid stability: Classification and a review," vol. 58, pp. 167–179, may 2016.

[9] T. S. Ustun, C. Ozansoy, and A. Zayegh, "Recent developments in microgrids and example cases around the world—a review," vol. 15, no. 8, pp. 4030–4041, oct 2011.

[10] B. Chen, J. Wang, X. Lu, C. Chen, and S. Zhao, "Networked microgrids for grid resilience, robustness, and efficiency: A review," vol. 12, no. 1, pp. 18–32, jan 2021.

[11] Z. Shuai, Y. Peng, X. Liu, Z. Li, J. M. Guerrero, and Z. J. Shen, "Dynamic equivalent modeling for multi-microgrid based on structure preservation method," vol. 10, no. 4, pp. 3929–3942, jul 2019.

[12] S. A. Arefifar, M. Ordonez, and Y. A.-R. I. Mohamed, "Voltage and current controllability in multi-microgrid smart distribution systems," vol. 9, no. 2, pp. 817–826, mar 2018.

[13] M. Pulcherio, M. S. Illindala, J. Choi, and R. K. Yedavalli, "Robust microgrid clustering in a distribution system with inverter-based DERs," vol. 54, no. 5, pp. 5152–5162, sep 2018.

[14] F. Ahmad, A. Rasool, E. Ozsoy, R. Sekar, A. Sabanovic, and M. Elitaş, "Distribution system state estimation-a step towards smart grid," vol. 81, pp. 2659–2671, jan 2018.

[15] C. Feng, F. Wen, L. Zhang, C. Xu, M. A. Salam, and S. You, "Decentralized energy management of networked microgrid based on alternating-direction multiplier method," vol. 11, no. 10, p. 2555, sep 2018.

[16] W.-J. Ma, J. Wang, V. Gupta, and C. Chen, "Distributed energy management for networked microgrids using online ADMM with regret," vol. 9, no. 2, pp. 847–856, mar 2018.

[17] Q. Zhang, K. Dehghanpour, Z. Wang, and Q. Huang, "A learning-based power management method for networked microgrids under incomplete information," vol. 11, no. 2, pp. 1193–1204, mar 2020.

[18] J. Meirinhos, D. Rua, L. Carvalho, and A. Madureira, "Multi-temporal optimal power flow for voltage control in MV networks using distributed energy resources," vol. 146, pp. 25–32, may 2017.

[19] M. Eskandari, L. Li, M. H. Moradi, P. Siano, and F. Blaabjerg, "Simultaneous reactive power sharing and voltage regulation in an autonomous networked microgrid," vol. 14, no. 7, pp. 1366–1377, feb 2020.

[20] W.-Y. Chiu, H. Sun, and H. V. Poor, "A multiobjective approach to multimicrogrid system design," vol. 6, no. 5, pp. 2263–2272, sep 2015.

[21] M. N. Alam, S. Chakrabarti, and A. Ghosh, "Networked microgrids: State-of-the-art and future perspectives," vol. 15, no. 3, pp. 1238–1250, mar 2019.

[22] M. Islam, F. Yang, and M. Amin, "Control and optimisation of networked microgrids: A review," vol. 15, no. 6, pp. 1133–1148, feb 2021.

[23] A. G. Tsikalakis and N. D. Hatziargyriou, "Centralized control for optimizing microgrids operation." IEEE, jul 2011.

[24] S. Burger, J. P. Chaves-Ávila, C. Batlle, and I. J. Pérez-Arriaga, "The value of aggregators in electricity systems," *MIT Center for Energy and Environment Policy Research: Cambridge, MA, USA*, 2016.

[25] Y. Wang, T. Zhao, C. Ju, Y. Xu, and P. Wang, "Two-level distributed volt/var control using aggregated PV inverters in distribution networks," *IEEE Transactions on Power Delivery*, vol. 35, no. 4, pp. 1844–1855, aug 2020.

[26] H. Kim and M. Thottan, "A two-stage market model for microgrid power transactions via aggregators," vol. 16, no. 3, pp. 101–107, nov 2011.

[27] M. S. Rahman, M. J. Hossain, J. Lu, F. H. M. Rafi, and S. Mishra, "A vehicle-to-microgrid framework with optimization-incorporated distributed EV coordination for a commercial neighborhood," *IEEE Transactions on Industrial Informatics*, vol. 16, no. 3, pp. 1788–1798, mar 2020.

[28] H. Almasalma, J. Engels, and G. Deconinck, "Peer-to-peer control of microgrids," *arXiv preprint arXiv:1711.04070*, 2017.

[29] T. Sousa, T. Soares, P. Pinson, F. Moret, T. Baroche, and E. Sorin, "Peer-to-peer and community-based markets: A comprehensive review," vol. 104, pp. 367–378, apr 2019.

[30] L. Ahmethodzic and M. Music, "Comprehensive review of trends in microgrid control," vol. 38, pp. 84–96, sep 2021.

[31] S. A. AREFIFAR, M. Ordonez, and Y. Mohamed, "Energy management in multi-microgrid systems — development and assessment," pp. 1–1, 2016.

[32] A. Ouammi, H. Dagdougui, and R. Sacile, "Optimal control of power flows and energy local storages in a network of microgrids modeled as a system of systems," vol. 23, no. 1, pp. 128–138, jan 2015.

[33] A. Gupta, Y. Badr, A. Negahban, and R. G. Qiu, "Energy-efficient heating control for smart buildings with deep reinforcement learning," vol. 34, p. 101739, feb 2021.

[34] M. Jalali, K. Zare, and H. Seyedi, "Strategic decision-making of distribution network operator with multi-microgrids considering demand response program," *Energy*, vol. 141, pp. 1059–1071, 2017.

[35] M. Eskandari, L. Li, M. H. Moradi, and P. Siano, "A nodal approach based state-space model of droop-based autonomous networked microgrids," *Sustainable Energy, Grids and Networks*, vol. 18, p. 100216, 2019.

[36] V. Toro and E. Mojica-Nava, "Microgrids coordination based on heterogeneous multi-agent systems," in *2015 IEEE 2nd Colombian Conference on Automatic Control (CCAC)*. IEEE, oct 2015.

[37] H. Dagdougui and R. Sacile, "Decentralized control of the power flows in a network of smart microgrids modeled as a team of cooperative agents," vol. 22, no. 2, pp. 510–519, mar 2014.

[38] Y. Han, K. Zhang, H. Li, E. A. A. Coelho, and J. M. Guerrero, "MAS-based distributed coordinated control and optimization in microgrid and microgrid clusters: A comprehensive overview," *IEEE Transactions on Power Electronics*, vol. 33, no. 8, pp. 6488–6508, aug 2018.

[39] Y. Wang, T.-L. Nguyen, Y. Xu, Q.-T. Tran, and R. Caire, "Peer-to-peer control for networked microgrids: Multi-layer and multi-agent architecture design," *IEEE Transactions on Smart Grid*, pp. 1–1, 2020.

[40] M. Dabbaghjamanesh, A. Kavousi-Fard, and Z. Y. Dong, "A novel distributed cloud-fog based framework for energy management of networked microgrids," *IEEE Transactions on Power Systems*, vol. 35, no. 4, pp. 2847–2862, jul 2020.

[41] S. Mao, Z. Dong, W. Du, and Y. Tang, "Distributed optimal economic dispatch with uncoordinated fixed step sizes for microgrids," in *2020 IEEE 29th International Symposium on Industrial Electronics (ISIE)*. IEEE, jun 2020.

[42] W.-J. Ma, J. Wang, V. Gupta, and C. Chen, "Distributed energy management for networked microgrids using online admm with regret," *IEEE Transactions on Smart Grid*, vol. 9, no. 2, pp. 847–856, 2016.

[43] Z. Lin, J. Chen, J. Ren, G. Song, and Y. Zhang, "Distributed optimal operation for distribution networks with multi-microgrid based on ADMM," in *2019 IEEE PES GTD Grand International Conference and Exposition Asia (GTD Asia)*. IEEE, mar 2019.

[44] P. Braun, T. Faulwasser, L. Grüne, C. M. Kellett, S. R. Weller, and K. Worthmann, "Hierarchical distributed admm for predictive control with applications in power networks," *IFAC Journal of Systems and Control*, vol. 3, pp. 10–22, 2018.

[45] S. Shin, P. Hart, T. Jahns, and V. M. Zavala, "A hierarchical optimization architecture for large-scale power networks," *IEEE Transactions on Control of Network Systems*, vol. 6, no. 3, pp. 1004–1014, sep 2019.

[46] H. Kim, J. Lee, S. Bahrami, and V. W. S. Wong, "Direct energy trading of microgrids in distribution energy market," *IEEE Transactions on Power Systems*, vol. 35, no. 1, pp. 639–651, jan 2020.

[47] Q. Xu, T. Zhao, Y. Xu, Z. Xu, P. Wang, and F. Blaabjerg, "A distributed and robust energy management system for networked hybrid AC/DC microgrids," *IEEE Transactions on Smart Grid*, vol. 11, no. 4, pp. 3496–3508, jul 2020.

[48] A. Parisio, C. Wiezorek, T. Kyntäjä, J. Elo, K. Strunz, and K. H. Johansson, "Cooperative mpc-based energy management for networked microgrids," *IEEE Transactions on Smart Grid*, vol. 8, no. 6, pp. 3066–3074, 2017.

[49] Z. Zeng, R. Zhao, and H. Yang, "Micro-sources design of an intelligent building integrated with micro-grid," vol. 57, pp. 261–267, feb 2013.

[50] T. Houser, "The economics of energy efficiency in buildings," *Transport*, vol. 1, no. 5, p. 6, 2009.

[51] D. Sturzenegger, D. Gyalistras, M. Gwerder, C. Sagerschnig, M. Morari, and R. S. Smith, "Model predictive control of a swiss office building," in *Clima-rheva world congress*, 2013, pp. 3227–3236.

[52] E. Žáčeková, Z. Váňa, and J. Cigler, "Towards the real-life implementation of MPC for an office building: Identification issues," *Applied Energy*, vol. 135, pp. 53–62, dec 2014.

[53] R. Carli, G. Cavone, S. B. Othman, and M. Dotoli, "IoT based architecture for model predictive control of HVAC systems in smart buildings," *Sensors*, vol. 20, no. 3, p. 781, jan 2020.

[54] B. Chen, Z. Cai, and M. Bergés, "Gnu-RL," in *Proceedings of the 6th ACM International Conference on Systems for Energy-Efficient Buildings, Cities, and Transportation*. ACM, nov 2019.

[55] M. Luzi, M. Vaccarini, and M. Lemma, "A tuning methodology of model predictive control design for energy efficient building thermal control," *Journal of Building Engineering*, vol. 21, pp. 28–36, jan 2019.

[56] S. Rastegarpour, S. Gros, and L. Ferrarini, "MPC approaches for modulating air-to-water heat pumps in radiant-floor buildings," *Control Engineering Practice*, vol. 95, p. 104209, feb 2020.

[57] K. Pandey and B. Basu, "Model predictive control for smart buildings: A simulated approach," in *Interdisciplinary Research in Technology and Management: Proceedings of the International Conference on Interdisciplinary Research in Technology and Management (IRTM, 2021), 26-28 February, 2021, Kolkata, India.* CRC Press, 2021, p. 283.

[58] J. Vasilj, S. Gros, D. Jakus, and M. Zanon, "Day-ahead scheduling and real-time economic MPC of CHP unit in microgrid with smart buildings," *IEEE Transactions on Smart Grid*, vol. 10, no. 2, pp. 1992–2001, mar 2019.

[59] N. Salimzadeh, F. Vahdatikhaki, and A. Hammad, "Bim-based surface-specific solar simulation of buildings," in *ISARC. Proceedings of the International Symposium on Automation and Robotics in Construction*, vol. 35. IAARC Publications, 2018, pp. 1–8.

[60] A. Ramos, M. A. Chatzopoulou, I. Guarracino, J. Freeman, and C. N. Markides, "Hybrid photovoltaic-thermal solar systems for combined heating, cooling and power provision in the urban environment," *Energy Conversion and Management*, vol. 150, pp. 838–850, oct 2017.

[61] A. A. Ammar, K. Sopian, M. A. Alghoul, B. Elhub, and A. M. Elbreki, "Performance study on photovoltaic/thermal solar-assisted heat pump system," *Journal of Thermal Analysis and Calorimetry*, vol. 136, no. 1, pp. 79–87, sep 2018.

[62] H. A. Hasan, K. Sopian, and A. Fudholi, "Photovoltaic thermal solar water collector designed with a jet collision system," *Energy*, vol. 161, pp. 412–424, oct 2018.

[63] A. L. Abdullah, S. Misha, N. Tamaldin, M. Rosli, and F. Sachit, "Theoretical study and indoor experimental validation of performance of the new photovoltaic thermal solar collector (PVT) based water system," *Case Studies in Thermal Engineering*, vol. 18, p. 100595, apr 2020.

[64] M. Carmona, A. P. Bastos, and J. D. García, "Experimental evaluation of a hybrid photovoltaic and thermal solar energy collector with integrated phase change material (PVT-PCM) in comparison with a traditional photovoltaic (PV) module," *Renewable Energy*, vol. 172, pp. 680–696, jul 2021.

[65] I. Prahastono, B. G. D. Wicaksono, G. K. Atmajaya, N. I. Sinisuka, I. S. Dinata, T. Fitriani, G. Widiyanto, and A. B. Saputra, "Feasibility study of PV-grid connected

system at the office building of TBBM cikampek," in *2019 2nd International Conference on High Voltage Engineering and Power Systems (ICHVEPS)*. IEEE, oct 2019.

[66] T. J. Soleja, M. F. Siddiqui, M. Kashan, and A. Waseem, "Economic feasibility analysis of on-grid PV system without battery storage for a commercial building in karachi, pakistan," in *2018 5th International Symposium on Environment-Friendly Energies and Applications (EFEA)*. IEEE, sep 2018.

[67] T. Phasha, B. A. Aderemi, S. Chowdhury, T. Olwal, and A. Abu-Mahfouz, "Design strategies of an off-grid solar PV plant for office buildings: A case study of johannesburg," in *2018 IEEE PES/IAS PowerAfrica*. IEEE, jun 2018.

[68] J. Solano, L. Olivieri, and E. Caamano, "HVAC systems using PV technology: Economic feasibility analysis in commercial buildings of ecuador," *IEEE Latin America Transactions*, vol. 14, no. 2, pp. 767–772, feb 2016.

[69] Syafii, Novizon, Wati, and D. Juliandri, "Feasibility study of rooftop grid connected PV system for peak load reduction," in *2018 5th International Conference on Electrical Engineering, Computer Science and Informatics (EECSI)*. IEEE, oct 2018.

[70] Y. Wang, Y. Xu, and J. Qiu, "Distributed finite-time control of aggregated energy storage systems for frequency regulation in multiarea microgrids," in *Distributed Control Methods and Cyber Security Issues in Microgrids*. Elsevier, 2020, pp. 149–176.

[71] M. Mehrtash, F. Capitanescu, P. K. Heiselberg, T. Gibon, and A. Bertrand, "An enhanced optimal PV and battery sizing model for zero energy buildings considering environmental impacts," *IEEE Transactions on Industry Applications*, vol. 56, no. 6, pp. 6846–6856, nov 2020.

[72] D. L. Rodrigues, X. Ye, X. Xia, and B. Zhu, "Battery energy storage sizing optimisation for different ownership structures in a peer-to-peer energy sharing community," *Applied Energy*, vol. 262, p. 114498, mar 2020.

[73] J. Koskela, A. Rautiainen, and P. Järventausta, "Using electrical energy storage in residential buildings – sizing of battery and photovoltaic panels based on electricity cost optimization," *Applied Energy*, vol. 239, pp. 1175–1189, apr 2019.

[74] K. Heine, A. Thatte, and P. C. Tabares-Velasco, "A simulation approach to sizing batteries for integration with net-zero energy residential buildings," *Renewable Energy*, vol. 139, pp. 176–185, aug 2019.

[75] J. Dulout, B. Jammes, C. Alonso, A. Anvari-Moghaddam, A. Luna, and J. M. Guerrero, "Optimal sizing of a lithium battery energy storage system for grid-connected photovoltaic systems," in *2017 IEEE Second International Conference on DC Microgrids (ICDCM)*. IEEE, jun 2017.

[76] H. A. Kazem and T. Khatib, "A novel numerical algorithm for optimal sizing of a photovoltaic/wind/diesel generator/battery microgrid using loss of load probability index," *International Journal of Photoenergy*, vol. 2013, pp. 1–8, 2013.

[77] J. Cai, H. Zhang, and X. Jin, "Aging-aware predictive control of PV-battery assets in buildings," *Applied Energy*, vol. 236, pp. 478–488, feb 2019.

[78] A. Ashrae, "Standard 55-2013: Thermal environmental conditions for human occupancy," *American Society of Heating, Refrigerating, and Air-Conditioning Engineers, Inc. Atlanta*, 2013.

[79] W. Fincher and M. Boduch, "Standards of human comfort: relative and absolute," 2009.

[80] K. K. Huynh, "Human thermal comfort." 2002.

[81] J. Kensby, A. Trüschel, and J.-O. Dalenbäck, "Potential of residential buildings as thermal energy storage in district heating systems – results from a pilot test," *Applied Energy*, vol. 137, pp. 773–781, jan 2015.

[82] I. Sengor, O. Erdinc, B. Yener, A. Tascikaraoglu, and J. P. S. Catalao, "Optimal energy management of EV parking lots under peak load reduction based DR programs considering uncertainty," *IEEE Transactions on Sustainable Energy*, vol. 10, no. 3, pp. 1034–1043, jul 2019.

[83] Y. Yang, Q.-S. Jia, G. Deconinck, X. Guan, Z. Qiu, and Z. Hu, "Distributed coordination of EV charging with renewable energy in a microgrid of buildings," *IEEE Transactions on Smart Grid*, vol. 9, no. 6, pp. 6253–6264, nov 2018.

[84] H. Li, Z. Wan, and H. He, "Constrained EV charging scheduling based on safe deep reinforcement learning," *IEEE Transactions on Smart Grid*, vol. 11, no. 3, pp. 2427–2439, may 2020.

[85] S. Iqbal, A. Xin, M. U. Jan, M. A. Abdelbaky, H. U. Rehman, S. Salman, S. A. A. Rizvi, and M. Aurangzeb, "Aggregation of EVs for primary frequency control of an industrial

microgrid by implementing grid regulation & charger controller," *IEEE Access*, vol. 8, pp. 141 977–141 989, 2020.

[86] L. Noel, G. Z. de Rubens, J. Kester, and B. K. Sovacool, "Beyond emissions and economics: Rethinking the co-benefits of electric vehicles (EVs) and vehicle-to-grid (v2g)," *Transport Policy*, vol. 71, pp. 130–137, nov 2018.

[87] A. Hassoune, M. Khafallah, A. Mesbahi, and T. Bouragba, "Smart topology of EVs in a PV-grid system based charging station," in *2017 International Conference on Electrical and Information Technologies (ICEIT)*. IEEE, nov 2017.

[88] V. Monteiro, J. Pinto, and J. L. Afonso, "Improved vehicle-for-grid (iV4g) mode: Novel operation mode for EVs battery chargers in smart grids," *International Journal of Electrical Power & Energy Systems*, vol. 110, pp. 579–587, sep 2019.

[89] J. Yusuf, A. S. M. J. Hasan, L. F. Enriquez-Contreras, and S. Ula, "A centralized optimization approach for bidirectional pev impacts analysis in a commercial building-integrated microgrid," 2021.

[90] Y. Dagdougui, A. Ouammi, and R. Benchrifa, "Energy management-based predictive controller for a smart building powered by renewable energy," vol. 12, no. 10, p. 4264, may 2020.

[91] S. Ferahtia, A. Djeroui, H. Rezk, A. Houari, S. Zeghlache, and M. Machmoum, "Optimal control and implementation of energy management strategy for a DC microgrid," vol. 238, p. 121777, jan 2022.

[92] H. Fontenot and B. Dong, "Modeling and control of building-integrated microgrids for optimal energy management – a review," vol. 254, p. 113689, nov 2019.

[93] V. S. K. M. Balijepalli, V. Pradhan, S. A. Khaparde, and R. M. Shereef, "Review of demand response under smart grid paradigm," in *ISGT2011-India*. IEEE, dec 2011.

[94] A. S. A. Awad, M. F. Shaaban, T. H. M. EL-Fouly, E. F. El-Saadany, and M. M. A. Salama, "Optimal resource allocation and charging prices for benefit maximization in smart PEV-parking lots," *IEEE Transactions on Sustainable Energy*, vol. 8, no. 3, pp. 906–915, jul 2017.

[95] M. Tavakkoli, S. Fattaheian-Dehkordi, M. Pourakbari-Kasmaei, M. Liski, and M. Lehtonen, "Bonus-based demand response using stackelberg game approach for

residential end-users equipped with HVAC system," *IEEE Transactions on Sustainable Energy*, vol. 12, no. 1, pp. 234–249, jan 2021.

[96] X.-D. Chen, L. Li, M.-L. Tseng, K. Tan, and M. H. Ali, "Improving power quality efficient in demand response: Aggregated heating, ventilation and air-conditioning systems," *Journal of Cleaner Production*, vol. 267, p. 122178, sep 2020.

[97] U. Amin, M. Hossain, and E. Fernandez, "Optimal price based control of HVAC systems in multizone office buildings for demand response," *Journal of Cleaner Production*, vol. 270, p. 122059, oct 2020.

[98] A.-Y. Yoon, Y.-J. Kim, T. Zakula, and S.-I. Moon, "Retail electricity pricing via online-learning of data-driven demand response of HVAC systems," *Applied Energy*, vol. 265, p. 114771, may 2020.

[99] R. Chandra, G. N. B. Yadav, and S. K. Panda, "Transactive control of air-conditioning systems in buildings for demand response," in *2020 IEEE PES Innovative Smart Grid Technologies Europe (ISGT-Europe)*. IEEE, oct 2020.

[100] M. K. Yadav, A. Verma, B. K. Panigrahi, and S. Mishra, "User comfort driven timetable linked AHU scheduling for ancillary service maximization of an educational building," *Energy and Buildings*, vol. 225, p. 110317, oct 2020.

[101] A. Brem, K. Bruton, and P. D. O'Sullivan, "Assessing the risk to indoor thermal environments on industrial sites offering AHU capacity for demand response," *Energies*, vol. 14, no. 19, p. 6261, oct 2021.

[102] Y. Lu, X. Yu, X. Jin, H. Jia, and Y. Mu, "Bi-level optimization framework for buildings to heating grid integration in integrated community energy systems," *IEEE Transactions on Sustainable Energy*, vol. 12, no. 2, pp. 860–873, apr 2021.

[103] E. Sperber, U. Frey, and V. Bertsch, "Reduced-order models for assessing demand response with heat pumps – insights from the german energy system," *Energy and Buildings*, vol. 223, p. 110144, sep 2020.

[104] Q. Meng, X. Ren, W. Wang, C. Xiong, Y. Li, Y. Xi, and L. Yang, "Reduction in on-off operations of an air source heat pump with active thermal storage and demand response: An experimental case study," *Journal of Energy Storage*, vol. 36, p. 102401, apr 2021.

[105] H. Mansy and S. Kwon, "Optimal HVAC control for demand response via chance-constrained two-stage stochastic program," *IEEE Transactions on Smart Grid*, vol. 12, no. 3, pp. 2188–2200, may 2021.

[106] H. Kim, M. Kim, and J. Lee, "A two-stage stochastic p-robust optimal energy trading management in microgrid operation considering uncertainty with hybrid demand response," *International Journal of Electrical Power & Energy Systems*, vol. 124, p. 106422, jan 2021.

[107] D. Thomas, O. Deblecker, and C. S. Ioakimidis, "Optimal operation of an energy management system for a grid-connected smart building considering photovoltaics' uncertainty and stochastic electric vehicles' driving schedule," *Applied Energy*, vol. 210, pp. 1188–1206, jan 2018.

[108] D. Mariano-Hernández, L. Hernández-Callejo, A. Zorita-Lamadrid, O. Duque-Pérez, and F. S. García, "A review of strategies for building energy management system: Model predictive control, demand side management, optimization, and fault detect & diagnosis," *Journal of Building Engineering*, vol. 33, p. 101692, jan 2021.

[109] M. A. Henson and D. E. Seborg, *Nonlinear process control*. Prentice Hall PTR Upper Saddle River, New Jersey, 1997.

[110] G. Bianchini, M. Casini, D. Pepe, A. Vicino, and G. G. Zanvettor, "An integrated model predictive control approach for optimal HVAC and energy storage operation in large-scale buildings," *Applied Energy*, vol. 240, pp. 327–340, apr 2019.

[111] A. Staino, H. Nagpal, and B. Basu, "Cooperative optimization of building energy systems in an economic model predictive control framework," *Energy and Buildings*, vol. 128, pp. 713–722, sep 2016.

[112] R. Ruusu, S. Cao, B. M. Delgado, and A. Hasan, "Direct quantification of multiple-source energy flexibility in a residential building using a new model predictive high-level controller," *Energy Conversion and Management*, vol. 180, pp. 1109–1128, jan 2019.

[113] M. Toub, C. R. Reddy, M. Razmara, M. Shahbakhti, R. D. Robinett, and G. Aniba, "Model-based predictive control for optimal MicroCSP operation integrated with building HVAC systems," *Energy Conversion and Management*, vol. 199, p. 111924, nov 2019.

[114] P. Lissa, C. Deane, M. Schukat, F. Seri, M. Keane, and E. Barrett, "Deep reinforcement learning for home energy management system control," *Energy and AI*, vol. 3, p. 100043, mar 2021.

[115] F. Alfaverh, M. Denai, and Y. Sun, "Demand response strategy based on reinforcement learning and fuzzy reasoning for home energy management," *IEEE Access*, vol. 8, pp. 39 310–39 321, 2020.

[116] E. Biyik and A. Kahraman, "A predictive control strategy for optimal management of peak load, thermal comfort, energy storage and renewables in multi-zone buildings," *Journal of Building Engineering*, vol. 25, p. 100826, sep 2019.

[117] C. Fan, F. Xiao, C. Yan, C. Liu, Z. Li, and J. Wang, "A novel methodology to explain and evaluate data-driven building energy performance models based on interpretable machine learning," *Applied Energy*, vol. 235, pp. 1551–1560, feb 2019.

[118] Y. Li, Z. O'Neill, L. Zhang, J. Chen, P. Im, and J. DeGraw, "Grey-box modeling and application for building energy simulations - a critical review," *Renewable and Sustainable Energy Reviews*, vol. 146, p. 111174, aug 2021.

[119] P. Kohlhepp, L. Gröll, and V. Hagenmeyer, "Characterization of aggregated building heating, ventilation, and air conditioning load as a flexibility service using gray-box modeling," *Energy Technology*, vol. 9, no. 9, p. 2100251, jul 2021.

[120] C. A. Thilker, P. Bacher, H. G. Bergsteinsson, R. G. Junker, D. Cali, and H. Madsen, "Non-linear grey-box modelling for heat dynamics of buildings," *Energy and Buildings*, vol. 252, p. 111457, dec 2021.

[121] M. H. Shamsi, U. Ali, E. Mangina, and J. O'Donnell, "A framework for uncertainty quantification in building heat demand simulations using reduced-order grey-box energy models," *Applied Energy*, vol. 275, p. 115141, oct 2020.

[122] F. Amara, K. Agbossou, A. Cardenas, Y. Dubé, and S. Kelouwani, "Comparison and simulation of building thermal models for effective energy management," vol. 06, no. 04, pp. 95–112, 2015.

[123] C. Keles, A. Karabiber, M. Akcin, A. Kaygusuz, B. B. Alagoz, and O. Gul, "A smart building power management concept: Smart socket applications with DC distribution," *International Journal of Electrical Power & Energy Systems*, vol. 64, pp. 679–688, jan 2015.

[124] Z. Wang, T. Hong, and M. A. Piette, "Building thermal load prediction through shallow machine learning and deep learning," *Applied Energy*, vol. 263, p. 114683, apr 2020.

[125] E. Sala-Cardoso, M. Delgado-Prieto, K. Kampouropoulos, and L. Romeral, "Activity-aware HVAC power demand forecasting," *Energy and Buildings*, vol. 170, pp. 15–24, jul 2018.

[126] A. Ghofrani, S. D. Nazemi, and M. A. Jafari, "HVAC load synchronization in smart building communities," *Sustainable Cities and Society*, vol. 51, p. 101741, nov 2019.

[127] L. Martirano, G. Parise, G. Greco, M. Manganelli, F. Massarella, M. Cianfrini, L. Parise, P. di Laura Frattura, and E. Habib, "Aggregation of users in a residential/commercial building managed by a building energy management system (BEMS)," *IEEE Transactions on Industry Applications*, vol. 55, no. 1, pp. 26–34, jan 2019.

[128] S. K. Howell, H. Wicaksono, B. Yuce, K. McGlinn, and Y. Rezgui, "User centered neuro-fuzzy energy management through semantic-based optimization," *IEEE Transactions on Cybernetics*, vol. 49, no. 9, pp. 3278–3292, sep 2019.

[129] M. Q. Raza, M. Nadarajah, and C. Ekanayake, "Demand forecast of PV integrated bioclimatic buildings using ensemble framework," *Applied Energy*, vol. 208, pp. 1626–1638, dec 2017.

[130] S. Yang, Z. Tan, Z. Liu, H. Lin, L. Ju, F. Zhou, and J. Li, "A multi-objective stochastic optimization model for electricity retailers with energy storage system considering uncertainty and demand response," *Journal of Cleaner Production*, vol. 277, p. 124017, dec 2020.

[131] J. Zhu, Y. Shen, Z. Song, D. Zhou, Z. Zhang, and A. Kusiak, "Data-driven building load profiling and energy management," *Sustainable Cities and Society*, vol. 49, p. 101587, aug 2019.

[132] J. Aguilar, A. Garces-Jimenez, N. Gallego-Salvador, J. A. G. D. Mesa, J. M. Gomez-Pulido, and A. J. Garcia-Tejedor, "Autonomic management architecture for multi-HVAC systems in smart buildings," *IEEE Access*, vol. 7, pp. 123 402–123 415, 2019.

[133] Y. F. Du, L. Jiang, C. Duan, Y. Z. Li, and J. S. Smith, "Energy consumption scheduling of HVAC considering weather forecast error through the distributionally robust approach," *IEEE Transactions on Industrial Informatics*, vol. 14, no. 3, pp. 846–857, mar 2018.

[134] S. Camal, F. Teng, A. Michiorri, G. Kariniotakis, and L. Badesa, "Scenario generation of aggregated wind, photovoltaics and small hydro production for power systems applications," *Applied Energy*, vol. 242, pp. 1396–1406, may 2019.

[135] V. Weiler, J. Stave, and U. Eicker, "Renewable energy generation scenarios using 3d urban modeling tools—methodology for heat pump and co-generation systems with case study application †," *Energies*, vol. 12, no. 3, p. 403, jan 2019.

[136] J. Yang, S. Zhang, Y. Xiang, J. Liu, J. Liu, X. Han, and F. Teng, "LSTM auto-encoder based representative scenario generation method for hybrid hydro-PV power system," *IET Generation, Transmission & Distribution*, vol. 14, no. 24, pp. 5935–5943, aug 2020.

[137] M. Taniguchi, N. Masuhara, and K. Burnett, "Water, energy, and food security in the asia pacific region," *Journal of Hydrology: Regional Studies*, vol. 11, pp. 9–19, 2017.

[138] Canada, Environment and Climate Change, "Greenhouse gas sources and sinks: executive summary 2021," Jul 2021. [Online]. Available: https://www.canada.ca/en/environment-climate-change/services/climate-change/greenhouse-gas-emissions/sources-sinks-executive-summary-2021.html

[139] N. Gilbert, "One-third of our greenhouse gas emissions come from agriculture," *Nature*, vol. 31, pp. 10–12, 2012.

[140] L. Lipper, P. Thornton, B. M. Campbell, T. Baedeker, A. Braimoh, M. Bwalya, P. Caron, A. Cattaneo, D. Garrity, K. Henry *et al.*, "Climate-smart agriculture for food security," *Nature climate change*, vol. 4, no. 12, pp. 1068–1072, 2014.

[141] R. Liao, S. Zhang, X. Zhang, M. Wang, H. Wu, and L. Zhangzhong, "Development of smart irrigation systems based on real-time soil moisture data in a greenhouse: Proof of concept," *Agricultural Water Management*, vol. 245, p. 106632, 2021.

[142] C. Lijun, D. Shangfeng, H. Yaofeng, and L. Meihui, "Linear quadratic optimal control applied to the greenhouse temperature hierarchal system," *IFAC-PapersOnLine*, vol. 51, no. 17, pp. 712–717, 2018.

[143] G. Serale, L. Gnoli, E. Giraudo, and E. Fabrizio, "A supervisory control strategy for improving energy efficiency of artificial lighting systems in greenhouses," *Energies*, vol. 14, no. 1, p. 202, jan 2021.

[144] M. Cossu, A. Yano, S. Solinas, P. A. Deligios, M. T. Tiloca, A. Cossu, and L. Ledda, "Agricultural sustainability estimation of the european photovoltaic greenhouses," *European Journal of Agronomy*, vol. 118, p. 126074, aug 2020.

[145] K. Ezzaeri, H. Fatnassi, A. Wifaya, A. Bazgaou, A. Aharoune, C. Poncet, A. Bekkaoui, and L. Bouirden, "Performance of photovoltaic canarian greenhouse: A comparison study between summer and winter seasons," *Solar Energy*, vol. 198, pp. 275–282, mar 2020.

[146] T. Alinejad, M. Yaghoubi, and A. Vadiee, "Thermo-environomic assessment of an integrated greenhouse with an adjustable solar photovoltaic blind system," *Renewable Energy*, vol. 156, pp. 1–13, aug 2020.

[147] W. E. Kolaly, W. Ma, M. Li, and M. Darwesh, "The investigation of energy production and mushroom yield in greenhouse production based on mono photovoltaic cells effect," *Renewable Energy*, vol. 159, pp. 506–518, oct 2020.

[148] H. B. Amara, S. Bouadila, H. Fatnassi, M. Arici, and A. A. Guizani, "Climate assessment of greenhouse equipped with south-oriented PV roofs: An experimental and computational fluid dynamics study," *Sustainable Energy Technologies and Assessments*, vol. 45, p. 101100, jun 2021.

[149] Y. Achour, A. Ouammi, D. Zejli, and S. Sayadi, "Supervisory model predictive control for optimal operation of a greenhouse indoor environment coping with food-energy-water nexus," *IEEE Access*, vol. 8, pp. 211 562–211 575, 2020.

[150] A. Ouammi, Y. Achour, D. Zejli, and H. Dagdougui, "Supervisory model predictive control for optimal energy management of networked smart greenhouses integrated microgrid," *IEEE Transactions on Automation Science and Engineering*, 2019.

[151] A. Ouammi, "Model predictive control for optimal energy management of connected cluster of microgrids with net zero energy multi-greenhouses," *Energy*, p. 121274, 2021.

[152] M. R. Sandgani and S. Sirouspour, "Energy management in a network of grid-connected microgrids/nanogrids using compromise programming," *IEEE Transactions on Smart Grid*, pp. 1–1, 2016.

[153] M. Falahi, S. Lotfifard, M. Ehsani, and K. Butler-Purry, "Dynamic model predictive-based energy management of DG integrated distribution systems," *IEEE Transactions on Power Delivery*, vol. 28, no. 4, pp. 2217–2227, oct 2013.

[154] B. Zhang, Q. Li, L. Wang, and W. Feng, "Robust optimization for energy transactions in multi-microgrids under uncertainty," *Applied Energy*, vol. 217, pp. 346–360, 2018.

[155] H. Dagdougui, A. Ouammi, and R. Sacile, “Optimal control of a network of power microgrids using the pontryagin's minimum principle,” vol. 22, no. 5, pp. 1942–1948, sep 2014.

[156] Z. Wang, B. Chen, J. Wang, and J. kim, “Decentralized energy management system for networked microgrids in grid-connected and islanded modes,” vol. 7, no. 2, pp. 1097–1105, mar 2016.

[157] M. Jalali, K. Zare, and H. Seyedi, “Strategic decision-making of distribution network operator with multi-microgrids considering demand response program,” vol. 141, pp. 1059–1071, dec 2017.

[158] D. Gregoratti and J. Matamoros, “Distributed energy trading: The multiple-microgrid case,” *IEEE Transactions on Industrial Electronics*, vol. 62, no. 4, pp. 2551–2559, apr 2015.

[159] R. Rostami and D. Görges, “Distributed model predictive control with event-based optimization,” *IFAC-PapersOnLine*, vol. 50, no. 1, pp. 8933–8938, jul 2017.

[160] A. Falsone, K. Margellos, S. Garatti, and M. Prandini, “Dual decomposition for multi-agent distributed optimization with coupling constraints,” *Automatica*, vol. 84, pp. 149–158, oct 2017.

[161] M. Razzanelli, E. Crisostomi, L. Pallottino, and G. Pannocchia, “Distributed model predictive control for energy management in a network of microgrids using the dual decomposition method,” *Optimal Control Applications and Methods*, vol. 41, no. 1, pp. 25–41, apr 2019.

[162] Z. Cheng and M.-Y. Chow, “Collaborative distributed ac optimal power flow: A dual decomposition based algorithm,” *Journal of Modern Power Systems and Clean Energy*, 2021.

[163] C. Feng, H. Xu, and B. Li, “An alternating direction method approach to cloud traffic management,” *IEEE Transactions on Parallel and Distributed Systems*, vol. 28, no. 8, pp. 2145–2158, 2017.

[164] Y. Wang, W. Yin, and J. Zeng, “Global convergence of ADMM in nonconvex nonsmooth optimization,” *Journal of Scientific Computing*, vol. 78, no. 1, pp. 29–63, jun 2018.

[165] S. Boyd, N. Parikh, and E. Chu, *Distributed optimization and statistical learning via the alternating direction method of multipliers*. Now Publishers Inc, 2011.

[166] K. Liu, T. Liu, Z. Tang, and D. J. Hill, "Distributed MPC-based frequency control in networked microgrids with voltage constraints," *IEEE Transactions on Smart Grid*, vol. 10, no. 6, pp. 6343–6354, nov 2019.

[167] Y. Liu, Y. Li, H. B. Gooi, Y. Jian, H. Xin, X. Jiang, and J. Pan, "Distributed robust energy management of a multimicrogrid system in the real-time energy market," *IEEE Transactions on Sustainable Energy*, vol. 10, no. 1, pp. 396–406, jan 2019.

[168] N. Nikmehr, "Distributed robust operational optimization of networked microgrids embedded interconnected energy hubs," *Energy*, vol. 199, p. 117440, may 2020.

[169] W. Zhang and Y. Xu, "Distributed optimal control for multiple microgrids in a distribution network," *IEEE Transactions on Smart Grid*, vol. 10, no. 4, pp. 3765–3779, 2018.

[170] Y. Shi, H. D. Tuan, A. V. Savkin, C.-T. Lin, J. G. Zhu, and H. V. Poor, "Distributed model predictive control for joint coordination of demand response and optimal power flow with renewables in smart grid," *Applied Energy*, vol. 290, p. 116701, may 2021.

[171] Q. Li, Y. Liao, K. Wu, L. Zhang, J. Lin, M. Chen, J. M. Guerrero, and D. Abbott, "Parallel and distributed optimization method with constraint decomposition for energy management of microgrids," *IEEE Transactions on Smart Grid*, pp. 1–1, 2021.

[172] G. Liu, T. Jiang, T. B. Ollis, X. Zhang, and K. Tomsovic, "Distributed energy management for community microgrids considering network operational constraints and building thermal dynamics," *Applied Energy*, vol. 239, pp. 83–95, apr 2019.

[173] W. Zhong, K. Xie, Y. Liu, C. Yang, S. Xie, and Y. Zhang, "Distributed demand response for multienergy residential communities with incomplete information," *IEEE Transactions on Industrial Informatics*, vol. 17, no. 1, pp. 547–557, jan 2021.

[174] A. Lesage-Landry and D. S. Callaway, "Dynamic and distributed online convex optimization for demand response of commercial buildings," *IEEE Control Systems Letters*, vol. 4, no. 3, pp. 632–637, jul 2020.

[175] J. Su, Y. Jiang, A. Bitlislioğlu, C. N. Jones, and B. Houska, "Distributed multi-building coordination for demand response," *IFAC-PapersOnLine*, vol. 53, no. 2, pp. 17 113–17 118, 2020.

[176] G. Ruan, H. Zhong, J. Wang, Q. Xia, and C. Kang, "Neural-network-based lagrange multiplier selection for distributed demand response in smart grid," *Applied Energy*, vol. 264, p. 114636, apr 2020.

[177] X. Wang, L. Liang, X. Zhang, and H. Sun, "Distributed real-time temperature and energy control of energy efficient buildings via geothermal heat pumps," *CSEE Journal of Power and Energy Systems*, 2021.

[178] WBCSD, "Transforming the market: Energy efficiency in buildings," 2009.

[179] IEA, "Energy technology perspectives 2012: Pathways to a clean energy system," Paris, 2012.

[180] X. Guan, Z. Xu, and Q.-S. Jia, "Energy-efficient buildings facilitated by microgrid," *IEEE Transactions on smart grid*, vol. 1, no. 3, pp. 243–252, 2010.

[181] M. C. Vlot, J. D. Knigge, and J. G. Slootweg, "Economical regulation power through load shifting with smart energy appliances," *IEEE transactions on smart grid*, vol. 4, no. 3, pp. 1705–1712, 2013.

[182] Z. Zhou, F. Zhao, and J. Wang, "Agent-based electricity market simulation with demand response from commercial buildings," *IEEE Transactions on Smart Grid*, vol. 2, no. 4, pp. 580–588, 2011.

[183] P. Palensky and D. Dietrich, "Demand side management: Demand response, intelligent energy systems, and smart loads," *IEEE transactions on industrial informatics*, vol. 7, no. 3, pp. 381–388, 2011.

[184] S. Arun and M. Selvan, "Intelligent residential energy management system for dynamic demand response in smart buildings," *IEEE Systems Journal*, vol. 12, no. 2, pp. 1329–1340, 2018.

[185] C. Chen, J. Wang, Y. Heo, and S. Kishore, "Mpc-based appliance scheduling for residential building energy management controller," *IEEE Transactions on Smart Grid*, vol. 4, no. 3, pp. 1401–1410, 2013.

[186] K. Ma, Y. Yu, B. Yang, and J. Yang, "Demand-side energy management considering price oscillations for residential building heating and ventilation systems," *IEEE Transactions on Industrial Informatics*, pp. 1–1, 2019.

[187] A. Y. Saber and G. K. Venayagamoorthy, "One million plug-in electric vehicles on the road by 2015," in *2009 12th International IEEE Conference on Intelligent Transportation Systems*. IEEE, 2009, pp. 1–7.

[188] S. Beer, T. Gómez, D. Dallinger, I. Momber, C. Marnay, M. Stadler, and J. Lai, "An economic analysis of used electric vehicle batteries integrated into commercial building microgrids," *IEEE Transactions on Smart Grid*, vol. 3, no. 1, pp. 517–525, 2012.

[189] H. K. Nguyen and J. B. Song, "Optimal charging and discharging for multiple phevs with demand side management in vehicle-to-building," *Journal of Communications and networks*, vol. 14, no. 6, pp. 662–671, 2012.

[190] M. Turcotte, "Commuting to work: Results of the 2010 general social survey," *Canadian Social Trends*, vol. 92, no. August, pp. 25–36, 2011.

[191] U.S. Department of Energy, "Web card - clean cities plug-in electric vehicle handbook for public charging station hosts," Jul. 2012.

[192] J. García-Villalobos, I. Zamora, J. San Martín, F. Asensio, and V. Aperribay, "Plug-in electric vehicles in electric distribution networks: A review of smart charging approaches," *Renewable and Sustainable Energy Reviews*, vol. 38, pp. 717–731, 2014.

[193] J. Van Roy, N. Leemput, F. Geth, R. Salenbien, J. Büscher, and J. Driesen, "Apartment building electricity system impact of operational electric vehicle charging strategies," *IEEE Transactions on Sustainable Energy*, vol. 5, no. 1, pp. 264–272, 2014.

[194] C. Guzman, K. Agbossou, and A. Cardenas, "Real-time emulation of residential buildings by hardware solution of multi-layer model," *IEEE Transactions on Smart Grid*, pp. 1–1, 2018.

[195] C. Guzmán, K. Agbossou, and A. Cardenas, "Real-time emulation of residential buildings by hardware solution of multi-layer model," *IEEE Transactions on Smart Grid*, 2018.

[196] A. Fleischhacker, H. Auer, G. Lettner, and A. Botterud, "Sharing solar PV and energy storage in apartment buildings: resource allocation and pricing," *IEEE Transactions on Smart Grid*, pp. 1–1, 2018.

[197] J. A. Pinzon, P. P. Vergara, L. C. Da Silva, and M. J. Rider, "Optimal management of energy consumption and comfort for smart buildings operating in a microgrid," *IEEE Transactions on Smart Grid*, vol. 10, no. 3, pp. 3236–3247, 2018.

[198] H. Kikusato, K. Mori, S. Yoshizawa, Y. Fujimoto, H. Asano, Y. Hayashi, A. Kawashima, S. Inagaki, and T. Suzuki, "Electric vehicle charge–discharge management for utilization of photovoltaic by coordination between home and grid energy management systems," *IEEE Transactions on Smart Grid*, vol. 10, no. 3, pp. 3186–3197, 2018.

[199] L. Ma, N. Liu, J. Zhang, and L. Wang, "Real-time rolling horizon energy management for the energy-hub-coordinated prosumer community from a cooperative perspective," *IEEE Transactions on Power Systems*, vol. 34, no. 2, pp. 1227–1242, 2018.

[200] S. Chen, H. B. Gooi, and M. Wang, "Sizing of energy storage for microgrids," *IEEE Transactions on Smart Grid*, vol. 3, no. 1, pp. 142–151, 2012.

[201] A. Thavlov and H. W. Bindner, "Thermal models for intelligent heating of buildings," in *4th International Conference on Applied Energy (ICAE 2012): Energy innovations for a sustainable world*, 2012.

[202] J. Li, G. Poulton, G. Platt, J. Wall, and G. James, "Dynamic zone modelling for hvac system control," *International Journal of Modelling, Identification and Control*, vol. 9, no. 1-2, pp. 5–14, 2010.

[203] H. Park, M. Ruellan, A. Bouvet, E. Monmasson, and R. Bennacer, "Thermal parameter identification of simplified building model with electric appliance," in *11th International Conference on Electrical Power Quality and Utilisation*. IEEE, 2011, pp. 1–6.

[204] D. Sturzenegger, "Model predictive building climate control: Steps towards practice," Ph.D. dissertation, 2014.

[205] Ontario Energy Board, "Toronto hydro-electric system limited," Dec. 2019.

[206] E. Rezaei and H. Dagdougui, "Optimal real-time energy management in apartment building integrating microgrid with multizone HVAC control," *IEEE Transactions on Industrial Informatics*, vol. 16, no. 11, pp. 6848–6856, nov 2020.

[207] H. Mansy and S. Kwon, "Optimal HVAC control for demand response via chance-constrained two-stage stochastic program," *IEEE Transactions on Smart Grid*, pp. 1–1, 2020.

[208] Y. Kim, "Optimal price based demand response of hvac systems in multizone office buildings considering thermal preferences of individual occupants buildings," *IEEE Transactions on Industrial Informatics*, vol. 14, no. 11, pp. 5060–5073, 2018.

[209] S. L. Arun and M. P. Selvan, "Intelligent residential energy management system for dynamic demand response in smart buildings," *IEEE Systems Journal*, vol. 12, no. 2, pp. 1329–1340, 2018.

[210] L. Yu, Y. Sun, Z. Xu, C. Shen, D. Yue, T. Jiang, and X. Guan, "Multi-agent deep reinforcement learning for HVAC control in commercial buildings," *IEEE Transactions on Smart Grid*, vol. 12, no. 1, pp. 407–419, jan 2021.

[211] E. Rezaei and H. Dagdougui, "A network of BIMGs participating in demand response using EVs and HVAC units," in *2019 IEEE 7th International Conference on Smart Energy Grid Engineering (SEGE)*. IEEE, aug 2019.

[212] M. Kermani, D. L. Carnì, S. Rotondo, A. Paolillo, F. Manzo, and L. Martirano, "A nearly zero-energy microgrid testbed laboratory: Centralized control strategy based on scada system," *Energies*, vol. 13, no. 8, p. 2106, 2020.

[213] A. Parisio, C. Wiezorek, T. Kyntaja, J. Elo, K. Strunz, and K. H. Johansson, "Cooperative MPC-based energy management for networked microgrids," *IEEE Transactions on Smart Grid*, vol. 8, no. 6, pp. 3066–3074, nov 2017.

[214] W. Zhang and Y. Xu, "Distributed optimal control for multiple microgrids in a distribution network," *IEEE Transactions on Smart Grid*, vol. 10, no. 4, pp. 3765–3779, jul 2019.

[215] Z.-Q. Luo and M. Hong, "On the linear convergence of the alternating direction method of multipliers." *Mathematical Programming*, vol. 162, 2017.

[216] T.-Y. Lin, S.-Q. Ma, and S.-Z. Zhang, "On the sublinear convergence rate of multi-block admm," *Journal of the Operations Research Society of China*, vol. 3, no. 3, pp. 251–274, 2015.

[217] Z. Jia, X. Gao, X. Cai, and D. Han, "The convergence rate analysis of the symmetric admm for the nonconvex separable optimization problems," *Journal of Industrial & Management Optimization*, vol. 17, no. 4, p. 1943, 2021.

[218] J. Zhou, Y. Xu, H. Sun, Y. Li, and M.-Y. Chow, "Distributed power management for networked AC–DC microgrids with unbalanced microgrids," *IEEE Transactions on Industrial Informatics*, vol. 16, no. 3, pp. 1655–1667, mar 2020.

[219] F. Amara, K. Agbossou, A. Cardenas, Y. Dubé, S. Kelouwani *et al.*, "Comparison and simulation of building thermal models for effective energy management," *Smart Grid and renewable energy*, vol. 6, no. 04, p. 95, 2015.

[220] A. Voskrebenzev, S. Riechelmann, A. Bais, H. Slaper, and G. Seckmeyer, "Estimating probability distributions of solar irradiance," *Theoretical and Applied Climatology*, vol. 119, no. 3, pp. 465–479, 2015.

[221] HydroQuebec. Structure of Rate Flex D. [Online]. Available: https://www.hydroquebec.com/residential/customer-space/rates/rate-flex-d-billing.html

[222] Homebyme, developed by Dassault Systèmes SE. [Online]. Available: https://home.by.me/en/about

[223] D. Sturzenegger, D. Gyalistras, V. Semeraro, M. Morari, and R. S. Smith, "Brcm matlab toolbox: Model generation for model predictive building control," in *2014 american control conference*. IEEE, 2014, pp. 1063–1069.

[224] H. Fjelde and N. von Uexkull, "Climate triggers: Rainfall anomalies, vulnerability and communal conflict in sub-saharan africa," *Political Geography*, vol. 31, no. 7, pp. 444–453, 2012.

[225] G. LaPlante, S. Andrekovic, R. G. Young, J. M. Kelly, N. Bennett, E. J. Currie, and R. H. Hanner, "Canadian greenhouse operations and their potential to enhance domestic food security," *Agronomy*, vol. 11, no. 6, p. 1229, 2021.

[226] J. Hare, B. Norton, and S. Probert, "Design of 'greenhouses': thermal aspects," *Applied Energy*, vol. 18, no. 1, pp. 49–82, 1984.

[227] A. Maher, E. Kamel, F. Enrico, I. Atif, and M. Abdelkader, "An intelligent system for the climate control and energy savings in agricultural greenhouses," *Energy Efficiency*, vol. 9, no. 6, pp. 1241–1255, 2016.

[228] J. Liu, Y. Chai, Y. Xiang, X. Zhang, S. Gou, and Y. Liu, "Clean energy consumption of power systems towards smart agriculture: roadmap, bottlenecks and technologies," *CSEE Journal of Power and Energy Systems*, vol. 4, no. 3, pp. 273–282, 2018.

[229] T. J. Jeaunita, V. Sarasvathi, M. Harsha, B. Bhavani, and T. Kavyashree, "An automated greenhouse system using agricultural internet of things for better crop yield," 2018.

[230] J. R. Llera, K. Deb, E. Runkle, L. Xu, and E. Goodman, "Evolving and comparing greenhouse control strategies using model-based multi-objective optimization," in *2018 IEEE Symposium Series on Computational Intelligence (SSCI)*. IEEE, 2018, pp. 1929–1936.

[231] S. Mirzamohammadi, A. Jabarzadeh, and M. S. Shahrabi, "Long-term planning of supplying energy for greenhouses using renewable resources under uncertainty," *Journal of Cleaner Production*, vol. 264, p. 121611, 2020.

[232] P. Zhuang, H. Liang, and M. Pomphrey, "Stochastic multi-timescale energy management of greenhouses with renewable energy sources," *IEEE Transactions on Sustainable Energy*, vol. 10, no. 2, pp. 905–917, 2018.

[233] Y. Su, L. Xu, and D. Li, "Adaptive fuzzy control of a class of mimo nonlinear system with actuator saturation for greenhouse climate control problem," *IEEE transactions on automation science and engineering*, vol. 13, no. 2, pp. 772–788, 2015.

[234] M.-H. Liang, L.-J. Chen, Y.-F. He, and S.-F. Du, "Greenhouse temperature predictive control for energy saving using switch actuators," *IFAC-PapersOnLine*, vol. 51, no. 17, pp. 747–751, 2018.

[235] M. C. Bozchalui, C. A. Cañizares, and K. Bhattacharya, "Optimal energy management of greenhouses in smart grids," *IEEE transactions on smart grid*, vol. 6, no. 2, pp. 827–835, 2014.

[236] G. Turcotte and A. Gosselin, "Influence of continuous and discontinuous supplemental lighting on the daily variation in gaseous exchange in greenhouse cucumber," *Scientia horticulturae*, vol. 40, no. 1, pp. 9–22, 1989.

[237] Rate d: Hydro-québec. [Online]. Available: https://www.hydroquebec.com/residential/customer-space/rates/rate-d.html

APPENDIX A A P2P EXAMPLE

This extension provides an example application for Algorithm 1 of Chapter 5 in a P2P network of greenhouses. Figure A.1 illustrates the topology of the network. In this network, greenhouse No. 3 directly connects to the aggregator and exchanges information with it, while greenhouses No. 1 and 2 connect to the aggregator and each other through link No. 1. The aggregator is responsible for coordinating greenhouses' energy exchanged with the main grid and managing the water reservoir. Link No. 1, on the other hand, is responsible for coordinating the power exchanged between greenhouses No. 1 and No. 2.

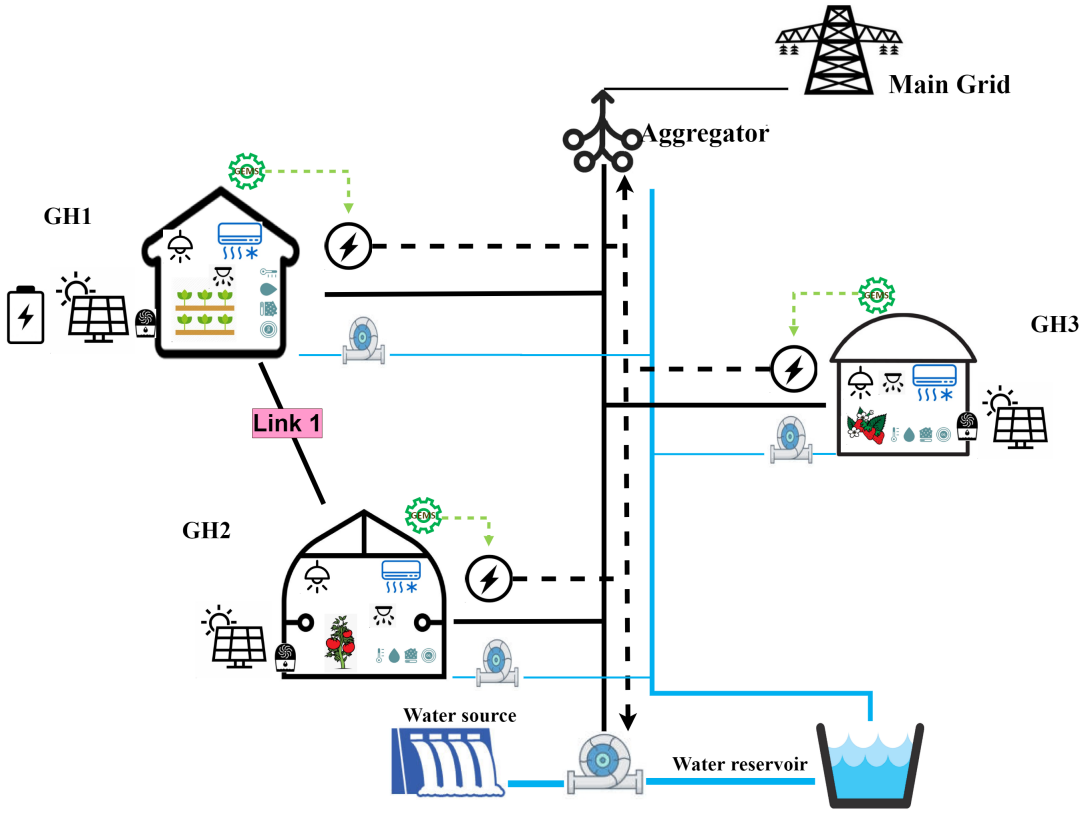

Figure A.1 The network topology

To illustrate the performance of the proposed algorithm, we consider a network of three greenhouses. PV panels are available only in Greenhouse No. 1, generating a power of up to 40 kW. In order to investigate exclusively the effects of P2P topology, the γs in (6.21) are adjusted to avoid the participation of the greenhouses in demand response schemes. Similar to Section 5.5, three scenarios are considered for solar irradiation at each 15 minutes time

step, and the network is simulated for a period of 24h.

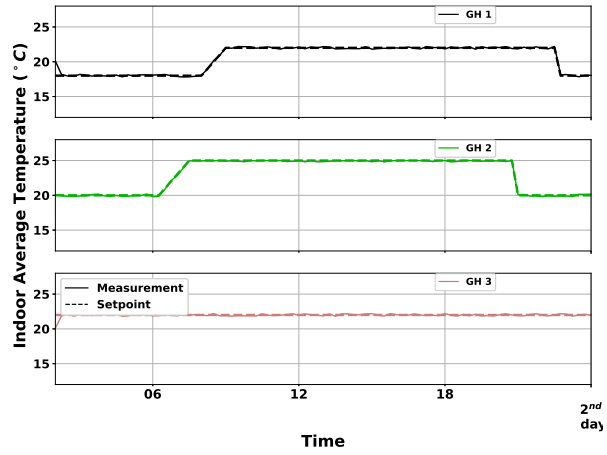

(a) Greenhouse indoor temperature.

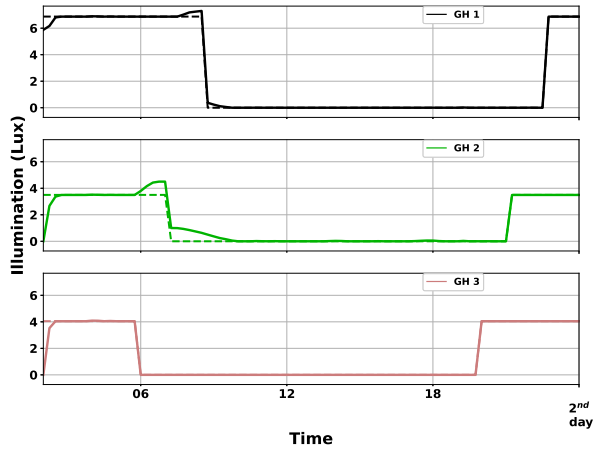

(b) Greenhouse interior lighting.

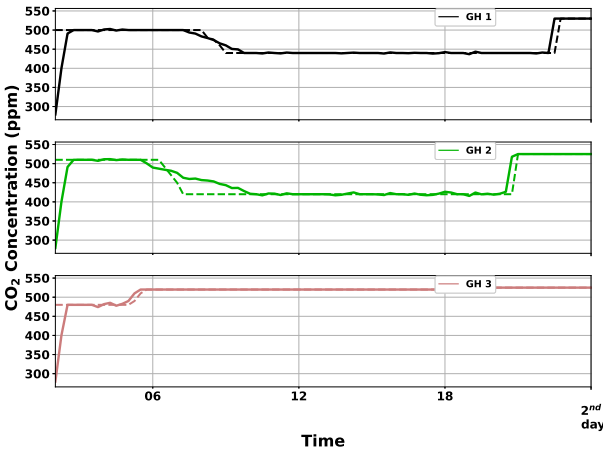

(c) Greenhouse CO_2 concentration level.

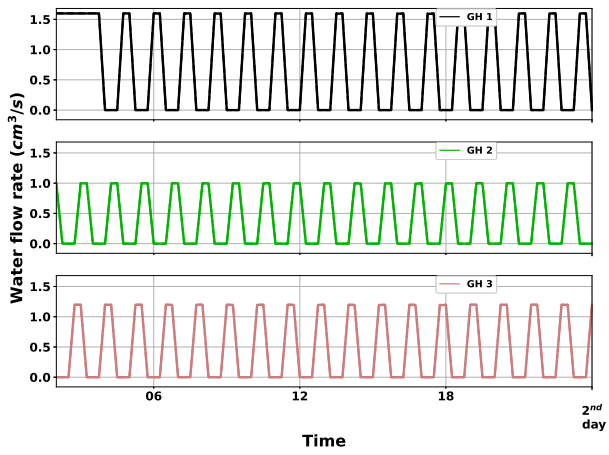

(d) Greenhouse CO_2 concentration level.

Figure A.2 Greenhouse climatic parameters

Figure A.2 shows the climatic conditions inside each greenhouse. As mentioned earlier, the high values of gammas ensure the perfect control of the indoor temperature, CO_2 level, lighting and watering system. Similarly, Fig. A.3 presents batteries SOC and their dis/charging powers. We randomly set the initial values of batteries between 60 and 70 percent, with a minimum admissible SOC of 18%.

Although the ADMM guarantees the convergence of the proposed algorithm, the convergence rate can sometimes be slow for real-time applications. For this reason, the algorithm uses

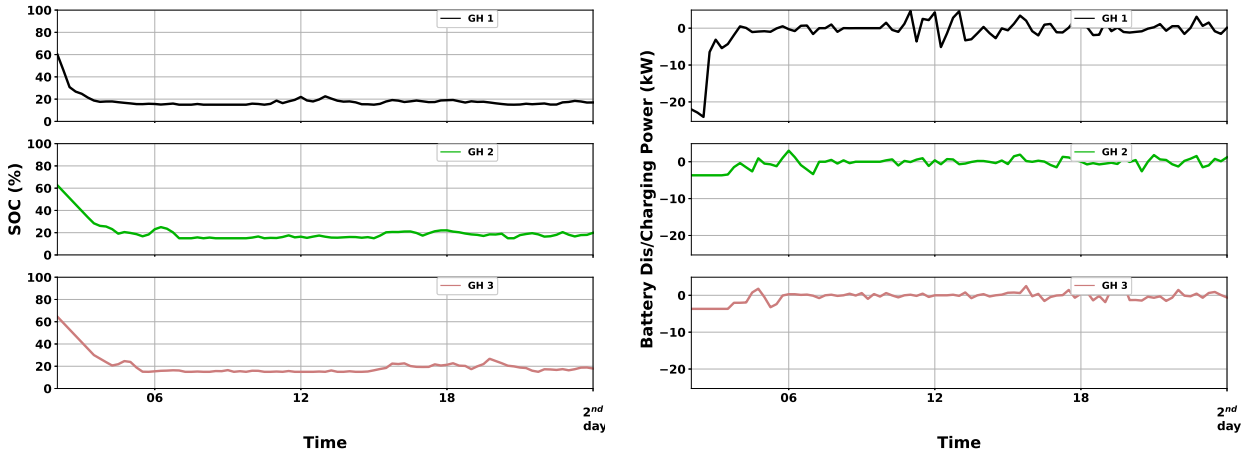

(a) SOC

(b) Dis/charging power

Figure A.3 Greenhouse battery condition

$maxItr$ and ϵ parameters for early stopping. We set $maxItr = 150$ and ϵ=2.4; however, the algorithm sometimes does not converge with these early stopping criteria, so a secondary control level is needed. At this level, the corresponding link (Link No. 1) decides whether the negotiation process was successful or not. If successful, the greenhouses will exchange the proposed link energy and buy/sell the difference between it and their proposed energy from/to the main grid. Otherwise, the corresponding link sets it to zero, and the greenhouses have to exchange the power they need with the main grid, Fig. A.4.

At each step, the greenhouses propose a new value for the amount of power exchange (dashed lines in Fig. A.4). The corresponding link (Link No. 1) then solves an optimization problem to find the optimal value (solid lines). Link No. 1 then proposes this optimal value to greenhouses and updates the trading price. This process continues till they reach a consensus or the algorithm meets the stopping conditions, and the link determines the amount (red lines).

This process for greenhouses No. 1 and 2 are illustrated in Figures A.4a and A.4b, respectively. In the early hours of the simulation (12:00 AM-08:00 AM), due to the energy stored in batteries, greenhouse No. 1 can sell some of this energy to GH 2 and vice versa. Around 08:30 AM, when GH 1 starts to generate PV power, it can sell the excess power to GH 2 instead of the main grid, Fig. A.5.

Due to *maxItr*, during the on-peak times (07:00 AM - 06:00 PM), the negotiation process usually ends before reaching a consensus. In this case, Link 1 compares the difference between

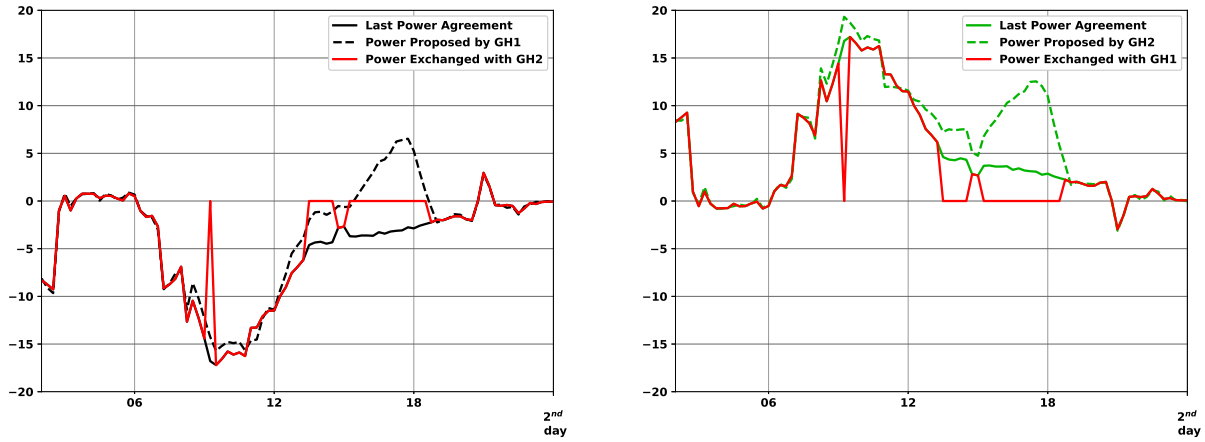

(a) GH No. 1 perspective

(b) GH No. 2 perspective

Figure A.4 The negotiation process

the proposed powers and the threshold ϵ. The negotiation process from 07:00 AM to 01:30 PM is almost successful, thanks to the PV power generated by GH 1, Fig. A.4. However, from 01:30 PM to 06:00 PM, the negotiation process is practically failed. The main reasons for this failure are lower levels of MDL, lack of sufficient PV power generated, and lack of energy storage in the battery. Therefore, the greenhouses buy their needs from the main grid, and as a result, the level of total power exchanged with the main grid is increasing, more than the MDL. After the on-peak times, when the MDL level rises, the negotiation

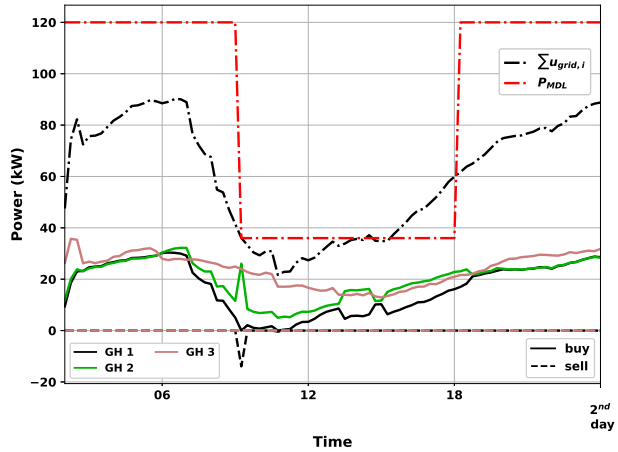

Figure A.5 The power exchanged with the main grid

process can continue between greenhouses again until the end of the day, with almost no other failures.

Finally, Fig. A.6 provides the information of the iterations in the negotiation process. Compared to previous case studies (Sections 6.4 and 5.5), although the average time per iteration is almost the same as before, the total time ($\simeq$ 600s) and number of iterations ($\simeq$ 150) per step are notable. Its main reason, as mentioned earlier, is that this case study is extreme. We assume just one greenhouse has RES, and none of the greenhouses are willing to reduce their consumption to participate in the DR program. There are usually more than one RES in the network in practice, and MGs are more eager to participate in the DR programs.

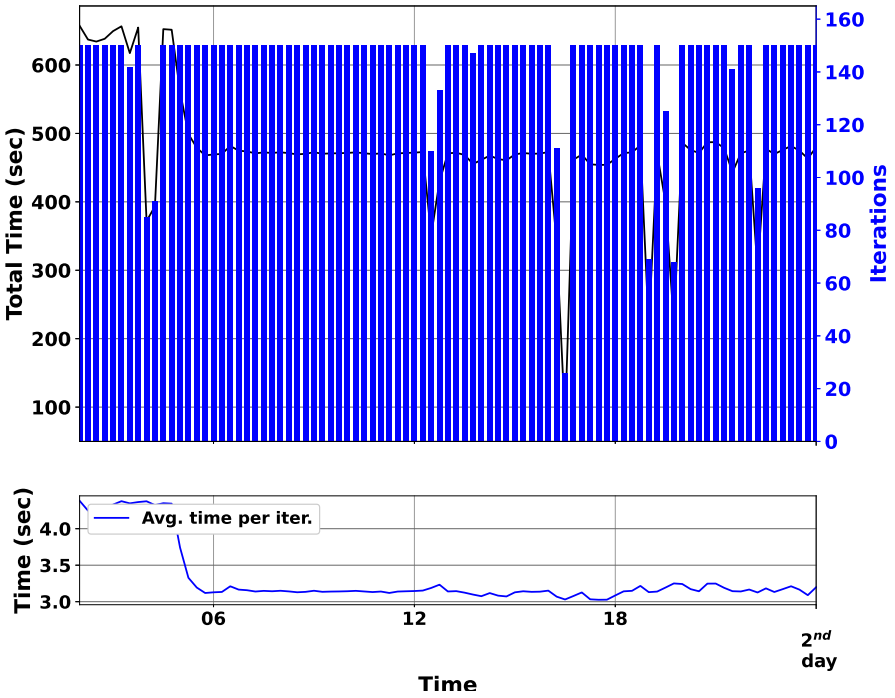

Figure A.6 Total time, average time per each iteration and total number of iterations